



Erasmus Mundus Joint Master in
ARCHaeological MATerials Science

Co-funded by the
Erasmus+ Programme
of the European Union



Green Mortars for Conservation: Utilizing agricultural and industrial waste for sustainable restoration.

**Regina Adomako
(m53971)**

A research paper submitted in partial fulfilment of the requirements for
the Master Of Science Degree In Archaeological Material Science
(ARCHMAT)

December, 2024.

Supervisors:

Dr. Nicola Schiavon

HERCULES Laboratory - Cultural Heritage, Studies and Safeguarding
University of Évora, Portugal

Dr. Silvestro Antonio Ruffolo

Department of Biology, Ecology, and Earth Sciences (DiBEST)
University of Calabria, Italy



UNIVERSIDADE
DE ÉVORA



ARISTOTLE
UNIVERSITY
OF THESSALONIKI



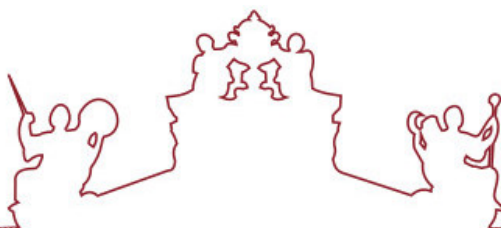
SAPIENZA
UNIVERSITÀ DI ROMA



SAPIENZA
UNIVERSITÀ DI ROMA



ARISTOTLE
UNIVERSITY OF
THESSALONIKI



**Universidade de Évora - Instituto de Investigação e Formação Avançada
Università degli Studi di Roma "La Sapienza" Aristotle University of
Thessaloniki**

Mestrado em Ciência dos Materiais Arqueológicos (ARCHMAT)

Dissertação

**Green Mortars for Conservation: Utilizing agricultural and
industrial waste for sustainable restoration**

Regina Adomako

Orientador(es) | Nicola Schiavon
Silvestro Antonio Ruffolo

Évora 2024

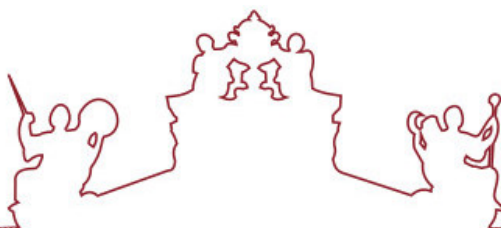




SAPIENZA
UNIVERSITÀ DI ROMA



ARISTOTLE
UNIVERSITY OF
THESSALONIKI



**Universidade de Évora - Instituto de Investigação e Formação Avançada
Università degli Studi di Roma "La Sapienza" Aristotle University of
Thessaloniki**

Mestrado em Ciência dos Materiais Arqueológicos (ARCHMAT)

Dissertação

**Green Mortars for Conservation: Utilizing agricultural and
industrial waste for sustainable restoration**

Regina Adomako

Orientador(es) | Nicola Schiavon
Silvestro Antonio Ruffolo

Évora 2024

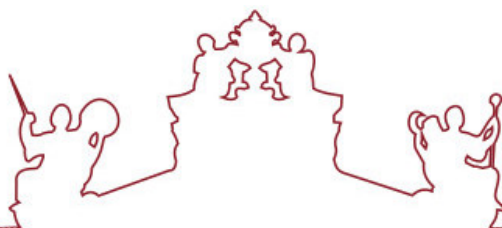




SAPIENZA
UNIVERSITÀ DI ROMA



ARISTOTLE
UNIVERSITY OF
THESSALONIKI



A dissertação foi objeto de apreciação e discussão pública pelo seguinte júri nomeado pelo Diretor do Instituto de Investigação e Formação Avançada:

Presidente | N. J. Almeida (Universidade de Évora)

Vogais | António Carlos Bettencourt Simões Ribeiro (LNEC - Laboratório Nacional de Engenharia Civil)
Donatella Magri (Università degli Studi di Roma "La Sapienza")
Eleni Pavlidou (Aristotle University of Thessaloniki)
Federico di Rita (Università degli Studi di Roma "La Sapienza")
Ioannis Kozaris ()
Nicola Schiavon (Universidade de Évora) (Orientador)

Table of Contents

Acknowledgements	vii
Abstract	viii
Resumo	ix
Abbreviations	x
List of Figures	xi
List of Tables and Equations	xiv
List of Appendices	xvi
Chapter 1:	1
Introduction	1
Background	1
Research objectives	3
Thesis Structure	4
Chapter 2:	5
Mortars	5
2.1 Composition of Mortars	6
2.1.1 Aggregates	6
2.1.2 Binders	9
2.1.3 Additives	11

Chapter 3:	18
Lime mortar in built heritage conservation	18
3.1 The use of lime mortars as repair mortars for built heritage conservation	20
3.2.1 Case studies.....	22
3.2 Repair mortars	26
Chapter 4:	28
Ground olive stones	28
4.1 Properties of Ground olive tree stones added to mortars.....	29
Chapter 5:	31
Materials and Methods	31
5.1 Materials used in the mortar preparation	33
5.1.1 Binder	33
5.1.2 Quartz sand aggregates	34
5.1.3 Ground Olive Stones (GOS).....	35
5.1.4 Nano Estel	35
5.1.5 Water.....	37
5.2 Methodologies in the preparation of test specimens.....	37
5.2.1 Mortar production	37
5.2.2 Testing Consistency of Wet Mortar Mixture	39
5.2.3 Moulding and Demoulding Mortars	39

5.3 Characterization of mortars in the hardened state	40
5.3.1 Colorimetry assessment	40
5.3.2 Salt crystallization tests.....	43
5.3.3 Water absorption by capillarity test.....	50
5.3.4 Mechanical tests	52
Chapter 6:	55
Results	55
6.1 Consistency test by flow table.....	55
6.2 Colourimetry assessment	56
6.3 Salt crystallization tests.....	61
6.4 Water absorption by capillarity	67
6.5 Mechanical Tests	73
6.5.1 Flexural strength test results.....	73
6.5.2 Compressive test results.....	76
Chapter 7:	79
Discussion.....	79
7.1 Consistency by flow table test.....	79
7.2 Colourimetry assessment	81
7.3 Salt Crystallization tests - Results	88
7.4 Water absorption by capillarity	99

7.5 Mechanical tests	101
Chapter 8:	106
Conclusions	106
Bibliography	110
Appendix	125

Acknowledgements

First of all, let me express my deepest gratitude to my amazing supervisors, Professor Nichola Schiavon and Professor Silvestro Antonio Ruffolo, for their invaluable guidance, support, and mentorship throughout my research journey, and for giving me the opportunity to learn and to grow. Your insights and expertise have been instrumental in shaping this work and my research ambitions. I did learn and will continue to learn a lot from you, as I proceed with my academic endeavours. Surely, you are the best supervisors anyone could ever have. Thank you so much.

A special thank you goes to Maria Antonietta Zicarelli, whose help throughout the entire thesis project was simply indispensable. Your support throughout the entire thesis project, is beyond measure. Your dedication and support were almost that of a supervisor, and for that, I am deeply grateful. You are the best!

I would also like to appreciate the faculty and staff at the Department of Biology, Ecology, and Earth Sciences (DiBEST), University of Calabria, Italy, for providing me with the resources, the environment needed to carry out this research and exposing me to colleagues who through their constant support and stimulating discussions, made this journey a rewarding experience.

A very big thank you to the European Union's Erasmus+ programme for funding my studies, the coordinators of the ARCHMAT program, for giving me this opportunity to participate in this program, as well as all the wonderful professors who taught us and gave their best in every instance. Your indispensable role in my education will forever be remembered.

To my family and friends, I owe endless thanks for their unwavering love and belief in me. Your support has been my greatest motivation.

Lastly, I would like to acknowledge the contributions of the many individuals who have directly or indirectly played a role in helping me complete this research. Your generosity and commitments have inspired me a lot.

Abstract

The construction industry faces growing environmental challenges due to its reliance on natural resources and the associated ecological impact. This study investigates the potential for using Ground Olive Stones (GOS), an agricultural byproduct, as a sustainable alternative to natural aggregates in lime-based repair mortars for the conservation and restoration of built heritage. The aim is to explore how GOS, when partially substituted for quartz aggregates, impacts the workability, durability, aesthetic compatibility, and resistance to environmental stresses, such as salt crystallization and moisture, in heritage conservation applications.

Seven different mortar mixtures were prepared, with varying proportions of GOS (ranging from 5% to 15%) and nano-silica to enhance their properties. The mortars were subjected to several standardized tests, including consistency by flow table, colorimetry, salt crystallization resistance, water absorption by capillarity, and mechanical strength assessments.

The results, when compared against a reference mortar without GOS show that while GOS offers environmental benefits by reducing the reliance on natural aggregates and repurposing agricultural waste, its use in conservation mortars must be carefully calibrated to balance the trade-offs between sustainability, durability, and aesthetic compatibility.

This study contributes to the growing field of sustainable construction materials by offering valuable insights into the use of agricultural byproducts in built heritage conservation.

Keywords: Built heritage conservation, Agricultural byproducts, Repair mortars, Compatibility, Ground Olive stones.

Resumo

A indústria da construção enfrenta desafios ambientais crescentes devido à sua dependência dos recursos naturais e ao impacto ecológico associado. Este estudo investiga o potencial de utilização de caroços de azeitona moídos (GOS), um subproduto agrícola, como alternativa sustentável aos agregados naturais em argamassas de reparação à base de cal para a conservação e restauro do património edificado. O objetivo é explorar como o GOS, quando parcialmente substituído por agregados de quartzo, impacta a trabalhabilidade, durabilidade, compatibilidade estética e resistência a tensões ambientais, como cristalização de sal e humidade, em aplicações de conservação de património.

Foram preparadas sete misturas diferentes de argamassas, com proporções variadas de GOS (variando de 5% a 15%) e nanossílica para potencializar as suas propriedades. As argamassas foram submetidas a diversos testes padronizados, incluindo avaliações de consistência por tabela de fluidez, colorimetria, resistência à cristalização de sal, absorção de água por capilaridade e resistência mecânica.

Os resultados, quando comparados com uma argamassa de referência sem GOS, mostram que, embora o GOS ofereça benefícios ambientais ao reduzir a dependência de agregados naturais e reaproveitar resíduos agrícolas, a sua utilização em argamassas de conservação deve ser cuidadosamente calibrada para equilibrar os compromissos entre sustentabilidade, durabilidade, e compatibilidade estética.

Este estudo contribui para o crescente campo dos materiais de construção sustentáveis, oferecendo informações valiosas sobre o uso de subprodutos agrícolas na conservação do património construído.

Palavras-chave: Conservação do património edificado, Subprodutos agrícolas, Argamassas de reparação, Compatibilidade, Caroços de azeitona moídos.

Abbreviations

GOS: Ground Olive Stones

HL: Hydrated Lime

POS5-HL: Mortar with 5% Ground Olive Stones and Hydrated Lime

POS10-HL: Mortar with 10% Ground Olive Stones and Hydrated Lime

POS15-HL: Mortar with 15% Ground Olive Stones and Hydrated Lime

POS5-HL-S: Mortar with 5% Ground Olive Stones, Hydrated Lime, and Nano-Silica

POS10-HL-S: Mortar with 10% Ground Olive Stones, Hydrated Lime, and Nano-Silica

POS15-HL-S: Mortar with 15% Ground Olive Stones, Hydrated Lime, and Nano-Silica

List of Figures

FIGURE 1: MORTAR COMPOSITION.....	6
FIGURE 2: MOH'S SCALE OF HARDNESS. RETRIEVED FROM: HTTPS://WWW.JEWELRYCULT.COM/JEWELRY/WHAT-IS-THE-MOHS-SCALE-OF-MINERAL-HARDNESS	8
FIGURE 3: LOCATION OF POZZUOLI. RETRIEVED FROM WWW.BRITANNICA.COM/PLACE/POZZUOLI . 11	
FIGURE 4: POZZOLANA. RETRIEVED FROM HTTPS://WWW.ARCHEOFLEGREI.IT/POZZOLANA-LA-POLVERE-PUTEOLI/POUZZOLANE15-20-03-Z-C340-C491/	11
FIGURE 5: THE LIME CYCLE	19
FIGURE 6: REPAIR MORTARS INCORPORATING A BLENDED COARSE STUFF LIME PUTTY MIXTURE APPLIED IN THE RESTORATION OF THE BELL TOWER AT THE TOWER OF LONDON, UK. RETRIEVED FROM: HTTPS://WWW.LIMESTUFF.CO.UK/BLOG/TOWER-OF-LONDON	22
FIGURE 7: THE RESTORATION OF THE COLOSSEUM'S HYPOGEA. RETRIEVED FROM HTTPS://WWW.TODSGROUP.COM/EN/SUSTAINABILITY/COLOSSEUM-RESTORATION-HYPOGEA .23	
FIGURE 8: REPAIRS AND RESTORATIONS OF THE ORATORY OF THE PARTAL PALACE IN THE ALHAMBRA, SPAIN. RETRIEVED FROM HTTPS://WWW.EUROPEANHERITAGEAWARDS.EU/WINNERS/ORATORY-PARTAL-PALACE-ALHAMBRA-SPAIN/	24
FIGURE 9: LEFT- UNMILLED OLIVE STONES, RIGHT- GROUND OLIVE STONE (100-300MICRONS). RETRIEVED FROM: WWW.BIO-POWDER.COM/EN/OLIVE-PIT/	28

FIGURE 10: CURING OF MORTAR SAMPLES - (A) – WET MORTAR MIXTURE IN A PRISM MOULD, (B) – DRIED MORTAR SAMPLES IN CUBE AND PRISM MOULDS, (C) – LABELLED WET MORTAR IN PRISM MOULDS.....	40
FIGURE 11: COLORIMETRY ASSESSMENT – (A) AND (B) – RESEARCHER TAKING COLORIMETRIC MEASUREMENTS, (C) – A SAMPLE WITH INDICATIONS ON WHERE MEASUREMENTS WERE TAKEN	42
FIGURE 12: PREPARATION OF A SOLUTION OF SODIUM SULPHATE – (A) - SODIUM SULPHATE (NA ₂ SO ₄), (B) – 84 GRAMS OF NA ₂ SO ₄ , (C) – 516 ML OF DISTILLED WATER, (D) – SOLUTION OF NA ₂ SO ₄ IN A WATER BATH	48
FIGURE 13: REPRESENTATION OF HOW THE SPECIMEN WERE CONTAMINATED WITH THE SODIUM SULPHATE SOLUTION WHILE MAINTAINING THE TEMPERATURE OF THE SOLUTION IN A WATER BATH.....	49
FIGURE 14: DRYING OF THE SPECIMENS AFTER IMMERSION	50
FIGURE 15: SET UP FOR WATER ABSORPTION BY CAPILLARITY TEST.....	51
FIGURE 16: LOADING ARRANGEMENT FOR FLEXURAL STRENGTH TEST	53
FIGURE 17: HALVED SPECIMENS AFTER FLEXURAL STRENGTH TEST.....	54
FIGURE 18: LOADING ARRANGEMENT OF THE COMPRESSIVE STRENGTH TEST.....	54
FIGURE 19: GRAPHICAL REPRESENTATION OF THE COLOUR DIFFERENCE	58
FIGURE 20: GRAPHICAL REPRESENTATION OF THE TOTAL COLOUR DIFFERENCE ΔE	60
FIGURE 21: GRAPHICAL REPRESENTATION OF THE RELATIVE MASS DIFFERENCE (%)......	66
FIGURE 22: GRAPHICAL REPRESENTATION OF THE CAPILLARY ABSORPTION CURVE.....	71
FIGURE 23: GRAPHICAL REPRESENTATION OF THE FLEXURAL STRENGTH TEST.....	75
FIGURE 24: GRAPHICAL REPRESENTATION OF THE SPECIMENS’ COMPRESSIVE STRENGTH	78

FIGURE 25: TQ SAMPLES AFTER THE 15 TH CYCLE SHOWING SIGNIFICANT MATERIAL LOSS AT THE END OF THE TEST	89
FIGURE 26: TQ SAMPLES AFTER THE 10 TH CYCLE SHOWING.....	89
FIGURE 27: POS-15-HL AFTER THE 12 TH CYCLE SHOWING A COMPLETE DISINTEGRATION	90
FIGURE 28: POS-5-HL-S AFTER COMPLETELY DISINTEGRATED AFTER THE 14 TH CYCLE	91
FIGURE 29: POS-10-HL-S AFTER THE 12 TH CYCLE COMPLETELY DISINTEGRATED	91
FIGURE 30: TQ SAMPLES SHOWING SIGNS OF MINOR BLISTERING AND TINY SALT CRYSTALS ON ITS SURFACE AFTER THE 3 RD CYCLE OF THE SALT CRYSTALLIZATION CYCLE.....	92
FIGURE 31: VISIBLE DETACHMENT ON THE TQ-HL SAMPLES AFTER THE 5 TH CYCLE OF THE SALT CRYSTALLISATION TEST.....	93
FIGURE 32: POS-HL-S SERIES SHOWING NO SIGNS OF SUFFERING THE SALT WEATHERING TEST AFTER THE 3 RD CYCLE AS COMPARED TO THE TQ-HL BELOW	95
FIGURE 33: TQ-HL SHOWING EARLY SIGNS OF BLISTERING AFTER THE 3 RD CYCLE.	95
FIGURE 34: POS-5-HL-S AFTER THE 10 TH CYCLE	96
FIGURE 35: THE LAST SAMPLE OF POS-10-HL-S DISINTEGRATING AFTER THE 12 TH CYCLE	96
FIGURE 36: THE LAST SAMPLE OF POS-15-HL-S DISINTEGRATING AFTER THE 12 TH CYCLE	96

List of Tables and Equations

TABLE 1: PHYSICAL AND CHEMICAL COMPOSITION OF THE HYDRATED LIME	34
TABLE 2: CHEMICAL AND PHYSICAL CHARACTERISTICS OF QUARTZITE	35
TABLE 3: CHEMICAL-PHYSICAL CHARACTERISTICS OF NANO ESTEL.....	36
TABLE 4: TYPE AND QUANTITY OF MATERIALS (G) USED TO MANUFACTURE OF MORTAR MIX	38
TABLE 5: MASS (G) OF SPECIMEN UNTIL A CONSTANT MASS (NOT GREATER THAN 0.01% OF THE INITIAL MASS)	47
TABLE 6: FLOW VALUES FROM CONSISTENCY TEST	56
TABLE 7: COLORIMETRIC VALUES OF SPECIMEN FROM THE COLOUR ASSESSMENT TEST	57
TABLE 8: COLOUR DIFFERENCE (ΔL^* , ΔA^* , ΔB^*)	58
TABLE 9: TOTAL COLOUR DIFFERENCE (ΔE)	60
TABLE 10: MASS (G) OF SPECIMEN AFTER WET AND DRY CYCLES OF SALT CRYSTALLIZATION	61
TABLE 11: ΔM : RELATIVE MASS DIFFERENCE (%) (MASS LOSS OR MASS GAIN).....	62
TABLE 12: AVERAGE VALUES OF THE RELATIVE MASS DIFFERENCE (%).....	64
TABLE 13: MASS OF SPECIMEN (G) AT TIME (TI)	67
TABLE 14: QI - AMOUNT OF WATER ABSORBED BY SPECIMEN PER UNIT AREA AT TIME (TI) IN (G/CM ²)	68
TABLE 15: DETERMINATION OF THE CAPILLARY WATER ABSORPTION CURVE QI (G/CM ²) / \sqrt{t}	70
TABLE 16: FLEXTURAL STRENGTH TEST RESULTS	73
TABLE 17: FLEXURAL TEST STRENGTH RESULTS	74
TABLE 18: DETERMINATION OF COMPRESSIVE STRENGTH OF SPECIMEN	77
TABLE 19: COMPRESSIVE STRENGTH OF SPECIMENS.....	77

TABLE 20: DESCRIPTION OF SALT DAMAGE TYPE ACCORDING TO ICOMOS INTERNATIONAL
SCIENTIFIC COMMITTEE FOR STONE (ISCS), [93].....125

List of Appendices

Table 20: Description of salt damage type according to ICOMOS International Scientific Committee for Stone (ISCS),	125
--	-----

Chapter 1:

Introduction

Background

The construction industry has a significant impact on environmental dynamics, mostly due to its large-scale use of natural resources, particularly aggregates. These materials, which include sand, gravel, and crushed stone, are basic components of mortars, concrete, and other building materials. But their long-term exploitation raises serious ecological issues. Extraction operations often lead to the destruction of habitats of living organisms, soil erosion, and landscape transformation, which in turn cause ecological disturbance and loss of biodiversity. Natural stone reserves have been significantly depleted due to the increased demand for concrete in buildings that use weight aggregates such as sand and gravel sizes of granitic fragments [2]. As the demand for construction materials continues to increase, it becomes crucial for the industry to prioritize sustainable practices and alternative materials to mitigate its environmental impact and preserve natural earth resources for future generations. The increasing demand for sustainable development has spurred a number of scholars to concentrate their research on repurposing discarded or recycled resources as possible building materials. Such approaches include responsible sourcing, recycling building debris, and incorporating alternative materials like agricultural and industrial wastes.

Additionally, the environmental impact of cement manufacture is significant, mainly due the high energy consumption and greenhouse gas emissions such as carbon dioxide (CO₂) which is released during the high temperatures at which raw materials like limestone and clay are heated in kilns during the cement manufacturing process [3]. As a result, a number of replacement materials for

natural aggregates and portions of cement have been researched for use in concrete mortar preparations. Among other things, agricultural wastes have been studied as materials to partially replace natural aggregates in mortars as well as a supplementary cementitious binder [4].

Meanwhile, due to the various issues posed by cement to historical buildings such as the presence of soluble salts in Ordinary Portland Cements which tends to leach and gradually degrade the surrounding material over time [5], conservation and restoration works on historical masonry have been testing the use lime as binders instead as it has proven to be more compatible comparatively [6]. Incompatibility with conventional materials, aesthetic concerns, mechanical and long-term maintenance issues are only a few of the significant difficulties and disadvantages associated with using cement in the conservation of historic buildings [7].

Although air lime mortars have proven to be compatible with historical masonry, it has some disadvantages such as slow setting, lack of durability, and inability to harden under water; characteristics which are able to undergo some changes when pozzolanic materials are added [8]. The addition of pozzolanic materials to lime mortars can improve the mechanical properties of the mortar due to pozzolanic reaction between silica and sometimes alumina oxides which is present in pozzolanic materials and the lime in the presence of water. Pozzolana is a type of siliceous or siliceous and aluminous material that, while not possessing significant cementitious properties by itself, can react chemically with calcium hydroxide (lime) in the presence of water to form compounds possessing cementitious properties [9]. This reaction is known as the pozzolanic reaction. The key to this reaction process is the availability of reactive silica (SiO_2) and, in some cases, alumina (Al_2O_3), which react with the lime to form calcium silicate hydrates (C-S-H) and calcium aluminate hydrates (C-A-H). These hydrates contribute to the hardening and strength development of the mortar. Various pozzolanic materials occur naturally in volcanic rocks and

certain sedimentary rocks, such as clays and shales while others are generated as byproducts of industrial processes, including the manufacture of fly ash, silica fume and rice husk ash [10]. While some pozzolans can be utilized in their raw state, others, like calcined clays, require thermal activation processes before use.

Research objectives

This thesis focuses on investigating the potential utilization of agricultural and industrial wastes such as Ground Olive Stones (GOS) in the preparation of a repair lime mortar for the purposes of conservation and restoration by substituting some volumetric proportions of the natural aggregates used with the wastes, in uncalcined form in an attempt to ensure sustainability without compromising the integrity of the historical material as well. The GOS is used as it is, just as a partial substitute of the natural aggregates used. Hence the objectives of the research include;

- An evaluation of the workability of mortars made with varying proportions of agricultural waste
- A determination of the durability of the repair mortar and its compatibility with historical mortar using a number of standardized tests.

The significance of this research is in its contribution to addressing the problem of disposing agricultural waste and the quest for a sustainable construction industry especially in the field of built heritage and monument conservation.

Thesis Structure

The structure of this thesis is divided into two main parts; The state of the art and the experimental development which is organized into seven chapters.

The first part comprises four chapters including Chapter 1 as an Introduction, providing an overview of the research topic, its significance, and the objectives of the study. Chapter 2 delves into the composition of traditional mortars, while Chapter 3 explores the use of lime mortars in conservation works, focusing on their historical context and practical applications. Chapter 4 investigates the properties of Ground olive stones (GOS) examining its potentials and influence on the mortar when utilized as a partial replacement of the natural aggregates in the preparation of a repair mortar.

The second part of the thesis, which presents and describes the experimental developments of the thesis consists of four chapters. Chapter 5 details the experimental methodology employed in the study, including procedures involved in the mixing and curing of the repair and reference mortars as well as the testing procedures and analysis methods. Chapter 6 presents the results and analysis of the experiments, discussing the performance of mortar mixtures incorporating GOS. Chapter 7 provides a comprehensive discussion of the findings, and Chapter 8 draws conclusions, based on the findings, and offers recommendations for future research. The thesis then concludes with a list of bibliographic references.

Chapter 2:

Mortars

Mortars are workable pastes made from a combination of binders, aggregates and water to bind building blocks together or fill the gaps between them. Sometimes additives (organic or inorganic) are also added for some desired properties. The aggregate adds volume to the mortar and influences its mechanical properties, while the binder and water make it workable and viscous. Other uses of mortars include waterproofing walls, rendering, preparatory layers for pigment application as in the case of frescoes and surface finishes. Moreover, the ability of a masonry mortar to bond with a substrate is its most important property which is influenced by its workability [11]. In addition, the technical guide provided by [12] suggests that a good mortar is one that is workable, cohesive, has sufficient strength, permeable, compatible and reasonably durable. The study of mortars reveals building techniques, chronology, geology and how people use the available raw materials as well as their search for raw materials that are not readily available to them. The classification of mortars can be based on the nature and type of binder used; lime, cement, clay and gypsum mortars. It can also be classified on the basis of its application; decoration, facings and masonry mortars. The manner in which mortars harden can also be a basis for its classification; hydraulic and aerial mortars.

2.1 Composition of Mortars

The basic constituents of mortars are aggregates, binder and water, sometimes with some additives.



Figure 1: Mortar composition

2.1.1 Aggregates

Aggregates add up to the bulk of the mortar mixture by filling up spaces and constitute about 60-75% of the total volume of mortar according to the Portland Cement Association [13]. Aggregates help to control the shrinkage of mortar as it dries and sets, thus minimizing the possibility of shrinkage-related cracking. Again, they increase strength and durability of the mixture and improves workability.

Aggregates are generally classified into two categories namely, coarse and fine aggregates. Fine aggregates are normally comprised of natural sand or crushed stone, with the majority of particles small enough to pass through a 0.95 cm sieve, while coarse aggregates include any particles larger than 0.48 cm, usually ranging from 0.48 to 3.81 cm in diameter [13].

Other physical characteristics of aggregates, such as the shape and texture, size gradation, reactivity, and bulk density, influence the strength, workability, and durability of mortars. For example, as the shape and texture of aggregate impact the properties of fresh mixture more than those of hardened mortar, smooth and rounded aggregates enhance workability, whereas rougher surfaces create stronger bonds between the paste and aggregate, leading to greater strength; the particle size distribution of aggregate affects the paste requirement for achieving workable concrete depending on the amount of void space and total surface area, and the density of aggregates is essential in mixture proportioning to determine weight-volume relationships [14].

The mineralogical composition of aggregates also influences the strength and durability of mortars. This composition is dependent on the source of aggregates used. Natural stone aggregates of sand and gravel grain size normally contain quartz, feldspars, micas and clay minerals, and calcium carbonates. These minerals, especially quartz, are known for their hardness and resistance to weathering. Crushed stone aggregates, derived from sources such as granite, limestone, and basalt, vary in their mineralogy. For example, granite primarily contains quartz, feldspars, and micas, while basalt is rich in pyroxene and plagioclase. Limestone, on the other hand, is composed primarily of calcite (calcium carbonate) and aggregates from industrial by-products such as slag; the by-product of steel production usually contains silicates and metal oxides [15]. Fly ash, which is the byproduct of coal combustion also contains aluminosilicates which improves strength and durability of mortars [16].

It is worthy to mention that the mineralogical composition of aggregates can vary widely based on their geological origin and the method of production. Common minerals present include quartz, feldspar, and calcite, each contributing different properties to the aggregate and, consequently, to the mortar in which they are used. Quartz, known for its hardness and resistance to weathering, is

one of the hardest common minerals, rated at 7 on the Mohs scale. Because of its resistance to scratches and fractures, chemical stability, and its resistance to high temperatures, quartz can be used in a wide range of applications that require longevity and durability [17].

This makes aggregates containing quartz highly resistant to mechanical wear, contributing to the durability of the mortar. Feldspar minerals which include orthoclase and plagioclase, have a hardness level of 6 on the Mohs scale.

The Mohs Scale of Mineral Hardness



Figure 2: Moh's scale of hardness. Retrieved from: <https://www.jewelrycult.com/jewelry/what-is-the-mohs-scale-of-mineral-hardness>

Though not as hard as quartz, they contribute to the durability of the aggregate due to the relatively high hardness. However, feldspars contain alkali elements such as potassium and sodium which can increase alkali concentration in pore solution which could lead to alkali-silica reaction (ASR) in the presence of reactive silicas in the mortar [18], hence potentially causing cracking and

expansion. The ASR mechanism can be represented by the following chemical equation: $2\text{NaOH (or KOH)} + \text{SiO}_2 \text{ (silica)} + \text{H}_2\text{O} \rightarrow \text{Na}_2\text{SiO}_3 \cdot \text{H}_2\text{O}$ (alkali-silica gel). This alkali-silica gel can absorb water and swell, leading to internal pressure, which when greater than the tensile strength of the mortar, results in cracking and deterioration of the mortar over time [19].

Calcite, the main mineral in limestone, is relatively soft, 3 on the Mohs scale. However, mortars containing calcite often demonstrate good initial setting characteristics, especially in lime-based mortars, where calcite forms during the carbonation process. In these systems, limestone is heated to produce quicklime, which is then slaked with water to form hydrated lime. Upon exposure to air, the hydrated lime reacts with atmospheric carbon dioxide, leading to the gradual formation of calcite (calcium carbonate), which contributes to the hardening of the mortar over time. It is important to distinguish between calcite formed through carbonation of the lime binder and calcite present as an aggregate material. In lime mortars, it is the carbonation of the binder that plays a critical role in the mortar's long-term setting and hardening process, rather than calcite as a component of the aggregates. Hence, understanding the mineralogical composition of aggregates helps to predict the behaviour of aggregates under different environmental and loading conditions, thereby ensuring the desired performance of the final product.

2.1.2 Binders

Binders constitute an important component in mortar as they act as a glue or a bonding agent that holds the aggregates and other additives together to ensure the mortar's structural integrity and provide the necessary adhesion to the building materials [20]. Mortars are used in construction for masonry work, plastering, and rendering, and their performance is primarily determined by the type and qualities of the binders used. Binders influence the mortar's physical and chemical qualities, such as its strength, the rate at which it sets, and how it reacts with other materials [21].

Types of binders used in mortars include cement, lime (non-hydraulic and hydraulic), gypsum and clay binders.

Cement is made from limestone and clay, which are heated to form clinker, then ground to a fine powder, whereas lime is made by slaking quicklime (calcium oxide) with water which hardens by reacting with carbon dioxide in the air (carbonation) [22]. Lime can be differentiated based on their reaction in the presence of water. According to Escadeillas et al [23], aerial lime, which is mostly made of calcium oxide or hydroxide, hardens slowly in the air through the process of carbonation in the presence of carbon dioxide and does not harden in response with water. Hydraulic lime on the other hand contains calcium hydroxide as well as calcium silicate compounds and calcium aluminates [23], produced by burning limestone that naturally contains clay and other impurities, which provide hydraulic properties thus, having the ability to set in the presence of water.

Binders enable mortar adhesion to masonry components ensuring that the bricks or stones are firmly held together. They also enhance the workability of mortar, making it easier to spread and apply. Binders are therefore important components of mortars, with a considerable impact on their characteristics and performance.

In essence, the specific requirements of the construction project influences the type of binder to be used, whether Portland cement, lime, gypsum, or clay such as strength, workability, compatibility, durability, and environmental factors. For instance, lime mortars are preferred in the case of historical masonry repair works as they have proven to be the most compatible with historical masonry as compared to cement even though they have high setting characteristics according to the literature.

2.1.3 Additives

Additives are normally included in mortars to improve its properties and performance. They are incorporated into the mortar mix to modify its characteristics and enhance certain properties such as its workability, setting time, durability, waterproof and strength [24]. These additives can either be organic or inorganic depending on their chemical composition. Examples include accelerators, waterproofing additives, plasticizers and superplasticizers, air-entraining agents and pigments. Correspondingly, the choice of additive used depends on the needs of the construction project and the properties they seek to attain.

2.1.3.1 Pozzolanic materials

Pozzolanic materials are additives added to mortars to confer hydraulic properties on the mortar. They have been used in building for ages to improve mortar characteristics and performance. Pozzolanic materials have been utilized since antiquity, with the Romans pioneering their use for constructions with great mechanical strength such as bridges [25] .



Figure 4: Pozzolana. Retrieved from <https://www.archeoflegrei.it/pozzolana-la-polvere-puteoli/pouzzolane15-20-03-z-c340-c491/>



Figure 3: Location of Pozzuoli. Retrieved from www.britannica.com/place/Pozzuoli

The term "pozzolana" is derived from the Italian town of Pozzuoli, near Mount Vesuvius, where extensive fine-grained volcanic ash deposits were the principal source of natural pozzolan [26]. The Romans realized that combining volcanic ash, lime, and water resulted in a strong and durable building material. Roman engineers also recognized the hydraulic properties of pozzolanic materials which made them ideal for underwater construction [27]. Pozzolans, such as volcanic ash, react with calcium hydroxide ($\text{Ca}(\text{OH})_2$) in wet conditions to form calcium silicate hydrate (C-S-H), the main binding phase responsible for strength and durability in cementitious materials. Since pozzolanic reactions; ($\text{Ca}(\text{OH})_2 + \text{H}_4\text{SiO}_4 \rightarrow \text{CaH}_2\text{SiO}_4 \cdot 2\text{H}_2\text{O}$) which can also be represented as C-S-H (Calcium silicate hydrates) occur in wet conditions, it for instance allowed the Romans to build harbours, piers, and other maritime structures that have survived for millennia. However in cases where natural pozzolans from volcanic activities are unavailable, other materials such as crushed bricks and tiles can be utilized. Examples of other artificial "pozzolanic" materials include industrial by-products such as fly ash, silica fume, ground granulated blast-furnace Slag (GGBS) and sugarcane bagasse ash. Rice husk ash and calcined clay such as metakaolin are other examples of pozzolanic materials utilized.

Despite the varied origins of pozzolanic materials, one characteristic they all have in common is that they are all rich in very fine-grained silica or alumina content typically in amorphous or glassy form that react with calcium hydroxide in the presence of water [12]. Whereas the silica reacts with calcium hydroxide to form calcium silicate hydrates (C-S-H), the alumina reacts with the calcium hydroxide to the form calcium aluminate hydrates (C-A-H) during the pozzolanic reaction. These hydration products are responsible for the strength and durability of the mortar since they tend to fill the pores within the mortar matrix thereby increasing its density and strength [28].

2.1.3.2 Animal Products

Organic materials such as egg whites, animal fat, milk, and even blood were sometimes added to mortars. These materials were believed to improve workability and durability. Egg whites were often used mixed into the mortar to improve consistency and workability due to its adhesive properties [29]. Whereas animal fat and milk could increase water resistance and flexibility. Such that, caseins, which make up 80% of milk proteins, are naturally phosphorylated, so in lime mortars, the anionic phosphate groups in caseins bind with calcium ions to form calcium caseinate, enhancing mortar adhesion, plasticity, and particularly compressive strength [30]. In addition, dried animal blood was historically added to building materials to enhance their properties, in that even a small amount significantly increases air retention, binding 5–25% more air which tends to improve workability, extensibility, and resilience against environmental conditions than conventional mortar [30].

2.1.3.3 Plant based additives

Various plant materials were incorporated into ancient mortars to increase tensile strength and durability.

For instance in ancient Greece, wood and straw fibres were specifically added to improve volume stability, while jute and straw were utilized in Indo-Muslim architecture to enhance bonding and minimize cracking [31]. Fibers are generally used to reduce cracking caused by plastic and drying shrinkage, as well as to increase tensile strength, toughness, and durability.

Plant extracts containing tannins were sometimes used for enhancing some mortar properties. According to [32], the presence of tannins and sucrose likely helped reduce crack formation, as indicated by increased resistivity and greater data stability. They mentioned that this effect may

stem from the polymerization of tannins and other polyphenols, which increases molecular size, filling micro-cracks formed during cement hydration and enhancing compressive strength and elasticity and consequently, the improving the durability properties which may be due to tannins and polyphenols like epicatechin, which form solid structures that reduce mortar porosity.

2.1.3.4 Pulverized bricks

Pulverized bricks or crushed terracotta were used as additives in Roman and Byzantine mortars to achieve hydraulic properties. This method provided enhanced resistance to water and helped mortars cure in damp conditions. Mortars and plasters made with crushed bricks and lime harden in the presence of water and exhibit high mechanical strength according to [33], whose research also opined that this durability made the mortars ideal for constructing aqueducts, bridges, and bathhouses since Roman times.

The addition of ceramic residues, like brick dust and crushed brick, to historic mortars was a common practice to enhance hydraulic properties was systematically applied over nearly two millennia, from the Hellenistic period through the Ottoman era, and adapted based on mortar type and structural needs, with a preference for local materials according to [34]. According to their research, they indicated that these additions improved lime-based mortar by increasing strength, humidity resistance, and reducing density, while recycling waste ceramics. This stems from the fact that bricks fired at low temperatures (600–900 °C) have pozzolanic potential, with aluminosilicates in the brick reacting with lime to create a stable, dense structure, particularly at the lime-brick interface [34].

2.1.3.5 Clay

In ancient times, particularly in regions with limited resources, clay was often added to lime mortars to improve plasticity and workability. It allowed for easier shaping and application, especially in masonry structures. Clay became widely used in construction due to its availability, low cost, and its ability to form a plastic paste that hardens through physicochemical processes when mixed with water, thereby enhancing the mortar's workability [35].

2.1.3.6 Plasticizers and superplasticizers

Plasticizers (water-reducing agents) are used to improve the workability of mortar without increasing the water content. They help create a more fluid mixture that is easier to apply while maintaining strength. Superplasticizers offer more advanced water-reducing capabilities, allowing for even lower water content without compromising workability and flow properties, resulting in a denser and more durable mortar [36]

2.1.3.7 Nano silica

Nano-silica is a more recent development in construction materials. It improves the properties of mortars by reacting with calcium hydroxide to form additional calcium silicate hydrates (C-S-H), enhancing the strength and durability of the mortar. It also helps refine the pore structure, improving density and reducing permeability. Such that its incorporation in mortar improves compressive and flexural strength, resistance to water penetration and sulphate attack, and reduces calcium leaching [37]. Nano-silica thus is particularly beneficial in modern heritage conservation applications where durability and resistance to weathering are crucial.

2.1.3.8 Other additives

Other modern additives include accelerators, which are designed to speed up the setting time of mortar, particularly useful in cold environments where slower setting can be problematic. Calcium chloride is a common accelerator, promoting faster hydration of cement and lime.

In contrast to accelerators, retarders, another form of modern additives delay the setting time of mortars, which can be beneficial in hot weather conditions or when large sections of a structure are being worked on. Gypsum is an example of a common retarder used in cement-based mortars.

Air-Entraining Agents are also additives that introduce microscopic air bubbles into the mortar, enhancing its freeze-thaw resistance by allowing room for water to expand as it freezes to prevent cracking in cold climates. Alkali salts of wood resins are commonly used as air-entraining agents.

Waterproofing additives are used to reduce the permeability of mortar, making it more resistant to water ingress. These are crucial in modern construction, particularly in basements and other underground structures. Examples include silicone-based compounds and hydrophobic chemicals.

Glass fibres, polypropylene fibres, and steel fibres are also some examples of additives commonly used in modern mortars to increase tensile strength, reduce shrinkage, and prevent cracking. Fiber-reinforced mortars are particularly useful in applications requiring enhanced flexibility and resistance to stress [38]. In contemporary sustainable practices, natural fibres such as coconut, jute, or flax are being explored as eco-friendly alternatives to synthetic fibres [39].

Pigments, another example of additives are added to mortars for aesthetic purposes, allowing for the customization of colour in modern construction. These can be natural, such as iron oxides, or synthetic, and are used to create uniform colour in decorative or finishing mortars.

Hydrophobic additives such as silicon resins, are used to create water-repellent mortars, especially in regions prone to moisture and dampness. Hydrophobic additives reduce water absorption and increase the lifespan of the mortar by making it resistant to water ingress. In a research by Hossain et. Al. [40] , it was observed that water-repellent admixtures in mortars decreased the density of the mortars, greatly reduced the capillary water absorption, and improved resistance to salt crystallization, achieving full water repellence. Overall, the study highlights how these admixtures can enhance the durability and environmental resistance of rendering mortars.

Finally, water is used to put all the dry ingredients of the mortar together into a workable paste.

Chapter 3:

Lime mortar in built heritage conservation

Lime mortars have been used in construction since antiquity, with evidence of their use in ancient Egyptian, Greek, and Roman masonry. Their compatibility with existing structures, breathability, and flexibility make them ideal for repair work as compared to cement mortars due to the various problems it causes to historical masonry. They are primarily composed of lime (calcium hydroxide) as the binder. The type of lime used can be classified into two categories: hydraulic lime and non-hydraulic lime. Lime is one of the oldest binding elements used in construction, aside mud and clay. Prior to the advent of concrete, lime mortar was used to build some of the world's most famous monuments and buildings; today, it is mostly used to restore them [41].

The raw material for lime production is limestone, mainly made of calcium carbonate (CaCO_3). The limestone is then converted into lime through the processes of calcination, hydration and carbonation. These make up what is known as the “lime cycle” (Figure 5).

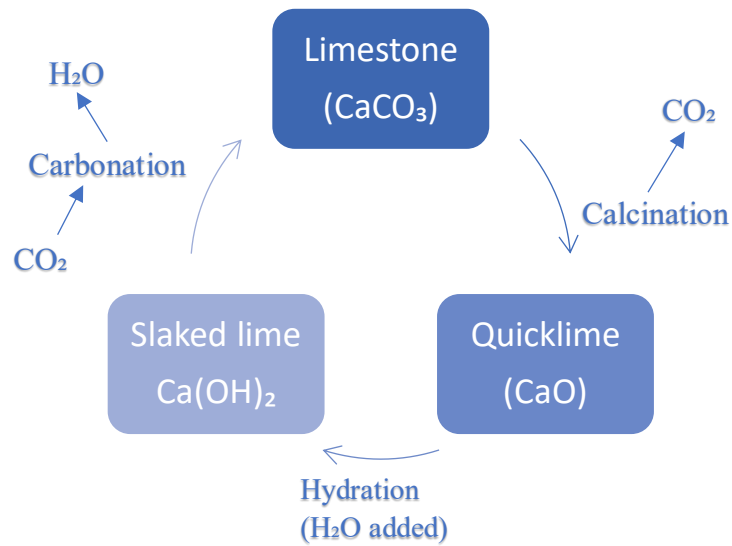
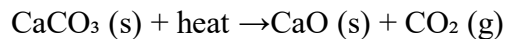


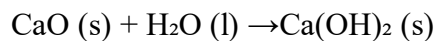
Figure 5: The lime cycle

Processes involved in the lime cycle;

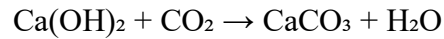
Calcination: a thermal decomposition process that involves heating limestone at high temperatures at approximately 900°C to produce quicklime (calcium oxide, CaO) and carbon dioxide (CO₂) in a specific kind of kiln [41]. This has a chemical reaction as



Hydration or slaking: the process of adding water to the quicklime to produce hydrated lime (calcium hydroxide, Ca(OH)₂). This process involves the exothermic reaction of quicklime with water thus releasing energy in the form of heat from the system. According to Hassibi, the process is known as hydration when the right amount of water is used to produce a dry powder, but is known as slaking when excess water is used to produce a pasty substance in this case [42]. This chemical reaction of this process is;



Carbonation: This is the reaction between the hydrated lime with carbon dioxide from the atmosphere to form calcium carbonate again after exposure to the atmosphere over a period of time. The reaction in this process is;



3.1 The use of lime mortars as repair mortars for built heritage conservation

Lime mortars are widely regarded as the most compatible materials for use in historical and archaeological masonry repair and conservation due to their chemical, physical, and mechanical properties closely aligning with those of the original mortars used in historic buildings, notwithstanding the challenges associated with lime mortars such as its longer setting time and low strength as compared to cement mortars [43].

These challenges, however, are less significant compared with those associated with the use of cement mortars due to: a) incompatibility with the old materials; b) high amount of soluble salts that may cause leaching and degrade the neighbouring ancient mortar through crystallization and/or hydration cycles [44]; c) higher compressive strength than that of the ancient material, and; d) lower vapour permeability which does not allow the material to breathe.

Lime-based mortars, on the other hand, have similar composition as that of most historical mortars which ensures a seamless integration and compatibility as it is recommended to utilize materials similar to the ancient materials in the design of repair mortars. Moreover, lime mortars are highly porous and “breathable”, which allows moisture to pass through the masonry preventing the

accumulation of moisture within the masonry framework; a very essential feature for the health of historic structures as it prevents moisture buildup within walls, which can lead to freeze-thaw damage, efflorescence, and biological development [45].

In addition, lime mortars are known to be less rigid than ordinary Portland cement mortars, providing flexibility that allows minor movements within the masonry unit to prevent cracks and structural damage, especially in ancient buildings [46]. Rigidity which refers to a material's resistance to bending under applied stress. A rigid material has a high modulus of elasticity [47], meaning it deforms very little when subjected to forces such as compression, tension, or shear. In the context of mortars, "rigidity" relates to how much a mortar can accommodate movements or stresses without deforming. That is, a rigid mortar, like one made with ordinary Portland cement (OPC), tends to be less capable of accommodating movements due to thermal expansion, settling, or external loads, and is more likely to crack under these conditions. This is because OPC mortars set and harden into a dense, inflexible matrix that resists deformation. On the other hand, lime mortars are less rigid, meaning they have a lower modulus of elasticity and can bend slightly under stress. This flexibility allows lime mortars to absorb and accommodate minor movements within the masonry structure, such as those caused by thermal expansion, moisture variations, or minor settlement. This flexibility helps prevent the formation of cracks, which is particularly beneficial in ancient buildings where maintaining structural integrity is important.

They are also chemically non-reactive with most historical masonry materials thus, reducing the possibility of the occurrence of chemical reactions that could cause decay. Unlike Portland cement, which can be extremely alkaline and aggressive, lime mortars have a positive interaction with traditional brickwork [46].

The above mentioned are some of the reasons why lime-based mortars are recommended for the repairs of historical structures coupled with issues of environmental concerns regarding their production and their relatively less expensive cost as a binder.

3.2.1 Case studies

As already mentioned, lime mortars have long been used in the restoration and conservation of historic buildings due to their compatibility with traditional materials and construction techniques. Their permeability, flexibility, and breathability make them ideal for preserving the structural integrity and authenticity of built heritage. Here are examples of notable case studies where lime mortars were successfully employed in built heritage conservation.

- Tower of London, UK

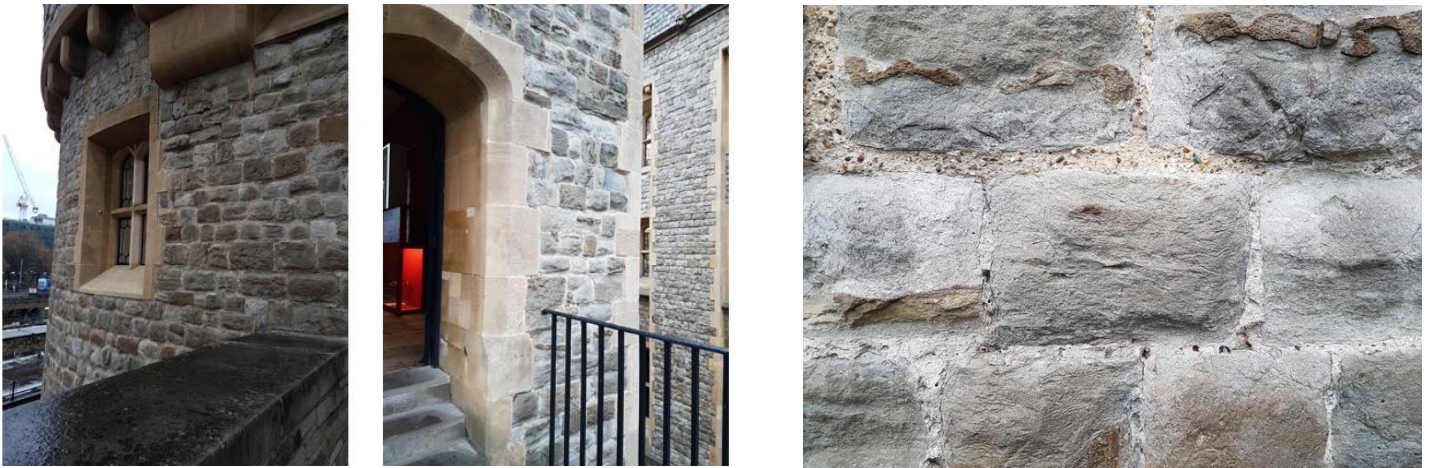


Figure 6: Repair mortars incorporating a blended coarse stuff lime putty mixture applied in the restoration of the bell tower at the Tower of London, UK. Retrieved from: <https://www.limestuff.co.uk/blog/tower-of-london>

The Tower of London, a UNESCO World Heritage site, underwent significant restoration using lime mortars to match the materials used in its original 11th-century construction. The restoration sought to ensure long-term durability while preserving historical integrity. Extensive testing led to

the development of a premixed hydraulic lime mortar that mimicked the historical material [48]. A hydraulic lime was chosen for its compatibility with the Tower's ancient stonework, offering breathability and flexibility that allowed moisture to escape and prevented structural damage. Eventually, the project successfully maintained the aesthetic and structural integrity of the Tower [49], preserving the historic landmark for future generations.

- The Colosseum, Rome, Italy



Figure 7: The restoration of the Colosseum's hypogea. Retrieved from <https://www.todsgroup.com/en/sustainability/colosseum-restoration-hypogea>

The Flavian's amphitheatre popularly known as the Colosseum, the monumental Roman amphitheatre, has undergone several restoration phases to repair damage caused by pollution, weathering, natural disasters, human activities and time. Central to these efforts has been the application of traditional lime mortars in the repair of its stone and brickwork, effectively

strengthening compromised sections while preserving the monument's historical integrity. This restoration according to Tod's [50], involved rebinding the travertine fragments with non-hydraulic lime mortar, injecting hydraulic lime mortar into areas of instability, and mechanically removing previous cement-based repairs that were deemed unsuitable. Additionally, lime-based mortar was employed for grouting cracks within the stone blocks. These interventions ensured material compatibility with the original Roman construction elements, including travertine and Roman concrete. The use of lime mortar also helped ensure compatibility with ancient Roman construction materials such as travertine and Roman concrete.

- The Alhambra, Granada, Spain

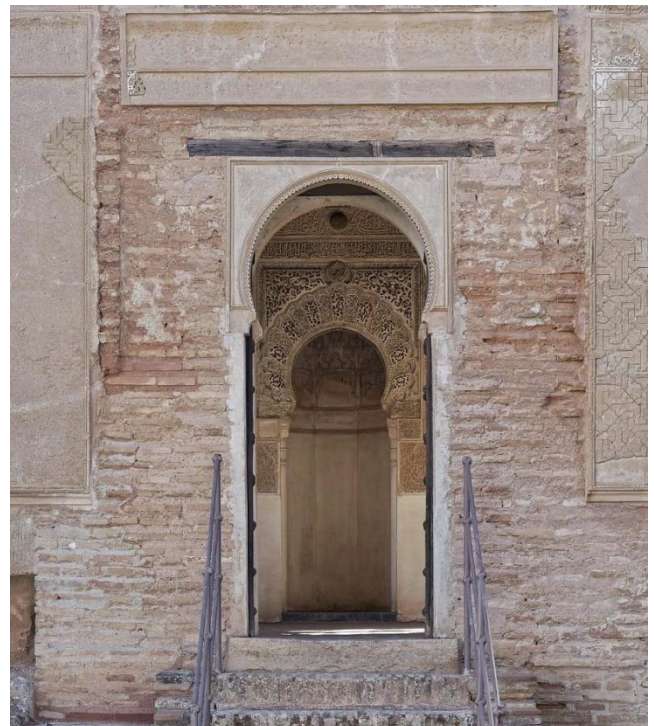


Figure 8: Repairs and restorations of the Oratory of the Partal Palace in The Alhambra, Spain. Retrieved from <https://www.europeanheritageawards.eu/winners/oratory-partial-palace-alhambra-spain/>

The Alhambra, a prime example of Nasrid architecture and one of the best-preserved Islamic palatine complexes from the medieval period, remains a significant heritage site in the Iberian Peninsula, constructed during the Islamic era (711–1492) [51]. Ongoing restoration initiatives have focused on safeguarding its intricate Islamic and mudéjar elements. A notable restoration was completed in 2017 on the Oratory of the Partal Palace, where lime mortars were employed to stabilize the original structure. Lime mortar stripes were applied along accessible edges to reinforce the brick wall fabric, while hydraulic mortar was injected into critical points prone to potential detachment [51].

These interventions were pivotal in preserving the monument's plaster and masonry, ensuring consistency with the materials used during the Nasrid period. This restoration effort earned the Grand Prix Europa Nostra in 2019, highlighting the effectiveness of traditional techniques, like lime mortar, in conserving the Alhambra's architectural legacy.

The case studies of the Tower of London, the Colosseum, and the Alhambra were selected for their representation of diverse lithologies. Each site uses different materials thus, the Tower of London features limestone and flint, the Colosseum includes travertine and Roman concrete, and the Alhambra is primarily constructed from bricks and plaster. The compatibility of lime mortars with these materials, especially in maintaining the original fabric and appearance, showcases lime's versatility in preserving a wide range of historical construction materials.

These case studies also illustrate how lime mortars perform under different environmental conditions. Such that, whereas The Tower of London faces heavy rainfall and humidity in a temperate maritime climate, requiring breathable mortars to prevent moisture damage, the Colosseum endures high levels of pollution, weathering, and seismic activity, necessitating lime mortars for flexibility and environmental resistance. The Alhambra on the other hand, in a semi-

arid Mediterranean climate, benefits from the ability of lime mortars to manage moisture fluctuations and protect delicate architectural details. These examples highlight the ability of lime mortars in adapting to different climatic challenges.

Lastly, the time periods represented by these monuments further emphasize lime mortars' enduring importance. The Tower of London from the 11th century, the Colosseum from the 1st century AD, and the Alhambra from the medieval Islamic era all demonstrate how lime mortars have been consistently used over centuries. The continued application of lime mortars in modern conservation underscores their historical relevance and effectiveness in preserving architectural heritage from different eras.

Thus, lime mortars play a crucial role in the restoration and conservation of historic buildings. The case studies of the Tower of London, the Colosseum, and the Alhambra are but a few cases of the restoration of heritage structures with lime-based mortars. Their compatibility with traditional building materials like stones and bricks makes them ideal for maintaining the original character of historic buildings. Such that the lime mortars allow moisture to move through the structure, helping to prevent damage while still providing support. By using lime mortars, conservators ensure that repairs are compatible with the original construction methods and materials, preserving both the structural integrity and historical significance of these sites.

3.2 Repair mortars

Repair mortars are a type of mortar designed specifically for the preservation and restoration of historical masonry, intended to match the physical and chemical features of the original mortar used in ancient buildings while ensuring compatibility and long-term durability. The major purpose of the repair mortar thus is to preserve the masonry's structural integrity and aesthetic look while

acknowledging its historical and architectural significance. In designing a repair mortar, one must take into account its purpose such as bedding, pointing, grout, render, plaster, flooring, and surface repairs as well as the environmental exposure and the role the mortar plays in the masonry unit it is found within [52].

In addition, during the design of a repair mortar, according to RILEM TC 203 [52], the compatibility of the substrate and the repair mortar must be met in order to ensure that other requirements such as durability, structural and environmental requirements are met while taking into account the properties of the substrate as well. This indicates how important it is for a repair mortar to be compatible with the historical material on which it is applied.

Chapter 4:

Ground olive stones

The use of agricultural by-products in the construction industry has recently gained attention due to their sustainability and cost-effectiveness [53]. Ground olive stones (GOS), a byproduct of the olive oil extraction, have shown potential as an additive or a partial replacement for traditional ingredients in mortar mixtures. However, they account for a significant amount of solid waste with millions of tons of olive stones produced annually around the world, primarily in Mediterranean regions where olive oil production is concentrated [54], whose disposal causes a major environmental concern. However it is currently being used in biofuel production due to its high calorific value which is around $17,000 \text{ kJ kg}^{-1}$, and is being explored for use in water treatment and in the construction industry [55].



Figure 9: Left- Unmilled olive stones, Right- Ground olive stone (100-300microns). Retrieved from: www.bio-powder.com/en/olive-pit/

Agricultural or industrial wastes are incorporated into mortar mixes either in their raw state or activated through calcination. According to a review by S. Blesson and A. U. Rao, calcined wastes

have higher reactivity than uncalcined wastes, enabling early strength development of the binder system [56]. Their research also indicates that agro-based wastes contain a high concentration of silica, which makes them exhibit pozzolanic reactivity.

4.1 Properties of Ground olive tree stones added to mortars

Utilizing agricultural and industrial by-products such as GOS in mortar mixes is a type of green construction practice that addresses the issue of waste disposal, while minimizing the use of natural resources such as aggregates in construction and cutting down production cost as well.

However, before incorporating non-traditional materials or substituting part of the traditional composition of mortars such as binder or aggregates with other materials such as agricultural wastes in mortars, the material must have certain characteristics similar to those of the traditional construction material so as to enable the replacement without compromising the integrity of the mortar as well.

Ground olive stone (GOS), is a lignocellulosic substance with cellulose, hemicellulose, and lignin as its main component, offers several benefits, such as affordability and availability, low density, renewable nature, lack of related health risks, but with a problem of high moisture absorption [57]. It is the solid residue generated after olive oil extraction. In this thesis, the GOS is used to partially substitute the natural quartz aggregates in varying portions in the synthesis of a repair mortar.

A mineralogical compositional analysis by [58] indicates that olive stone ash mostly consist of silicon oxide SiO_2 and calcite $CaCO_3$ as their inorganic components. An energy dispersive X-ray analysis by [59] also reveals Silicon and Calcium as the major chemical composition in olive stone

waste with other elements found in lesser proportions. The presence of Silicon in olive stones is also confirmed in a research by [60].

The effect of ground olive stones on the mechanical characteristics of mortars has been the subject of a number of investigations. One important finding has been that adding olive stones usually results in a lower mortar density and improve thermal insulation [61], but potentially compromise its compressive strength. Ferreiro et al. [62], for example, found that the amount of GOS used to substitute fine crushed limestone aggregates decreased the mechanical properties of the cement mortar as the proportion of GOS increased. Nevertheless, they also pointed out an appropriate application range of 0–30% where the decrease in the strength of the mortar is not very significant and is acceptable for application [62]. This is also confirmed in a research by Cheboub et al. [63] where it was discovered that replacing natural sand with crushed olive kernel aggregates (COK) in a self-compacting lightweight mortar decreased the tensile and compressive strengths, but within the acceptable range limits as stated in the RILEM guidelines for lightweight building.

Although increasing the amount of GOS in a mortar mixture decreases certain properties like workability and setting time, the mechanical strength of the mortar increases with an increase in GOS content up to a certain limit as a partial replacement of sand as reported by Abdulwahid & Al-Akhras [64].

Ground olive stones (GOS) have evidently attracted significant interest as a sustainable material in the construction industry, particularly in cement-based mortars. However, there is a significant gap in research regarding their use in lime-based mortars, which are essential for conservation purposes. This thesis research therefore aims to address this gap by exploring the potential and implications of incorporating GOS in lime-based mortars as partial replacement of quartz sand aggregates for the conservation of built heritage.

Chapter 5:

Materials and Methods

This research investigates the utilization of agricultural and industrial waste, specifically ground olive stones (GOS), in the development of repair mortars for conservation purposes. The primary objective is to replace a portion of the natural aggregates with GOS to produce a lightweight repair mortar, while promoting sustainability without compromising the structural integrity of historical materials. Lightweight concrete is generally defined as any type of concrete with an oven-dry density below 2000 kg/m^3 [65]. Lower density is beneficial for conservation projects, particularly in historical structures, where reducing the overall weight of repairs can prevent further strain or damage to aged or fragile heritage materials. Lightweight mortars can also be advantageous for specific restoration applications where weight considerations are critical, such as repairing weak or delicate sections of walls or structures that cannot support heavy materials.

GOS in this case, was used to partially replace quartz aggregates to produce a lighter mortar due to its lower density compared to traditional rock mineral aggregates. Several studies on organic waste materials, including GOS, have demonstrated their ability to lower the density of mortars while maintaining acceptable performance. So the porous, fibrous nature of GOS may reduce the overall density of the mortar mixture, and make it less heavier, a characteristic particularly advantageous in works where lighter mortars can minimize additional stress on aged structures.

Studies involving other agricultural by-products like rice husk ash, palm oil clinker, and sawdust as organic aggregates substitute have shown that replacing traditional aggregates with organic materials can reduce the weight of mortar [62], [66], [67]. These studies demonstrated that the

reduction in density is achievable because the organic materials generally have lower densities than natural mineral aggregates. Though fewer studies have been conducted specifically on GOS, research has indicated that organic waste materials from agriculture contribute to lighter cementitious composites due to their lower bulk densities and porous structures. Since GOS are organic, low-density materials, when used as a partial replacement for natural rock or rock mineral aggregates in mortars, can significantly reduce the overall density of the mixture. Investigations into GOS in concrete and mortar formulations have shown that they lead to lower density and improved sustainability by replacing part of the natural aggregates.

To this end, seven different mortar mixtures were prepared. One mixture, devoid of GOS, serves as the control sample. The remaining six mixtures incorporate varying proportions of GOS, substituting 5% to 15% of the total volume of natural aggregate used, with a binder-to-aggregate ratio of 1:3.

The properties of the GOS mortars are enhanced by mixing with a suspension of nano silica; Nanoestel to improve their bonding and mechanical properties. Studies have shown that nano-silica can significantly improve the properties of cementitious materials due to its high surface area [68], and reactivity [69], which contribute to a denser microstructure and better bonding at the micro-level. Nano-silica has high pozzolanic reactivity such that when added to a mortar, it reacts with the calcium hydroxide ($\text{Ca}(\text{OH})_2$) produced during lime hydration to form additional calcium silicate hydrate (C-S-H), which is the key binding phase in cementitious materials. This reaction helps to fill in voids and improve the overall density and bonding of the mortar, helping to mitigate potential weaknesses that could arise from the inclusion of GOS

In addition, nano-silica particles which are extremely fine, with a size typically less than 100 nm help to fill in the tiny pores in the mortar matrix, leading to a denser and more cohesive material.

The finer microstructure enhances the interfacial transition zone (ITZ) between the aggregate and the binder, leading to improved bonding [70], [71]. This is particularly beneficial when using alternative aggregates like GOS, where bonding might otherwise be weaker due to differences in surface texture and composition compared to natural aggregates. Numerous studies have also demonstrated that the addition of nano-silica can increase the compressive and tensile strength of mortars due to the improved microstructure and better bonding within the matrix.

The mortar mixtures were prepared using distilled water and tested for consistency with the flow table method. Subsequently, the mixtures were moulded into cubic specimens (5cm x 5cm x 5cm), (5cm x 5cm x 2cm) and prism specimens (4cm x 4cm x 16cm). The samples were then cured, demoulded, and allowed to set for 28 days and 90 days, respectively.

The hardened cubic samples were subjected to tests for salt crystallization, colorimetry, and water absorption by capillarity. Additionally, the prism specimens underwent mechanical strength assessments, including flexural and compressive strength tests. Detailed methodologies and results are discussed in the subsequent sections of this thesis.

5.1 Materials used in the mortar preparation

This section presents the characterization of the materials used in the production of the mortar mixes that were studied experimentally.

5.1.1 Binder

The binder used in this study was a hydrated lime Calce Idrata Speciale CL70-S provided by Unicalce S.p.A., located in Lecco, Italy being a product available on the national market and sold

in paper bags. The physical and chemical composition of the binder as specified in the technical sheet is indicated in Table 1.

Table 1: Physical and chemical composition of the hydrated lime

Description	Fine solid powder
Colour	White
Odour	None
Total CaO + MgO	> 85.0%
MgO	< 2.0%
Residual CO ₂	≤ 12.0%
Sulphates (SO ₄ ²⁻)	< 0.1%
Free Lime (CaO)	72.0 - 84.0%
Bulk Density (kg/m ³)	400-500
Solubility in water (Ca(OH) ₂) (g/l)	1.7
pH of Saturated Solution	12.5
Moisture Content	< 1.0%
Residue on 0.200 mm Sieve	≤ 2.0%
Residue on 0.090 mm Sieve	≤ 7.0%
Penetration (mm)	28-30

5.1.2 Quartz sand aggregates

The natural sand aggregates utilized in this study consist of a quartz sand aggregate, supplied by CTS s.r.l., based in Altavilla Vicentina, Italy. This product, widely available in the Italian national market, commercially distributed in plastic containers possesses an average grain diameter size of 0.1 to 0.3 mm. According to the technical documentation provided by the supplier, the quartzite is devoid of organic matter, vegetative components, clay, and any friable materials. Furthermore, the

petrographic analysis revealed an absence of impurities such as gypsum, anhydrite, amorphous silica, and mica. Table 2 presents the detailed chemical and physical characteristics of the quartzite as outlined in the technical sheet.

Table 2: Chemical and physical characteristics of quartzite

Chemical Composition	(w/t%)	Physical Characteristics	
SiO ₂ (Silicon Dioxide)	99.500	Colour	Whitish
Al ₂ O ₃ (Aluminium Oxide)	0.1200	Origin	Natural
Fe ₂ O ₃ (Iron Oxide)	0.017	Grain	Rounded
TiO ₂ (Titanium Dioxide)	0.028	Absolute density (g/cm ³)	2.65
CaO (Calcium Oxide)	0.23	Apparent density (g/cm ³)	1.50

5.1.3 Ground Olive Stones (GOS)

The GOS was supplied by BioPowder.com based in Spain and is available and is sold in plastic containers with grain sizes within 0.1 to 0.3mm.

5.1.4 Nano Estel

In order to enhance the properties of the GOS used in the mixture, Nano Estel was used. The Nano Estel is a colloidal aqueous dispersion of nano-sized silica with consolidating and stabilizing properties, suitable for application on natural stones, bricks, terracotta, mortars, and plasters [72]. This refers to a stable mixture where tiny silica particles, on the nanometre (nm) scale (typically less than 100 nm), are evenly distributed or suspended in water, such that the particles are small enough to remain suspended and dispersed, forming a colloid. Nano silica is normally used as a consolidant to effectively strengthen deteriorated porous materials like stone, brick, terracotta and

mortars. Their nano dimension allows them to penetrate into microscopic pores and structures. As they aggregate, they bond with the material, filling in these voids and increasing the overall strength and durability of the material, making them useful for applications such as materials consolidation [73].

The commercial Nano Estel used in this research was provided by CTS s.r.l. in Altavilla Vicentina, Italy. It is an inorganic consolidant which consists of an aqueous colloidal suspension of silica nanoparticles, with an average size of about 20 nm, a silica content of 30% by weight and an alkaline pH (approximately 10). Table 3 displays the consolidant's chemical and physical characteristics as listed on the technical sheet.

It was applied diluted with distilled water in the ratio of distilled water to Nano Estel (2:1) dilution. The diluted Nano Estel was subsequently incorporated into the GOS at a ratio of 0.35 relative to the quantity of GOS.

Table 3: Chemical-physical characteristics of Nano Estel

Description	Aqueous suspension of silica nanoparticles
Appearance	Colourless liquid
Active matter content (w/t%)	30
Particle size (nm)	<20
Density (g/cm ³ , at 20 °C)	1.2
Viscosity (mPa·s, at 20 °C)	6.0
pH	10 approx.

5.1.5 Water

Distilled water was used throughout the experiment to eliminate impurities, minerals, and contaminants that could affect the results. It ensures consistency and control in experimental conditions, preventing unwanted chemical reactions and allows to isolate the effects of the variables being tested. In this research, distilled water was used to prepare mortar mixtures to accurately assess the properties and reactions of ground olive stones (GOS) and other components without interference from impurities.

5.2 Methodologies in the preparation of test specimens

5.2.1 Mortar production

The first step in the preparation of mortars is the weighing of its constituents using a scale with 0.01g of precision. Seven different mixtures are prepared with varying percentages of GOS ranging from (0 – 15%) of the total volume of aggregates used. Each mixture is identified by the amount of GOS it contains. Hence the following mortar mixtures are eventually made;

- TQ-HL : 100% quartz aggregates
- POS5-HL : 95% of quartz aggregates, 5% of GOS
- POS10-HL: 90% of quartz aggregates, 10% of GOS
- POS15-HL: 85% of quartz aggregates, 15% of GOS
- POS5-HL-S: 95% of quartz aggregates, 5% of GOS + Nano silica
- POS10-HL-S: 90% of quartz aggregates, 10% of GOS + Nano silica
- POS15-HL-S: 85% of quartz aggregates, 5% of GOS + Nano silica

Each mixture is prepared by initially weighing all dry components; aggregates, hydrated lime (binder), and GOS. The dry materials are manually mixed together in a bowl by hand, and water is added until the desired consistency is achieved. The quantity of binder was kept constant across all mixtures to maintain consistency. The quantity of GOS however, is inversely proportional to the volume of the aggregates such that, as the GOS content increases, the amount of aggregate decreases. In the mixtures containing diluted nano silica, the diluted nano silica is 0.35 of the amount of GOS used. The reference mortar specimen (TQ-HL) is made without GOS, and is tested for consistency with the Flow Table method according SIST EN 1015-3:2001 [74]. The rest of the specimen are made with varying proportions of GOS and tested for consistency aimed at achieving that of the reference specimen. Thus, Table 4 indicates the proportion of materials used in preparing the mortar samples.

Mortar Composition (g)

Table 4: Type and quantity of materials (g) used to manufacture of mortar mix

Specimen	Quartz sand	Hydrated lime	Water	Water to Binder ratio	GOS	Diluted Nano silica (ml)
<i>TQ-HL</i>	718.50	85.20	149.10	1.75	0	0
<i>POS5-HL</i>	680.96	85.20	188.29	2.21	13.31	0
<i>POS10-HL</i>	645.12	85.20	193.40	2.27	26.62	0
<i>POS15-HL</i>	609.28	85.20	195.96	2.30	39.94	0
<i>POS5-HL-S</i>	680.96	85.20	159.30	1.88	13.31	4.50
<i>POS10-HL-S</i>	645.12	85.20	159.30	1.88	26.62	9.45
<i>POS15-HL-S</i>	609.28	85.20	159.30	1.88	39.94	14

5.2.2 Testing Consistency of Wet Mortar Mixture

The wet mortar mixtures are subjected to the Flow table test, to determine the workability and consistence of the freshly mixed mortar according to the SIST EN 1015-3:2001 standard before being moulded. The principle behind the flow table test is to measure the workability or fluidity of freshly mixed concrete by observing its ability to spread. This is achieved by allowing the sample of mortar to flow freely when the confining truncated conical mould is removed, followed by subjecting the flow table to a series of controlled jolts; 15 times in this case. This procedure is repeated three times for each mortar mixture. The degree of spread, or flow, is measured after each trial, and the average spread is calculated to provide a quantitative measure of the mortar's consistency. The reference mortar specimen, designated as TQ-HL, is prepared without the addition of GOS and serves as a reference for the consistency test such that the other specimens with varying proportions of GOS are prepared and subjected to the same consistency test, with the objective of achieving a consistency similar to that of the reference specimen.

5.2.3 Moulding and Demoulding Mortars

After testing the consistency of the mortars, the mixtures were moulded into wooden moulds of various dimensions for specific tests to evaluate their properties. The dimensions used were; 5cm x 5cm x 5cm moulds for water absorption by capillarity test, 5cm x 5cm x 2cm moulds for salt crystallization and colourimetry tests, and 4cm x 4cm x 16cm moulds for mechanical tests (flexural strength and compressive strength).

For each of the seven mortar mixtures, three samples were prepared in each of these dimensions, resulting in a total of nine samples per mortar mixture. Consequently, a total of 63 samples were produced.

After filling the moulds with the fresh mortar, the mixtures were compacted and levelled off with a trowel for a smooth and even surface as seen in Figure 10. The samples were then left uncovered in the laboratory to set for about 7 days. The samples were later carefully demoulded and labelled for identification.

The time interval from demoulding to the commencement of testing varied depending on the specimen type, thus, 28 days for the cubic specimens and 90 days for the prism specimens.

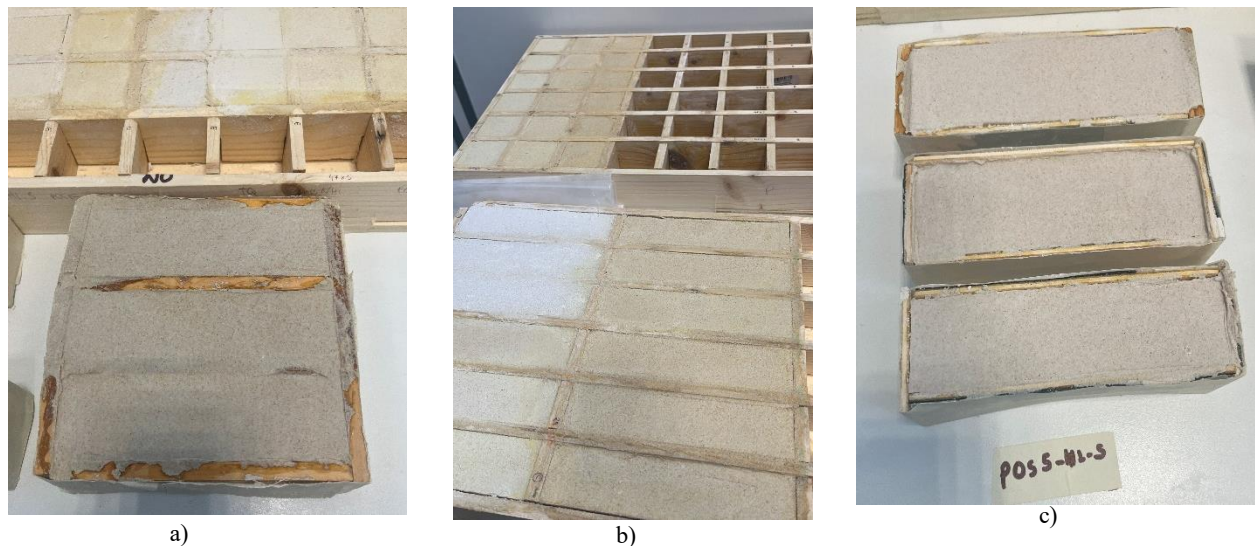


Figure 10: Curing of mortar samples - (a) – wet mortar mixture in a prism mould, (b) – dried mortar samples in cube and prism moulds, (c) – labelled wet mortar in prism moulds

5.3 Characterization of mortars in the hardened state

5.3.1 Colorimetry assessment

After hardening for 28 days, the cubic specimens (5cm x 5cm x 2cm) were tested for colorimetric assessment according to UNI EN 15886:2010 [75]. This test provides an objective and quantifiable measure of colour by detecting any changes in their appearance over time. “The method involves

determining the colour of a surface through instrumental quantification, expressing the colour numerically according to international standards set by the International Commission on Illumination (CIE). The colours are represented within a "colour space," where any visible colour is defined by three coordinates" - [75].

The colour measurements were conducted using a PCE-CSM 7 portable colorimeter. For each sample, data were collected from five distinct points: the top left corner, the top right corner, the bottom left corner, the bottom right corner, and the centre. The average values of the L*, a*, and b* coordinates were then calculated from these five points to evaluate the colour change in the samples with varying concentrations of GOS. The total colour difference (ΔE) of the specimens in the CIELAB colour space was evaluated by $\Delta E = \sqrt{(\Delta L^2 + \Delta a^2 + \Delta b^2)}$.

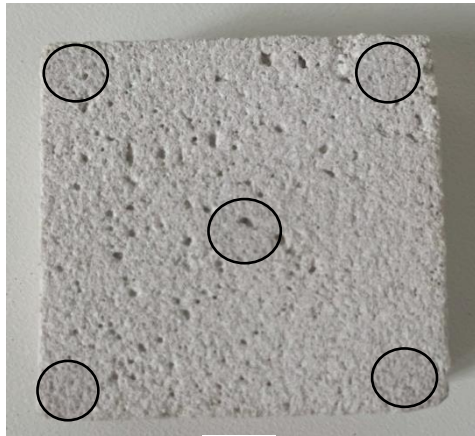
In the CIE colour space, the L* value represents the lightness component, ranging from 0 (black) to 100 (white). The a* value denotes the red-green axis, where positive values indicate a shift towards red and negative values indicate a shift towards green. The b* value represents the yellow-blue axis, with positive values indicating a shift towards yellow and negative values indicating a shift towards blue.



a)



b)



c)

Figure 11: Colorimetry assessment – (a) and (b) – Researcher taking colorimetric measurements, (c) – a sample with indications on where measurements were taken

In this study, the colorimetric assessment was conducted to provide an objective and quantifiable measure of colour stability in the specimens over time. This test is essential for evaluating the impact of the varying concentrations of GOS on the colour properties of the mortars after the hardening. The test was aimed at detecting any potential changes in appearance, which is critical for assessing the aesthetic durability and performance of the mortar. The use of a portable colorimeter and the subsequent analysis of the L^* , a^* , and b^* coordinates from multiple points on the surface enabled a reliable monitoring of colour variations to ensure that any deviations in colour due to the addition of GOS are captured.

5.3.2 Salt crystallization tests

After drying and hardening for 28 days, the cubic specimen (5cm x 5cm x 2cm) were subjected to salt crystallization test according to the SIST EN 12370:2000 [76] standard and modified in accordance with the recommendations of RILEM TC 271-ASC [77], aiming to simulate real-world conditions that may not be fully covered by one standard alone.

In this modified test, the SIST EN 12370:2000 standard, which prescribes full immersion of samples in a salt solution and drying at 105°C, was adapted based on RILEM TC 271-ASC recommendations to better simulate real-world conditions. The RILEM guidelines suggest partial immersion, at approximately 10% of the sample's length submerged allowing the solution to move upward through capillary action, closely mirroring how salt-laden moisture rises gradually from the ground in natural environments. Furthermore, RILEM specifies a lower drying temperature of 45°C, more representative of ambient conditions, to avoid potential sample alterations that could result from higher drying temperatures.

These modifications yield a testing method that more accurately reflects the environmental challenges the material will face over time, providing a nuanced and practical understanding of its durability, particularly for applications in heritage conservation. By doing so, the testing process is tailored to reflect the environmental conditions that the material is expected to face in actual use, such as the temperature conditions and the salt accumulation processes.

The salt crystallization test was conducted to evaluate the resistance of the specimens to salt-induced weathering, a critical factor in determining the long-term durability of materials used in conservation and restoration. In particular, salt crystallization can lead to internal stresses due to

the formation and growth of salt crystals within the pores of the material, which may result in micro-cracks, granular disintegration, and eventual structural deterioration.

Soluble salts significantly impact the durability of porous building materials used to build much of the world's architectural heritage, in as much as they are made from porous materials like stones and mortars as well as bricks and ceramics which are vulnerable to salt damage [78]. Therefore, it becomes crucial to understand how salts crystallize and damage these materials to predict and enhance their durability.

Understanding how the specimens in this case withstand this form of weathering is essential for predicting their performance in real-world conditions, especially in environments subject to saline exposure. This is because it provides insights into the mortars' behaviour and resilience when exposed to environmental conditions similar to those in real-world settings. Thus, in many historical buildings and structures, particularly those located in coastal areas, urban environments, or regions with fluctuating moisture levels, materials are frequently exposed to saline solutions.

The saline solutions involved in the degradation of historical buildings includes a variety of sulphates, chlorides, and nitrates, each stemming from different sources and exerting unique impacts on the structural materials. Sodium chloride (NaCl), commonly sourced from marine environments is highly soluble and can cause efflorescence [79]. Magnesium sulphate ($MgSO_4$), often found in groundwater, forms crystals of ettringite and gypsum that may exert crystallization pressures within the pores of stone and mortar, causing cracking, softening and degradation [80] and spalling.

Spalling happens due to the growth in volume of expansive salts accumulating close to the masonry surface, which creates pressure from compression, ultimately causing the material to break apart

[81]. Gypsum crystals ($CaSO_4 + 2H_2O$) mostly found in black sulphated crust, can form on calcium carbonate surfaces through the “sulphation” reaction between sulfuric acid from SO_2 atmospheric pollution and calcareous materials like limestone, marble and mortars. The formation of gypsum within the mortar can result in swelling and ultimately lead to the development of cracks and fissures. Under specific conditions, the pressure exerted during this process can become sufficient to cause blistering or spalling of the adjacent brick or stone materials [81] .

Some of the mechanism by which soluble salts damage historical buildings is through the processes of crystallization and hydration. Thus, salts dissolved in water can penetrate porous building materials such as stone, brick, plaster, and mortar. When water evaporates, due to strong insolation depending on the material porosity , salts may crystallize within the pores or at the surface of the building. Depending on the rate of the evaporation, two phenomenon are likely to occur: efflorescence and subflorescence.

Efflorescence occurs when water containing dissolved salts migrates to the surface of a porous material. This migration is driven by capillary action, where the water moves through the micro-pores of the material. So, as the water reaches the surface and encounters the air, it evaporates due to environmental conditions such as sunlight or wind. The salts dissolved in the water are left behind and crystallize on the surface, forming white, powdery deposits. While efflorescence is primarily an aesthetic issue, it is a visible sign that salts and moisture are actively moving within the structure [82].

Subflorescence, on the other hand, is a more destructive phenomenon compared to the phenomenon of efflorescence, as it occurs below the surface of the material. In this process, the saline solution travels less far through the capillary pores before the water begins to evaporate. This early evaporation happens below the surface, leading to the crystallization of salts within the

pores. Unlike efflorescence, subflorescence is not visible on the surface; however, the salt crystals exert crystallization pressures within the confined spaces of the material's pores causing higher damage to the material [83]. This pressure can, in fact, disrupt the internal structure of the material, leading to spalling, micro-cracking, and eventual disintegration. The concealed nature of subflorescence makes it particularly insidious, as significant damage can occur before any external signs are evident.

Moreover, some salts are hygroscopic, which means they can absorb and retain water from the surrounding environmental humidity. This ability causes cycles of dissolution and crystallization that repeatedly imposes stress on the material's microstructure. Over time, these cycles can significantly weaken the structural integrity of the material, making it susceptible to further damage from other environmental factors like frost action.

Hence, if the material has poor resistance to salt crystallization, it can lead to a range of destructive effects such as micro-cracking, granular disintegration, and surface scaling. Over time, these decay can accumulate and result in significant structural damage or even loss of material. Therefore, by assessing how well the specimens resist salt crystallization, the research can predict how the repair mortar will perform in such environments. This knowledge is critical for choosing materials that will endure in conservation efforts, ensuring the preservation of the structure while minimizing the need for frequent repairs or replacements.

The specimens were initially dried and weighed until a constant mass was achieved. To ensure a constant mass, the samples were first measured and then subjected to drying in an oven at a temperature of $(105 \pm 5) ^\circ\text{C}$ for 24 hours. Following this, they were cooled in a desiccator for approximately 20 minutes before being weighed again. This cycle of drying, cooling, and weighing was repeated three times (24 hours each cycle) until a constant mass was obtained.

The criterion for achieving a constant mass was determined by calculating the difference between the mass after cooling and the initial mass prior to heating. The procedure was continued until the difference between two consecutive mass measurements, taken at an interval of 24 ± 2 hours, did not exceed 0.1% of the initial measurement. Table 5 indicates the mass of the samples measured until a constant was achieved; IM: Initial measurements, M1: Measurement after 24 hours, M2: Measurement after 48 hours, M3: Measurement after 72 hours.

Table 5: Mass (g) of specimen until a constant mass (not greater than 0.01% of the initial mass)

Specimen	(IM)	(M1)	(M2)	(M3)	0.1% of the I.M	Difference b/n IM & M1	Difference b/n M1 & M2	Difference b/n M2 & M3 (Constant mass)
TQ-HL-1	87.43	87.29	87.28	87.27	0.09	0.14	0.01	0.01
TQ-HL-2	84.12	84	83.98	83.98	0.08	0.12	0.02	0
TG-HL-3	89.79	89.67	89.66	89.66	0.09	0.12	0.01	0
POS5-HL-1	84.66	84.38	84.39	84.37	0.08	0.28	-0.01	0.02
POS5-HL-2	80.26	79.97	79.93	79.95	0.08	0.29	0.04	-0.02
POS5-HL-3	78.59	78.32	78.29	78.32	0.08	0.27	0.03	-0.03
POS10-HL-1	76.61	76.17	76.16	76.17	0.08	0.44	0.01	-0.01
POS10-HL-2	78.58	78.15	78.12	78.14	0.08	0.43	0.03	-0.02
POS10-HL-3	83.67	83.19	83.14	83.17	0.08	0.48	0.05	-0.03
POS15-HL-1	69.88	69.33	69.29	69.27	0.07	0.55	0.04	0.02
POS15-HL-2	73.77	73.16	73.14	73.13	0.07	0.61	0.02	0.01
POS15-HL-3	74.03	74.45	73.39	73.37	0.07	-0.42	1.06	0.02
POS5-HL-S-1	88.44	88.11	88.08	88.08	0.09	0.33	0.03	0
POS5-HL-S-2	88.51	88.15	88.13	88.11	0.09	0.36	0.02	0.02
POS5-HL-S-3	89.88	89.46	89.45	89.43	0.09	0.42	0.01	0.02
POS10-HL-S-1	82.37	81.79	81.6	81.47	0.10	0.60	0.20	0.10
POS10-HL-S-2	87.38	86.8	86.64	86.62	0.09	0.58	0.16	0.02
POS10-HL-S-3	83.43	82.85	82.77	82.71	0.08	0.58	0.08	0.06
POS15-HL-S-1	79.1	78.36	78.33	78.31	0.08	0.74	0.03	0.02
POS15-HL-S-2	66.49	65.78	65.72	65.7	0.07	0.71	0.06	0.02
POS15-HL-S-3	75.13	74.39	74.37	74.34	0.08	0.74	0.02	0.03

After drying to a constant mass, the samples were measured again before the start of the first cycle. A sodium sulphate solution (Na_2SO_4) was prepared by dissolving 84 grams of sodium sulphate in 516 millilitres of distilled water, mixing it with a magnetic stirrer until all the salt was completely dissolved. The solution was then placed in a water bath to maintain the temperature at $(20 \pm 0.5)^\circ\text{C}$.

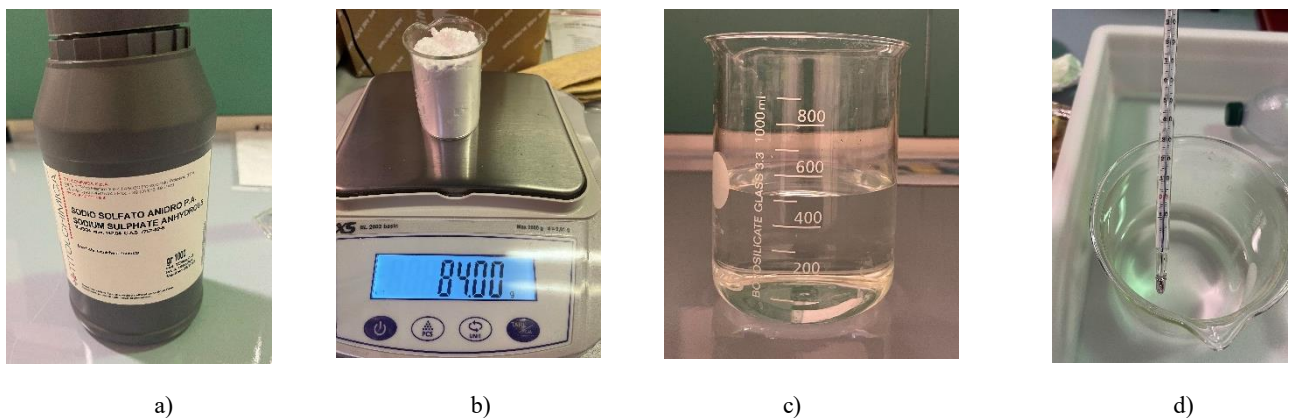


Figure 12: Preparation of a solution of sodium sulphate – (a) - Sodium Sulphate (Na_2SO_4), (b) – 84 grams of Na_2SO_4 , (c) – 516 ml of distilled water, (d) – Solution of Na_2SO_4 in a water bath

The dried samples were then carefully placed in a plastic container positioned within a water bath to maintain the solution's temperature at $(20 \pm 0.5)^\circ\text{C}$. The solution was carefully poured into the container until it covered approximately 10% of the height of the samples from the bottom. This was done to ensure contamination by capillary absorption of the salt solution from the bottom surface, following the recommendations of RILEM TC 271-ASC. The container was then covered to minimize evaporation, and the specimens were left to soak for 2 hours.



Figure 13: Representation of how the specimen were contaminated with the sodium sulphate solution while maintaining the temperature of the solution in a water bath

After soaking for 2 hours, the specimens were removed and then dried in an oven at 45°C for 8 hours. Subsequently, they were allowed to cool to room temperature for 12 hours, after which they were weighed and photographed. A new solution was prepared, and the cycle was repeated 15 times, except for specimens that broke before the fifteenth cycle. The results, which is the relative mass difference ΔM (mass loss or gain) are expressed as a percentage of the initial dry mass M_d and the number of cycles required to induce failure in cases where the specimen has disintegrated or has broken into two or more pieces before the final drying, in the equation $\Delta M = \frac{M_f - M_d}{M_d} \times 100$. Where M_f is mass of the dried specimen in grams, after the 15th cycle, or the number of cycles required to induce failure in cases where the specimen has broken into two or more pieces before the final drying, and M_d is the mass of the dried specimen with label before first cycle, in grams.



Figure 14: Drying of the specimens after immersion

5.3.3 Water absorption by capillarity test

An assessment of the durability and performance of the mortar specimen in conditions where it may be exposed to moisture was done by determining their water absorption by capillarity according to UNI EN 15801:2010 [84]. This test was performed on the cubic specimen with dimensions (5cm x 5cm x 5cm) in the Diagnostics and Conservation of cultural heritage laboratory at the Department of Biology, Ecology, and Earth Sciences, University of Calabria. The test was done to understand the permeability and porosity of the repair mortar, which are critical factors in determining its performance, particularly in environments exposed to water or high humidity.

The test procedure involves drying the samples to a constant mass, weighing them, and then placing them on a saturated layer of absorbent paper about 1cm thickness, which is positioned at the bottom of a container filled with distilled water. The samples are periodically weighed after specific intervals to measure the amount of water absorbed by capillary action. The absorption is calculated as a function of the increase in mass over time, allowing for the determination of the

capillary absorption coefficient, which reflects the mortar's permeability and porosity with the equation.

In this research, the samples were first dried to a constant mass in an oven at a temperature of 60 ± 2 °C until their mass change was less than 0.1% after two successive measurements in 24 hours to ensure that the test starts with a completely dry sample. Once the samples were dried and cooled to room temperature in a desiccator, they were weighed to determine the mass of the dried specimen, which is the initial mass (m_0) of the samples. The dried samples were then placed on a saturated layer of absorbent paper about 1 ± 0.5 cm thick, which was placed at the bottom of a flat bottomed container filled with distilled water.



Figure 15: Set up for water absorption by capillarity test

The samples were left in this position and later weighed after 10, 20, 30 and 60 minutes and after 4, 6, 24, 48, 72, 96, 128, 152 and 176 hours. After the immersion time has elapsed, the samples were removed from the saturated layer of paper, surface water was then removed using a damp cloth, and the samples were weighed immediately. This is the wet mass (M_i) of the sample. The amount of water absorbed by the specimen through capillary action, calculated by the difference between the wet mass at time (t_i) and the initial dry mass of the sample (m_0) as a function of time in relation to the samples' surface area in contact with the water was expressed as $Q_i =$

$[(m_i - m_0) / A]$. The test ended when the variation between two consecutive weighing within a 24-hour period did not exceed 1% of the total mass of water absorbed by the specimen.

5.3.4 Mechanical tests

After hardening for 90 days, the prism specimen with dimensions (4cm x 4cm x 16cm) were mechanically assessed to evaluate of their physical properties under various forces or loads to assess its strength, durability, and structural performance. Two mechanical tests were performed; compressive strength tests and flexural strength tests. These tests provide an understanding of how well the mortars can withstand structural and environmental stresses. This is essential because, for heritage materials and in the designing of repair mortars, it becomes vital to match or closely approximate the mechanical properties of the repair material to that of the original materials to ensure compatibility and to maintain the structural integrity of the heritage structure.

5.3.4.1 Flexural test

A flexural strength test is a method used to determine the ability of a material to resist deformation under load. It measures the material's tensile strength when subjected to bending. In this test, a sample (usually a beam) is supported at both ends while a force is applied at the midpoint. The load is increased until the sample breaks, and the maximum force that the sample can withstand before failure is recorded as its flexural strength. This test is usually used to evaluate the performance of materials under bending stresses.

In this research, the flexural strength test was conducted with the prismatic specimens (4 x 4 x 16 cm) using three-point loading to determine the flexural strength of the hardened mortars at 90 days in accordance with the EN 1015-11:2019 [85], standard at the Department of Engineering, University of Calabria. During the test, a sample is positioned in contact with two support rollers,

and a concentrated load is applied at the midpoint of the sample. The load is then increased uniformly at a rate of 0.20MPa/S, until failure occurs within a timeframe of 30 to 90 seconds. Three samples were tested for each mortar specimen and the average value was presented as the final flexural strength.

The flexural strength (f) corresponds to the maximum force recorded by the machine, and it was determined with the equation: $f = 1.5 \times \frac{(F.l)}{b.d^2}$. Where F is the maximum load applied to the specimen, in kilo newton (KN), l is the distance between the support rollers, in millimetres (mm), b is the width of specimen, in millimetres (mm), and d is the depth of the specimen, in millimetres (mm).

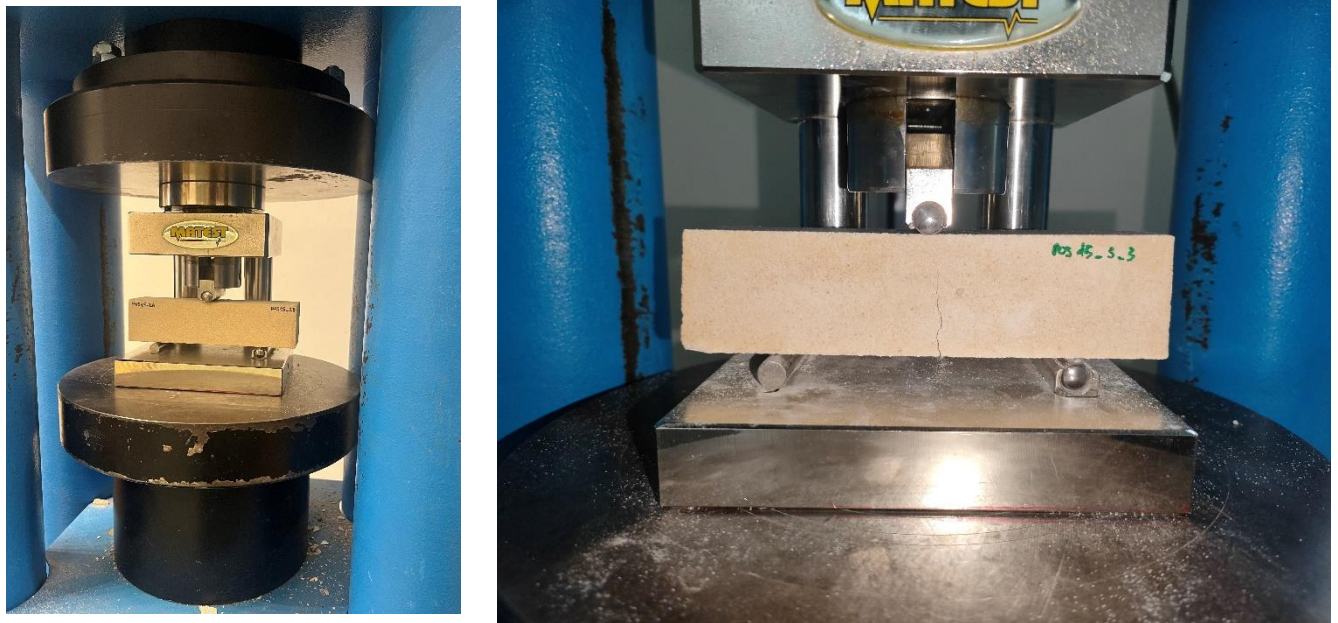


Figure 16: Loading arrangement for flexural strength test

5.3.4.2 Compressive strength test

Compressive strength is a measure of a material's ability to withstand axial loads that compress it. The test involves applying a uniaxial load to a specimen until failure occurs, and the maximum load per unit area is recorded as the compressive strength. This property provides insights into the material's capacity to resist crushing under applied forces.

In this research, the compressive strength of the specimen was determined using the half remains of the samples after the flexural strength test according to the EN 1015-11:2019 [85], standard. During the test, each sample was placed in the testing machine and compressed, with a load applied at a rate of 0.20 MPa/s to ensure that failure occurred within a time frame of 30 to 90 seconds. The compressive strength was then determined by dividing the maximum load recorded during the test by the compressed area of the sample expressed in the equation; $f = \frac{F}{A}$, where F is the maximum the maximum load applied to the specimen, in Kilo newtons (KN), and A is the area of the compressed sample surface.



Figure 18: Halved specimens after flexural strength test

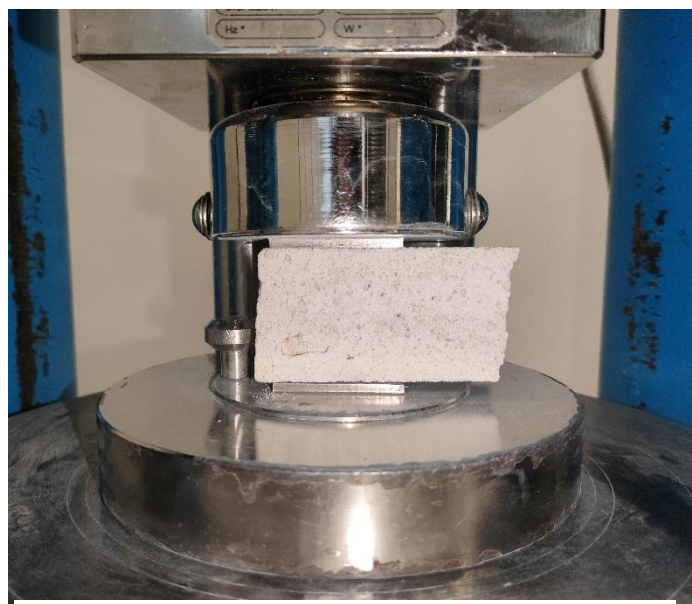


Figure 17: Loading arrangement of the compressive strength test

Chapter 6:

Results

6.1 Consistency test by flow table

The workability of the wet mortar mixtures was evaluated by determining their consistency using a flow table test. The flow table test is a standard method used to assess the workability and consistency of fresh mortar mixtures by measuring how much the mortar spreads when subjected to slight jolting. In the test, fresh mortar is placed into a cone mould on a table, which is then raised and dropped 15 times from a set height. This action causes the mortar to spread, and the final diameter of the spread is measured to determine its flow value. A larger spread indicates higher workability, while a smaller spread suggests a stiffer, less workable mixture.

The flow values reported in this study are the averages of three measurements, each representing the expanded diameter of the fresh mortar, measured with a ruler. Initially, all mixtures were prepared using the same water content as the reference sample (TQ), but the paste was stiff and not workable enough. To achieve workable consistency, additional water was added, especially for the POS-HL samples as the GOS content increased. This is reflected in the increasing water/binder ratios for the POS-HL series. On the contrary, the nano silica-modified samples (POS-HL-S series) required less water to achieve similar workability, as seen by the lower, consistent water/binder ratio of 1.88.

Table 6: Flow values from consistency test

Specimen	Water/Binder ratio	Flow values
<i>TQ</i>	1.75	126.75
<i>POS5-HL</i>	2.21	127.5
<i>POS10-HL</i>	2.27	127.83
<i>POS15-HL</i>	2.3	127.5
<i>POS5-HL-S</i>	1.88	126.33
<i>POS10-HL-S</i>	1.88	126.5
<i>POS15-HL-S</i>	1.88	128.33

From the flow values in Table 6, it is evident that the specimens containing GOS and nano silica required a constant water addition to maintain workability. Although the water-to-binder ratio in these samples was higher than that of the reference sample (TQ), it was still lower than the ratio required for the mixtures with GOS but without nano silica.

6.2 Colourimetry assessment

The colorimetry test was conducted primarily to ensure visual compatibility of the repair mortars with GOS inclusion in comparison with the reference sample by monitoring their colour changes, ensuring the long-term durability of the repair and its ability to blend seamlessly with the existing structures, particularly when exposed to environmental factors. In heritage conservation and restoration, aesthetic consistency is crucial, as visible differences in colour between the original material and the repair mortar can detract from the historical and architectural integrity of the structure. Therefore, colorimetry tests of repair mortars aid in achieving both functional and aesthetic harmony in restoration projects.

The average values of the L^* , a^* , and b^* coordinates calculated from five points on each of the mortar specimen are presented in Table 7 below.

Table 7: Colorimetric values of specimen from the colour assessment test

<i>Specimen</i>	L^*	a^*	b^*
<i>TQ-HL</i>	88.54	0.63533	2.48
<i>POS5-HL</i>	86.39	1.38933	5.95
<i>POS10-HL</i>	84.47	2.048	7.78
<i>POS15-HL</i>	84.18	2.32267	8.70
<i>POS5-HL-S</i>	86.99	1.18467	4.93
<i>POS10-HL-S</i>	84.18	2.23667	6.93
<i>POS15-HL-S</i>	83.34	2.65867	8.01

From the colorimetric values, the reference sample (TQ) exhibits an L^* value of 88.54, representing the lightest mortar among the test samples while POS15-HL-S with 15% replacement with GOS and nanosilica results in an L^* value of 83.34, representing the darkest sample. Also, it is observed that as the GOS content increases, the a^* values steadily increase, signifying a stronger red tint in the mortars with GOS. The b^* values which reflect the shift along the blue-yellow axis, with positive values indicating a yellow hue, also show a clear trend as GOS content increases indicating that the mortars are becoming more yellow as more GOS is added.

The colour difference (ΔL^* , Δa^* and Δb^*) of the samples and the reference sample was analysed by subtracting the L^* , a^* , and b^* values of the sample from the L^* , a^* , and b^* values of the reference sample and expressed as the delta values.

Table 8: Colour difference (ΔL^* , Δa^* , Δb^*)

<i>Specimen</i>	ΔL^*	Δa^*	Δb^*
<i>POS5-HL</i>	-2.15	0.75	3.47
<i>POS10-HL</i>	-4.08	1.41	5.30
<i>POS15-HL</i>	-4.37	1.69	6.22
<i>POS5-HL-S</i>	-1.57	0.55	2.45
<i>POS10-HL-S</i>	-4.37	1.60	4.46
<i>POS15-HL-S</i>	-5.20	2.02	5.53

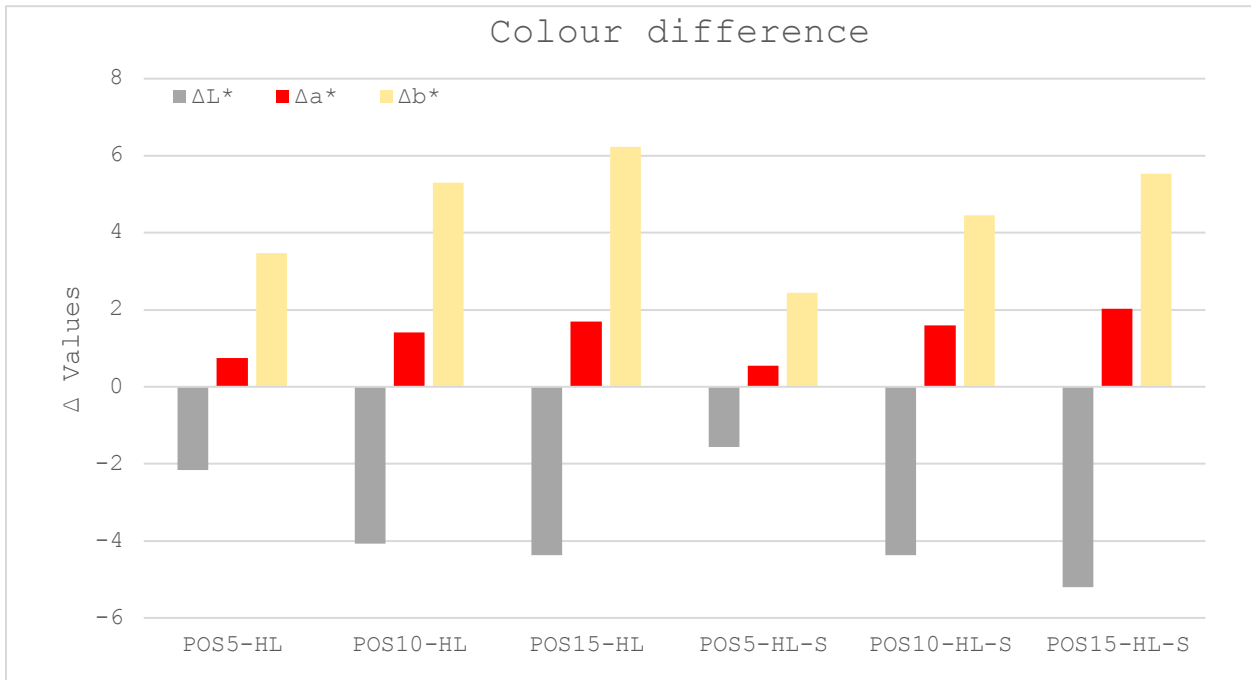


Figure 19: Graphical representation of the colour difference

From the data above, it is observed that all specimens have negative ΔL^* values, indicating that they are darker than the reference sample. The darkening effect increases as GOS content increases. For example, POS15-HL (-4.37) is darker than POS5-HL (-2.15). Meanwhile the nano silica-modified specimens (POS-HL-S series) generally show a smaller reduction in lightness compared to the POS-HL. For example, POS5-HL-S has a ΔL^* of -1.57, which is lighter than POS5-HL at -2.15.

An important exception to the overall trend is observed in the ΔL^* value of POS15-HL-S. Thus, while the other nano silica-modified samples show less darkening compared to their non-modified samples, POS15-HL-S has a significantly more negative ΔL^* value (-5.20), indicating that it is darker than even the corresponding non-modified sample POS15-HL (-4.37).

In addition, all specimens show positive Δa^* values, meaning they shift towards the red spectrum compared to the reference sample. This red shift increases slightly with the addition of more GOS. For example, POS15-HL has a Δa^* of 1.69, while POS5-HL has a Δa^* of 0.75. The nano silica-modified samples once again have slightly lower Δa^* values than their non-modified counterparts, indicating a smaller shift towards red. For example, POS15-HL-S has a Δa^* of 2.02, while POS15-HL has 1.69.

Lastly, all the specimens exhibit positive Δb^* values, indicating a shift towards the yellow spectrum compared to the reference sample. The yellow shift increases as the GOS content rises. Such that, POS15-HL has a Δb^* of 6.22, compared to POS5-HL at 3.47. The POS-HL-S series generally have smaller Δb^* values compared to the POS-HL equivalents. For instance, POS15-HL-S has a Δb^* of 5.53, compared to POS15-HL at 6.22.

The total colour difference (ΔE) between the reference sample and each of the other specimen with GOS, which is the geometrical distance between their positions in the CIELAB colour space was evaluated by $\Delta E = \sqrt{(\Delta L^2 + \Delta a^2 + \Delta b^2)}$. This provides a numerical value representing the overall colour difference between the reference sample and each of the other specimens with GOS.

Table 9: Total colour difference (ΔE)

Specimen	Delta values
TQ-HL, POS5-HL	8.63
TQ-HL, POS10-HL	23.34
TQ-HL, POS15-HL	30.32
TQ-HL, POS5-HL-S	4.37
TQ-HL, POS10-HL-S	20.74
TQ-HL, POS15-HL-S	30.87

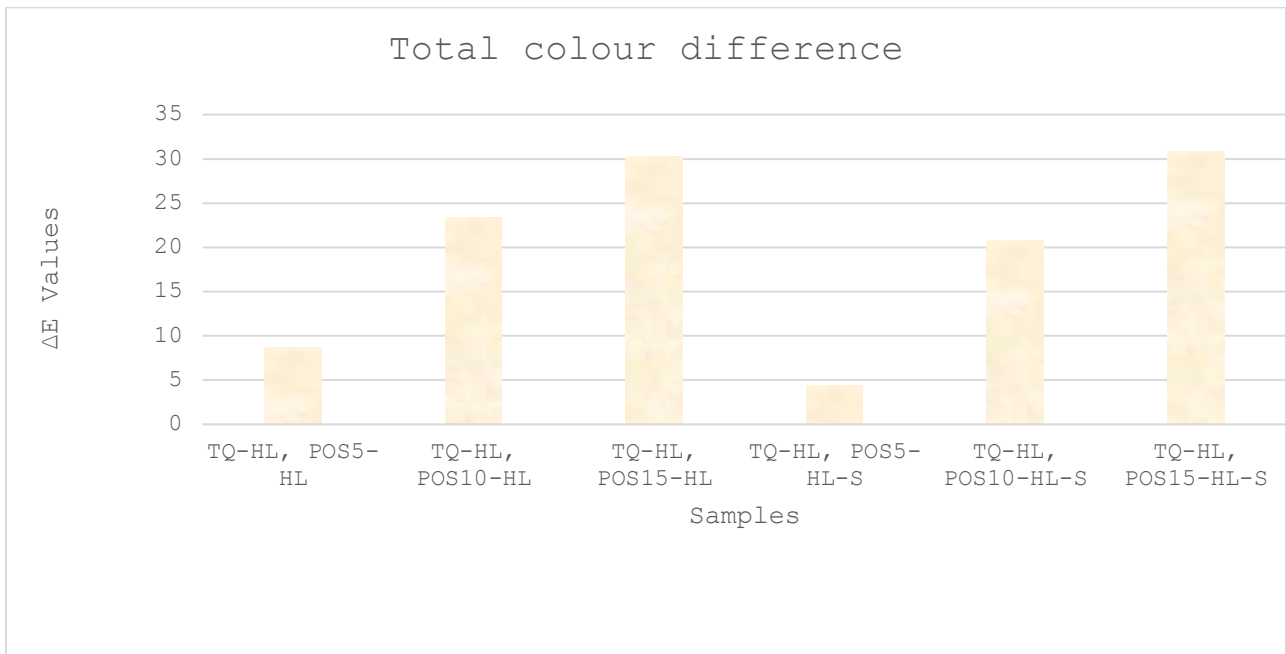


Figure 20: Graphical representation of the Total colour difference ΔE

From the data in Table 9 and Figure 20 above, it is observed that as the GOS content increases from 5% to 15% in the POS-HL series, the total colour difference (ΔE) increases significantly. For POS5-HL, the ΔE is 8.63. The value jumps to 23.34 for POS10-HL and the highest value at 30.32 in the case of POS15-HL. The POS-HL-S series however, tend to have lower ΔE values compared to their unmodified counterparts, especially for lower GOS content. For example: POS5-HL-S has a ΔE of 4.37, which is significantly lower than the 8.63 of POS5-HL. POS10-HL-S has a ΔE of

20.74 which is also slightly lower than the 23.34 of POS10-HL. However, at 15% GOS content, the POS15-HL-S sample has a slightly higher ΔE value of 30.86 compared to its unmodified counterpart POS15-HL which has a ΔE value of 30.32.

6.3 Salt crystallization tests

The results of the accelerated salt weathering tests are reported in this section. All the samples were subjected to 15 cycles of wet and dry cycles of salt crystallisation test. However, some samples disintegrated before the 15th cycle. Table 10 reports the mass of the specimens (in grams) after each cycle, prior to the start of the next cycle. For specimens that fractured before the start of the subsequent cycle, their final recorded mass is shown, and they are excluded from further measurements. These instances are denoted by “#0”, indicating that no measurements were taken after the cycle in which the specimen broke.

Table 10: Mass (g) of specimen after wet and dry cycles of salt crystallization

Specimen	Md: Mass before 1st cycle	Mass after 1st cycle (M1)	Mass after 2nd Cycle (M2)	Mass after 3rd cycle (M3)	Mass after 4th cycle (M4)	Mass after 5th cycle (M5)	Mass after 6th cycle (M6)	Mass after 7th cycle (M7)
TQ-HL-1	87.25	90.77	94.22	96.44	97.19	95.93	97.96	97.96
TQ-HL-2	83.97	87.18	90.35	92.37	93.3	91.23	94.36	94.41
TG-HL-3	89.64	92.46	95.2	97.94	99.09	97.56	100.67	101.16
POS5-HL-1	84.46	88.01	90.91	93.73	94.81	92.61	95.41	96.27
POS5-HL-2	80.03	83.06	85.51	87.4	88.89	86.85	90.03	90.43
POS5-HL-3	78.38	81.08	83.36	85.75	87	85.04	88.27	88.67
POS10-HL-1	76.39	79.32	81.71	83.98	85.42	82.89	86.61	87.25
POS10-HL-2	78.26	81.55	84.09	86.51	87.76	85.09	89.47	90.24
POS10-HL-3	83.38	86.98	89.26	91.33	92.96	90.04	94.88	95.88
POS15-HL-1	69.57	73.37	76.18	78.71	79.38	75.82	80.62	80.76
POS15-HL-2	73.4	77.45	80.09	82.15	83.23	80.29	84.22	85.13
POS15-HL-3	73.64	77.62	80.5	82.84	83.8	80.61	84.97	85.81
POS5-HL-S-1	88.17	89.72	90.99	93.08	94.64	93	95.98	96.37
POS5-HL-S-2	88.23	89.61	90.58	92.16	93.59	92.32	95.07	95.6
POS5-HL-S-3	89.45	91.23	92.54	94.81	96.18	94.51	97.75	98.08
POS10-HL-S-1	81.24	83.61	86.48	89.03	89.91	87.18	90.52	90.57
POS10-HL-S-2	86.65	88.69	90.5	92.82	93.94	91.49	93.96	94.2
POS10-HL-S-3	82.66	84.54	86.13	88.38	89.4	87.18	90.18	90.14

POS15-HL-S-1	78.58	80.57	81.84	88.83	84.75	83.15	86.07	86.96
POS15-HL-S-2	65.83	67.47	68.51	70.02	70.87	69.52	71.7	72.53
POS15-HL-S-3	74.63	76.49	77.54	79.22	80.07	78.78	81.31	82.11
Specimen	Mass after 8th cycle (M8)	Mass after 9th cycle (M9)	Mass after 10th cycle (M10)	Mass after 11th cycle (M11)	Mass after 12th cycle (M12)	Mass after 13th cycle (M13)	Mass after 14th Cycle (M14)	Mass after 15th cycle (M15)
TQ-HL-1	98.04	98.32	96.74	96.3	95.62	94.06	90.05	89.07
TQ-HL-2	94.38	94.21	92.74	91.62	88.58	85.76	79.77	79.05
TG-HL-3	101.34	101.56	100.15	101.45	100.94	96.03	94.79	80.84
POS5-HL-1	96.23	96.19	93.61	92.97	90.3	87.21	87.04	83.39
POS5-HL-2	90.26	90.11	86.22	86.22	78.19	61.36	58.24	57.4
POS5-HL-3	88.36	88.15	85.54	78.58	77.32	73.27	#0	#0
POS10-HL-1	86.86	86.97	84.36	82.85	80.37	71.93	#0	#0
POS10-HL-2	90.2	90.27	87.06	83.84	82.79	76.87	#0	#0
POS10-HL-3	95.78	95.77	92.68	88.95	84.3	#0	#0	#0
POS15-HL-1	80.34	80.03	76.5	68.17	61.93	33.68	#0	#0
POS15-HL-2	84.47	84.23	78.2	69.2	#0	#0	#0	#0
POS15-HL-3	85.38	85.17	82.3	78.5	70.52	#0	#0	#0
POS5-HL-S-1	96.15	95.63	90.16	68.1	#0	#0	#0	#0
POS5-HL-S-2	95.31	94.74	90.29	93.8	93.32	86.08	58.24	66.99
POS5-HL-S-3	97.74	93.37	90.43	83.83	#0	#0	#0	#0
POS10-HL-S-1	90.06	89.45	85.77	80.69	66.01	16.71	#0	#0
POS10-HL-S-2	93.55	91.93	71.88	#0	#0	#0	#0	#0
POS10-HL-S-3	89.41	88.94	85.51	83.34	#0	#0	#0	#0
POS15-HL-S-1	86.45	86.11	68.07	80.42	#0	#0	#0	#0
POS15-HL-S-2	72.2	69.61	83.64	71.69	67.02	#0	#0	#0
POS15-HL-S-3	81.95	81.86	79.86	71.26	#0	#0	#0	#0

The results, in accordance with SIST EN 12370:2000, are expressed as the relative mass difference (ΔM), representing the mass loss or gain as a percentage of the initial dry mass (M_d) and the number of cycles required to induce failure in cases where the specimen has disintegrated or has broken into two or more pieces before the final drying are calculated with the equation $\Delta M = \frac{M_f - M_d}{M_d} \times 100$. where M_f represents the final mass of the specimen after a given cycle, and M_d is the initial dry mass.

Table 11: ΔM : Relative mass difference (%) (Mass loss or mass gain)

Specimen	$\Delta M1$ (%)	$\Delta M2$ (%)	$\Delta M3$ (%)	$\Delta M4$ (%)	$\Delta M5$ (%)	$\Delta M6$ (%)	$\Delta M7$ (%)	$\Delta M8$ (%)
TQ-HL-1	4.03	7.99	10.53	11.39	9.95	12.28	12.28	12.37
TQ-HL-2	3.82	7.60	10.00	11.11	8.65	12.37	12.43	12.40

TG-HL-3	3.15	6.20	9.26	10.54	8.84	12.30	12.85	13.05
POS5-HL-1	4.20	7.64	10.98	12.25	9.65	12.96	13.98	13.94
POS5-HL-2	3.79	6.85	9.21	11.07	8.52	12.50	13.00	12.78
POS5-HL-3	3.44	6.35	9.40	11.00	8.50	12.62	13.13	12.73
POS10-HL-1	3.84	6.96	9.94	11.82	8.51	13.38	14.22	13.71
POS10-HL-2	4.20	7.45	10.54	12.14	8.73	14.32	15.31	15.26
POS10-HL-3	4.32	7.05	9.53	11.49	7.99	13.79	14.99	14.87
POS15-HL-1	5.46	9.50	13.14	14.10	8.98	15.88	16.08	15.48
POS15-HL-2	5.52	9.11	11.92	13.39	9.39	14.74	15.98	15.08
POS15-HL-3	5.40	9.32	12.49	13.80	9.46	15.39	16.53	15.94
POS5-HL-S-1	1.76	3.20	5.57	7.34	5.48	8.86	9.30	9.05
POS5-HL-S-2	1.56	2.66	4.45	6.08	4.64	7.75	8.35	8.02
POS5-HL-S-3	1.99	3.45	5.99	7.52	5.66	9.28	9.65	9.27
POS10-HL-S-1	2.92	6.45	9.59	10.67	7.31	11.42	11.48	10.86
POS10-HL-S-2	2.35	4.44	7.12	8.41	5.59	8.44	8.71	7.96
POS10-HL-S-3	2.27	4.20	6.92	8.15	5.47	9.10	9.05	8.17
POS15-HL-S-1	2.53	4.15	13.04	7.85	5.82	9.53	10.66	10.02
POS15-HL-S-2	2.49	4.07	6.36	7.66	5.61	8.92	10.18	9.68
POS15-HL-S-3	2.49	3.90	6.15	7.29	5.56	8.95	10.02	9.81

Specimen	$\Delta M9$ (%)	$\Delta M10$ (%)	$\Delta M11$ (%)	$\Delta M12$ (%)	$\Delta M13$ (%)	$\Delta M14$ (%)	$\Delta M15$ (%)
TQ-HL-1	12.69	10.88	10.37	9.59	7.81	3.21	2.09
TQ-HL-2	12.19	10.44	9.11	5.49	2.13	-5.00	-5.86
TG-HL-3	13.30	11.72	13.17	12.61	7.13	5.75	-9.82
POS5-HL-1	13.89	10.83	10.08	6.91	3.26	3.05	-1.27
POS5-HL-2	12.60	7.73	7.73	-2.30	-23.33	-27.23	-28.28
POS5-HL-3	12.46	9.13	0.26	-1.35	-6.52	#0	#0
POS10-HL-1	13.85	10.43	8.46	5.21	-5.84	#0	#0
POS10-HL-2	15.35	11.24	7.13	5.79	-1.78	#0	#0
POS10-HL-3	14.86	11.15	6.68	1.10	#0	#0	#0
POS15-HL-1	15.04	9.96	-2.01	-10.98	-51.59	#0	#0
POS15-HL-2	14.75	6.54	-5.72	#0	#0	#0	#0
POS15-HL-3	15.66	11.76	6.60	-4.24	#0	#0	#0
POS5-HL-S-1	8.46	2.26	-22.76	#0	#0	#0	#0
POS5-HL-S-2	7.38	2.33	6.31	5.77	-2.44	-33.99	-24.07
POS5-HL-S-3	4.38	1.10	-6.28	#0	#0	#0	#0
POS10-HL-S-1	10.11	5.58	-0.68	-18.75	-79.43	#0	#0
POS10-HL-S-2	6.09	-17.05	#0	#0	#0	#0	#0
POS10-HL-S-3	7.60	3.45	0.82	#0	#0	#0	#0
POS15-HL-S-1	9.58	-13.37	2.34	#0	#0	#0	#0
POS15-HL-S-2	5.74	27.05	8.90	1.81	#0	#0	#0
POS15-HL-S-3	9.69	7.01	-4.52	#0	#0	#0	#0

The data presented in

Table 12 below provides the average relative mass difference (ΔM) for each mortar mixture over the cycles of salt crystallization. This relative mass difference represents the mass loss or gain as a percentage of the initial dry mass, and it helps evaluate the durability of the different mortar mixtures under salt crystallization according to the SIST EN 12370:2000 standard. The average values were calculated for specimen that had at least two samples not broken. The reported average values after each cycle however are based only on the specimens where at least two samples remained intact, ensuring that the averages reflect the performance of specimens that have not completely disintegrated.

Table 12: Average values of the relative mass difference (%)

Cycle	Specimen						
	TQ-HL	POS5-HL	POS10-HL	POS15-HL	POS5-HL-S	POS10-HL-S	POS15-HL-S
0	0.00	0.00	0.00	0.00	0.00	0.00	0.00
M1	3.67	3.81	4.12	5.46	1.77	2.52	2.51
M2	7.26	6.95	7.16	9.31	3.11	5.03	4.04
M3	9.93	9.86	10.00	12.52	5.34	7.88	8.52
M4	11.02	11.44	11.82	13.76	6.98	9.08	7.60
M5	9.14	8.89	8.41	9.28	5.26	6.12	5.66
M6	12.32	12.69	13.83	15.34	8.63	9.65	9.13
M7	12.52	13.37	14.84	16.20	9.10	9.75	10.29
M8	12.61	13.15	14.61	15.50	8.78	9.00	9.83
M9	12.73	12.98	14.69	15.15	6.74	7.93	8.34
M10	11.02	9.23	10.94	9.42	1.90	-2.67	6.90
M11	10.89	6.02	7.42	-0.38	-7.58	0.07	2.24
M12	9.23	1.09	4.03	-7.61	#0	#0	#0
M13	5.69	-8.86	-3.81	#0	#0	#0	#0
M14	1.32	-12.09	#0	#0	#0	#0	#0
M15	-4.53	-14.77	#0	#0	#0	#0	#0

From the data, it is observed that in the initial phase (Cycles 1-4), all mortar mixtures, including the reference sample TQ-HL, experienced an increase in mass due to salt accumulation. The

highest mass increase occurs in the POS15-HL sample (15% GOS), which had a ΔM of 5.46% after the first cycle and reached 13.76% after the 4th cycle. The nano silica-modified mortars (POS5-HL-S, POS10-HL-S, and POS15-HL-S) show relatively smaller mass increases in the first four cycles. For instance, POS5-HL-S only increased by 1.77% after the first cycle, compared to 3.67% in the reference sample.

After the 5th cycle however, all the specimen experience a mass loss. Interestingly, after the 6th cycle, all specimens begin to gain mass again, likely due to further accumulation of salts within the damaged mortar structure, as new salts may form during repeated wet-dry cycles. For example, POS15-HL increases its mass from 9.28% in the 5th cycle to 15.34% after the 6th cycle, and POS10-HL increases from 8.41% to 13.83%. The nano silica-modified specimens also follow this trend. POS5-HL-S sees an increase in mass from 5.26% in the 5th cycle to 8.63% after the 6th cycle.

The mass gain continues through cycles 7 to 9, with all specimens showing moderate increment. For instance, TQ-HL rises from 9.14% (cycle 5) to 12.73% after the 9th cycle. POS10-HL also rises from 8.41% after cycle 5 to 14.69% after the 9th cycle and POS15-HL-S increases from 5.66% (cycle 5) to 9.83% (cycle 9).

After the 10th cycle, the majority of specimens begin to experience severe mass loss. This is especially true for GOS-modified specimens, which show negative values indicating mass loss and the breakage of one sample from the specimen. For example, POS5-HL drops sharply to -14.77% by the 15th cycle as one of its samples broke after the 13th cycle, and POS10-HL disintegrates before reaching the final cycle with one of its samples breaking after the 13th cycle.

Nano silica-modified samples, such as POS5-HL-S, also experience mass loss, though less severe than their unmodified counterparts, with POS5-HL-S showing a mass loss of -7.58% by the 11th cycle. But none of them survived beyond the 11th cycle, as all the samples had disintegrated or broken apart.

It can be observed that even though the TQ-HL sample survived all 15 cycles, it suffered considerable damage, dropping from 12.73% (cycle 9) to 11.02% (cycle 10), ending at -4.53% by the 15th cycle. POS5-HL, with only two intact samples, also experienced significant mass loss, dropping from 12.98% (cycle 9) to 9.23% (cycle 10), and eventually to -14.77% by the 15th cycle. Specimens containing higher GOS content like the POS10-HL and POS15-HL, and all nano silica-modified samples disintegrated before the 15th cycle. These trends are graphically presented Figure 21 below.

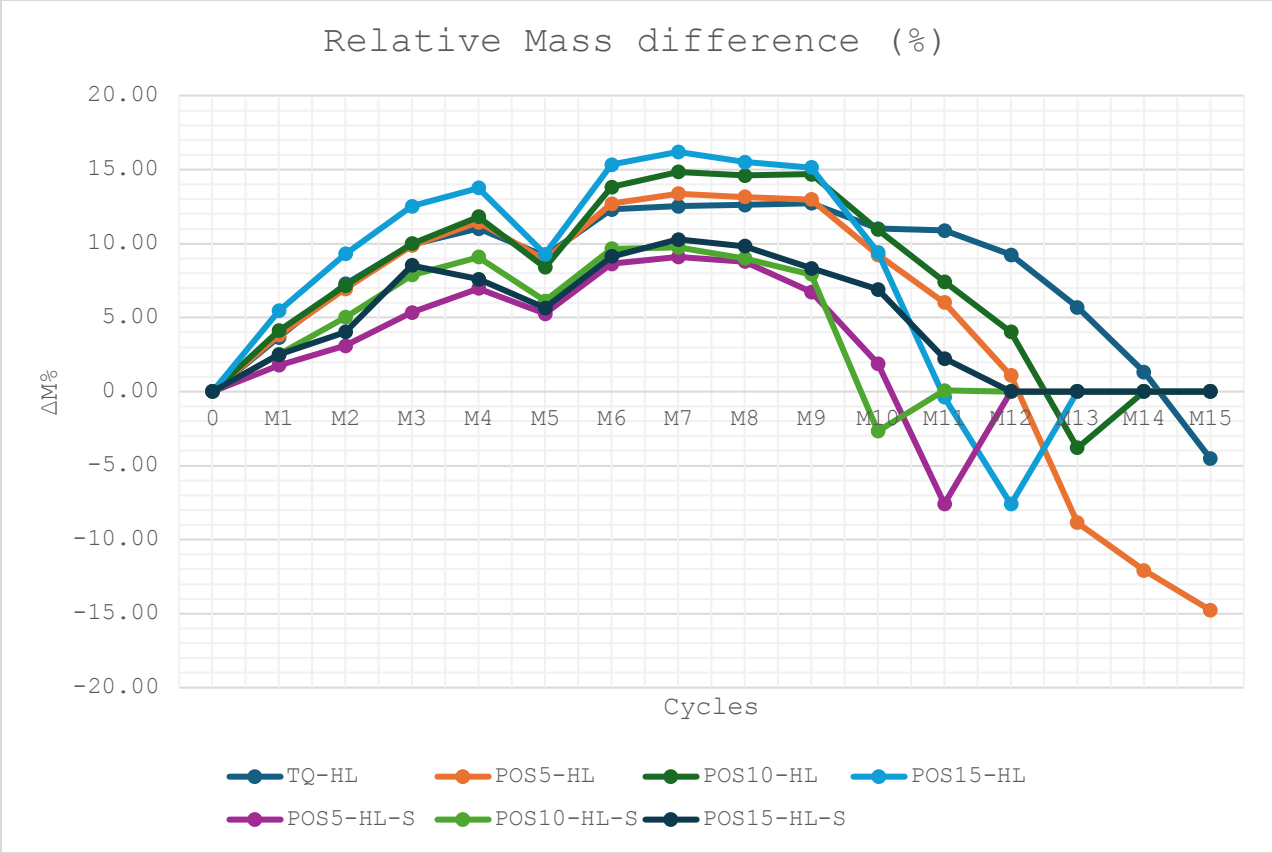


Figure 21: Graphical representation of the relative mass difference (%)

6.4 Water absorption by capillarity

The following section presents the results from the water absorption by capillary action test done on the cubic specimen to assess the permeability and porosity of the repair mortar. The test ended after 7 days when the variation between two consecutive weighing within a 24-hour period did not exceed 1% of the total mass of water absorbed by the specimen. The samples were removed from the saturated layer of paper after specific time intervals and weighed immediately.

Table 13: Mass of specimen (g) at time (ti)

Specimen	Mo (ti= 0)	M1 (ti=10mins)	M2 (ti=20mins)	M3 (ti=30mins)	M4 (ti=60 mins)	M5 (ti=4hrs)	M6 (ti=6hrs)
TQ-HL-1	207.32	215.83	218.91	222.39	228.32	230.40	230.47
TQ-HL-2	199.23	209.97	213.39	216.30	220.65	221.80	221.87
TQ-HL-3	200.66	210.07	213.76	216.54	221.40	223.55	223.56
POS5-HL-1	187.43	194.40	196.61	198.19	200.92	208.05	208.95
POS5-HL-2	194.18	199.63	201.31	202.55	204.66	211.56	212.98
POS5-HL-3	196.12	203.08	205.4	207.13	209.86	217.09	218.27
POS10-HL-1	178.48	183.27	186.28	188.94	194.03	205.92	206.79
POS10-HL-2	175.76	179.09	181.56	183.88	187.96	198.21	199.47
POS10-HL-3	176.83	179.72	182.48	184.79	188.62	198.72	200.15
POS15-HL-1	164.54	166.85	167.91	168.43	169.35	180.08	187.88
POS15-HL-2	172.38	174.38	175.8	176.81	179.03	196.92	200.42
POS15-HL-3	173.25	175.69	177.70	179.36	182.83	200.97	202.81
POS5-HL-S-1	197.94	205.65	207.80	209.28	212.75	218.39	219.30
POS5-HL-S-2	198.99	205.87	207.78	209.17	212.34	218.46	219.50
POS5-HL-S-3	195.99	202.67	204.53	205.9	209.02	215.24	216.39
POS10-HL-S-1	189.50	195.68	197.25	198.38	201.02	207.55	209.36
POS10-HL-S-2	188.97	194.78	196.24	197.27	199.76	206.51	208.49
POS10-HL-S-3	185.07	190.74	192.16	193.2	195.59	202.17	204.19
POS15-HL-S-1	175.49	182.40	184.36	185.92	189.33	198.43	200.26
POS15-HL-S-2	179.60	186.58	188.36	189.81	193.04	201.90	203.97
POS15-HL-S-3	178.18	185.30	187.11	188.59	191.63	200.58	202.64

Specimen	M7 (ti=24hrs)	M8 (ti=48hrs)	M9 (ti=72hrs)	M10 (ti=96hrs)	M11 (ti=128hrs)	M12 (ti=152hrs)	M13 (ti=176hrs)
TQ-HL-1	231.09	231.62	231.66	231.91	231.95	232.07	232.18
TQ-HL-2	222.44	223.17	223.34	223.47	223.65	223.66	223.74
TQ-HL-3	224.14	224.85	224.87	225.09	225.24	225.25	225.3
POS5-HL-1	210.38	211.06	211.28	211.5	211.68	211.81	211.88
POS5-HL-2	215.62	216.33	216.59	216.99	217.16	217.34	217.42
POS5-HL-3	220.61	220.85	221.02	221.25	221.52	221.58	221.65
POS10-HL-1	207.48	208.01	208.44	209.22	209.53	209.87	210.09
POS10-HL-2	200.84	201.33	201.75	202.46	202.8	203.09	203.33
POS10-HL-3	201.66	202.12	202.53	203.29	203.62	203.96	204.12
POS15-HL-1	193.66	194.63	195.52	196.81	197.45	197.94	198.27
POS15-HL-2	202.77	203.53	204.2	205.2	205.74	206.22	206.51
POS15-HL-3	204.25	205	205.67	206.87	207.22	207.72	208.03

POS5-HL-S-1	220.39	221.66	222.2	222.49	223.11	223.68	223.94
POS5-HL-S-2	220.77	222.01	222.54	223.09	223.63	223.96	224.27
POS5-HL-S-3	217.76	218.87	219.42	219.83	220.31	220.89	221.17
POS10-HL-S-1	211.99	213.5	214.19	214.71	215.24	215.78	216.04
POS10-HL-S-2	211.42	212.75	213.46	213.94	214.49	211.3	211.56
POS10-HL-S-3	207.18	208.59	209.27	209.8	210.31	210.88	211.12
POS15-HL-S-1	202.46	204.37	205.46	206.38	206.76	207.43	207.77
POS15-HL-S-2	206.48	208.35	209.56	210.15	210.77	214.93	215.31
POS15-HL-S-3	204.95	206.88	208.08	208.73	209.35	209.86	210.22

The amount of water absorbed by the specimen through capillary action per unit area, calculated by the difference between the wet mass at time (t_i) and the initial dry mass of the sample (m_0) as a function of time in relation to the samples' surface area in contact with the water was expressed as $Q_i = [(m_i - m_0) / A]$.

Table 14: Q_i - Amount of water absorbed by specimen per unit area at time (t_i) in (g/cm²)

Specimen	M1 ($t_i=10$ mins)	M2 ($t_i=20$ mins)	M3 ($t_i=30$ mins)	M4 ($t_i=60$ mins)	M5 ($t_i=4$ hrs)	M6 ($t_i=6$ hrs)
TQ-HL-1	340.4	463.6	602.8	840	923.2	926
TQ-HL-2	429.6	566.4	682.8	856.8	902.8	905.6
TQ-HL-3	376.4	524	635.2	829.6	915.6	916
POS5-HL-1	278.8	367.2	430.4	539.6	824.8	860.8
POS5-HL-2	218	285.2	334.8	419.2	695.2	752
POS5-HL-3	278.4	371.2	440.4	549.6	838.8	886
POS10-HL-1	191.6	312	418.4	622	1097.6	1132.4
POS10-HL-2	133.2	232	324.8	488	898	948.4
POS10-HL-3	115.6	226	318.4	471.6	875.6	932.8
POS15-HL-1	92.4	134.8	155.6	192.4	621.6	933.6
POS15-HL-2	80	136.8	177.2	266	981.6	1121.6
POS15-HL-3	97.6	178	244.4	383.2	1108.8	1182.4
POS5-HL-S-1	308.4	394.4	453.6	592.4	818	854.4
POS5-HL-S-2	275.2	351.6	407.2	534	778.8	820.4
POS5-HL-S-3	267.2	341.6	396.4	521.2	770	816
POS10-HL-S-1	247.2	310	355.2	460.8	722	794.4
POS10-HL-S-2	232.4	290.8	332	431.6	701.6	780.8
POS10-HL-S-3	226.8	283.6	325.2	420.8	684	764.8

POS15-HL-S-1	276.4	354.8	417.2	553.6	917.6	990.8
POS15-HL-S-2	279.2	350.4	408.4	537.6	892	974.8
POS15-HL-S-3	284.8	357.2	416.4	538	896	978.4

Specimen	M7 (ti=24hrs)	M8 (ti=48hrs)	M9 (ti=72hrs)	M10 (ti=96hrs)	M11 (ti=128hrs)	M12 (ti=152hrs)	M13 (ti=176hrs)
TQ-HL-1	950.8	972	973.6	983.6	985.2	990	994.4
TQ-HL-2	928.4	957.6	964.4	969.6	976.8	977.2	980.4
TQ-HL-3	939.2	967.6	968.4	977.2	983.2	983.6	985.6
POS5-HL-1	918	945.2	954	962.8	970	975.2	978
POS5-HL-2	857.6	886	896.4	912.4	919.2	926.4	929.6
POS5-HL-3	979.6	989.2	996	1005.2	1016	1018.4	1021.2
POS10-HL-1	1160	1181.2	1198.4	1229.6	1242	1255.6	1264.4
POS10-HL-2	1003.2	1022.8	1039.6	1068	1081.6	1093.2	1102.8
POS10-HL-3	993.2	1011.6	1028	1058.4	1071.6	1085.2	1091.6
POS15-HL-1	1164.8	1203.6	1239.2	1290.8	1316.4	1336	1349.2
POS15-HL-2	1215.6	1246	1272.8	1312.8	1334.4	1353.6	1365.2
POS15-HL-3	1240	1270	1296.8	1344.8	1358.8	1378.8	1391.2
POS5-HL-S-1	898	948.8	970.4	982	1006.8	1029.6	1040
POS5-HL-S-2	871.2	920.8	942	964	985.6	998.8	1011.2
POS5-HL-S-3	870.8	915.2	937.2	953.6	972.8	996	1007.2
POS10-HL-S-1	899.6	960	987.6	1008.4	1029.6	1051.2	1061.6
POS10-HL-S-2	898	951.2	979.6	998.8	1020.8	893.2	903.6
POS10-HL-S-3	884.4	940.8	968	989.2	1009.6	1032.4	1042
POS15-HL-S-1	1078.8	1155.2	1198.8	1235.6	1250.8	1277.6	1291.2
POS15-HL-S-2	1075.2	1150	1198.4	1222	1246.8	1413.2	1428.4
POS15-HL-S-3	1070.8	1148	1196	1222	1246.8	1267.2	1281.6

To determine the capillary water absorption curve, the calculated values of Q_i were plotted on a graph as a function of the square root of time (\sqrt{t}). Prior to plotting the curve, the average Q_i values were calculated for each specimen. Additionally, the time intervals, originally recorded in minutes

and hours, were converted into seconds before calculating the square root of the time values for accurate analysis of the water absorption curve.

Table 15: Determination of the capillary water absorption curve Q_i (g/cm^2) $/\sqrt{t}$

	Absorption time (\sqrt{t})	TQ-HL	POS5-HL	POS10-HL	POS15-HL	POS5-HL-S	POS10-HL-S	POS15-HL-S
Mo (ti = 0)	0	0	0	0	0	0	0	0
M1 (ti=10mins)	24.49	382.13	258.4	146.80	90	283.60	235.46	280.13
M2 (ti=20mins)	34.64	518	341.2	256.67	149.87	362.53	294.80	354.13
M3 (ti=30mins)	42.43	640.27	401.86	353.87	192.40	419.07	337.47	414
M4 (ti=60mins)	60	842.13	502.80	527.20	280.53	549.20	437.73	543.07
M5 (ti=4hrs)	120	913.87	786.26	957.07	904	788.93	702.53	901.87
M6 (ti=6hrs)	146.97	915.87	832.93	1004.53	1079.20	830.27	780	981.33
M7 (ti=24hrs)	293.94	939.47	918.40	1052.13	1206.80	880	894	1074.93
M8 (ti=48hrs)	415.69	965.73	940.13	1071.87	1239.87	928.27	950.67	1151.07
M9 (ti=72hrs)	509.12	968.80	948.80	1088.67	1269.60	949.87	978.40	1197.73
M10 (ti=96hrs)	587.88	976.80	960.13	1118.67	1316.13	966.53	998.80	1226.53
M11 (ti=128hrs)	678.82	981.73	968.40	1131.73	1336.53	988.40	1020	1248.13
M12 (ti=152hrs)	739.73	983.60	973.33	1144.67	1356.13	1008.13	992.27	1319.33
M13 (ti=176hrs)	795.99	986.80	976.27	1152.93	1368.53	1019.47	1002.40	1333.73

The data in Table 15 shows the capillary water absorption curve, illustrating the Q_i values (water absorbed per unit area) over time for the different specimens. From the data, it can be observed that all specimens show a gradual increase in Q_i (g/cm^2) values over time as water absorption continues. The rate of increase is more rapid during the early stages (10 to 60 minutes), and it slows down as time progresses (after 6 hours).

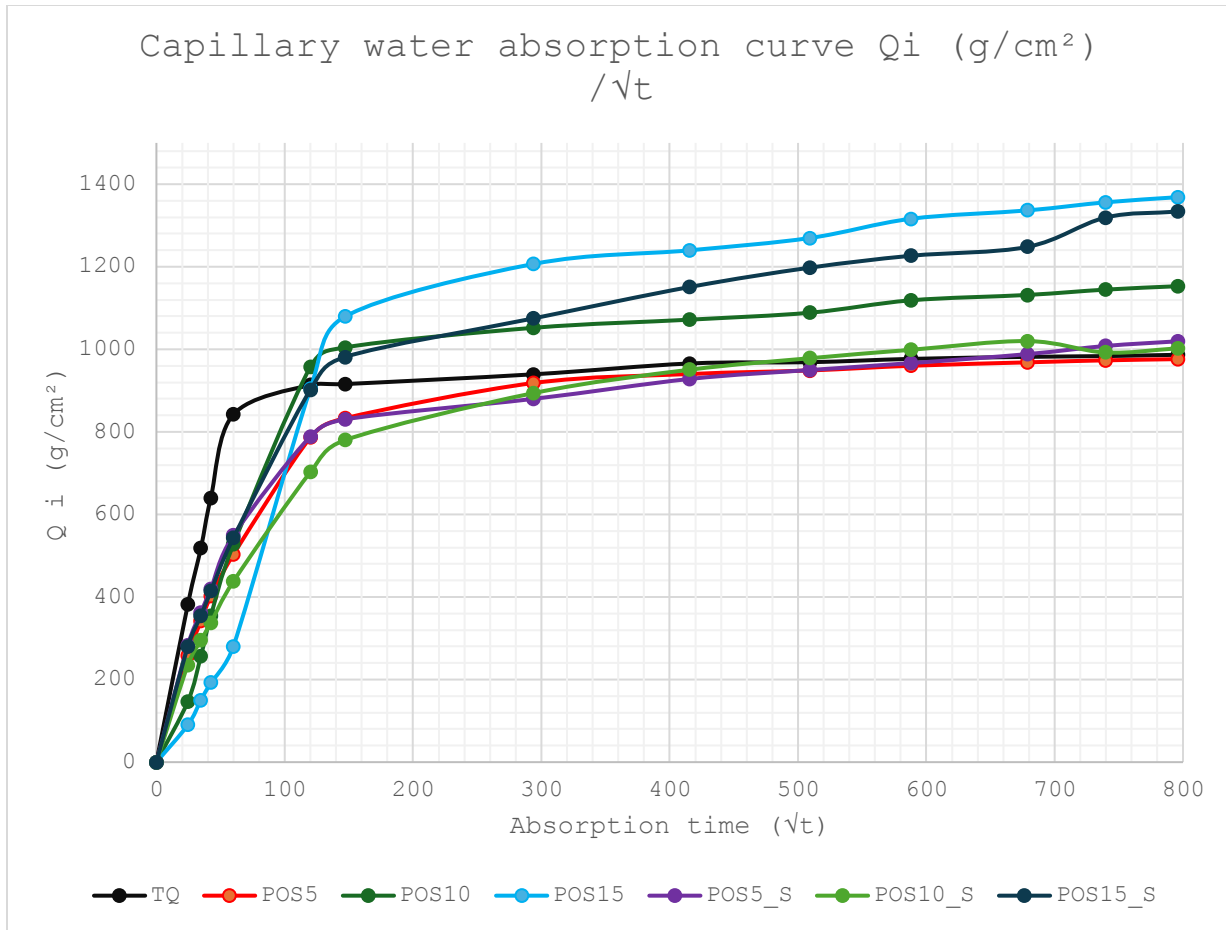


Figure 22: Graphical representation of the capillary absorption curve

The TQ-HL reference sample has the highest initial water absorption rate at $382.13 \text{ g}/\text{cm}^2/\sqrt{t}$, while the GOS-modified samples show lower initial absorption rates. POS5-HL with a value of $258.40 \text{ g}/\text{cm}^2/\sqrt{t}$, POS10-HL with $146.80 \text{ g}/\text{cm}^2/\sqrt{t}$ and POS15-HL with $90.00 \text{ g}/\text{cm}^2/\sqrt{t}$. This indicates that as the GOS content increases, the initial water absorption decreases, with the highest GOS content POS15-HL showing the lowest water absorption initially.

Meanwhile the nano silica-modified samples on the other hand show varying initial absorption values with the value of POS5-HL-S at $283.60 \text{ g}/\text{cm}^2/\sqrt{t}$ (higher than POS5-HL but lower than that of the TQ), POS10-HL-S at $235.46 \text{ g}/\text{cm}^2/\sqrt{t}$ (higher than POS10-HL but lower than that of

the TQ), and POS15-HL-S at $280.13 \text{ g/cm}^2/\sqrt{t}$ (higher than POS15-HL, but lower than that of the TQ).

At 60 minutes, the reference sample (TQ-HL) continues to have a high absorption value ($842.13 \text{ g/cm}^2/\sqrt{t}$), but the GOS-modified specimens show a substantial increase with POS5-HL at $502.80 \text{ g/cm}^2/\sqrt{t}$, POS10-HL at $527.20 \text{ g/cm}^2/\sqrt{t}$, and POS15-HL at $280.53 \text{ g/cm}^2/\sqrt{t}$. Similarly, the nano silica-modified samples continue to absorb water with POS5-HL-S at $549.20 \text{ g/cm}^2/\sqrt{t}$, POS10-HL-S at $437.73 \text{ g/cm}^2/\sqrt{t}$, and POS15-HL-S at $543.07 \text{ g/cm}^2/\sqrt{t}$.

By 176 hours, it can be observed that the GOS-modified samples absorb more water than the reference sample except POS5-HL. Thus, POS5-HL has a Q_i value of $976.27 \text{ g/cm}^2/\sqrt{t}$, whilst POS10-HL has $1152.93 \text{ g/cm}^2/\sqrt{t}$, and POS15-HL at $1368.53 \text{ g/cm}^2/\sqrt{t}$. The nano silica-modified samples also show high absorption after 176 hours such that POS5-HL-S has a Q_i value of $1019.47 \text{ g/cm}^2/\sqrt{t}$, POS10-HL-S with $1002.40 \text{ g/cm}^2/\sqrt{t}$, and POS15-HL-S at $1333.73 \text{ g/cm}^2/\sqrt{t}$ all of which are greater than the value of TQ-HL which is at $986.80 \text{ g/cm}^2/\sqrt{t}$.

6.5 Mechanical Tests

The hardened specimen were mechanically tested to evaluate their flexural strength and compressive strengths. The results is presented in this section.

6.5.1 Flexural strength test results

The test results indicated below in Table 16 is a representation of the point of failure; in this case cracks at a given load. In essence the specimen are subjected to a uniformly increasing pressure until it eventually breaks, the maximum load the specimen endures until it breaks is recorded. The

sample's flexural strength is then recorded in Mega Pascal (MPa) with the expression:

$$f = 1.5 \times \frac{(F.l)}{b.d^2}$$

Where l is the distance between the axes of the support rollers, in millimetres (mm), b is the width of specimen, in millimetres (mm), d is the depth of the specimen, in millimetres (mm) and F is the maximum load applied to the specimen, in Kilo newtons (kN).

Table 16: Flextural strength test results

Specimen	l (mm)	b (mm)	d (mm)	F (kN)	f (MPa)
TQ-HL-1	100	40	40	0.52	1.22
TQ-HL-2	100	40	40	0.41	0.96
TQ-HL-3	100	40	40	0.45	1.05
POS5-HL-1	100	40	40	0.41	0.96
POS5-HL-2	100	40	40	0.45	1.05
POS5-HL-3	100	40	40	0.34	0.80
POS10-HL-1	100	40	40	0.16	0.38
POS10-HL-2	100	40	40	0.27	0.63
POS10-HL-3	100	40	40	0.30	0.70
POS15-HL-1	100	40	40	0.27	0.63
POS15-HL-2	100	40	40	0.29	0.68
POS15-HL-3	100	40	40	0.30	0.70
POS5-HL-S-1	100	40	40	0.20	0.47
POS5-HL-S-2	100	40	40	0.20	0.47
POS5-HL-S-3	100	40	40	0.27	0.63
POS10-HL-S-1	100	40	40	0.21	0.49
POS10-HL-S-2	100	40	40	0.21	0.49
POS10-HL-S-3	100	40	40	0.21	0.49
POS15-HL-S-1	100	40	40	0.16	0.38
POS15-HL-S-2	100	40	40	0.13	0.30
POS15-HL-S-3	100	40	40	0.16	0.38

The average value is of the three samples tested for each mortar specimen is presented as the final flexural strength of the specimen.

Table 17: Flexural test strength results

<i>Samples</i>	<i>Flexural strength (MPa)</i>	<i>Stand. Deviation</i>
<i>TQ-HL</i>	1.08	0.13
<i>POS5-HL</i>	0.94	0.13
<i>POS10-HL</i>	0.57	0.17
<i>POS15-HL</i>	0.67	0.04
<i>POS5-HL-S</i>	0.52	0.09
<i>POS10-HL-S</i>	0.49	0.00
<i>POS15-HL-S</i>	0.35	0.04

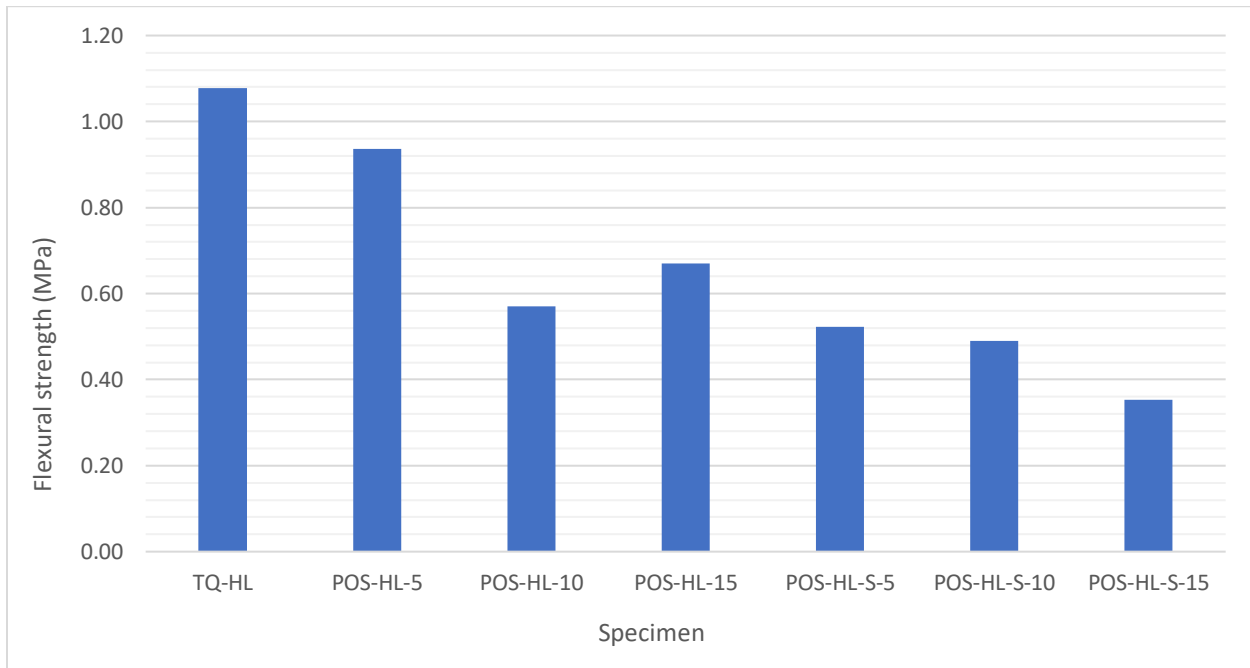


Figure 23: Graphical representation of the flexural strength test

From the results, it can be observed that the reference mortar (TQ-HL), serving as the benchmark for comparison, demonstrated the highest flexural strength of 1.08 MPa. The addition of GOS caused a reduction in flexural strength compared to the reference sample, with POS5-HL achieving

0.94 MPa, which closely matched the control sample. As GOS content increased, the flexural strength declined more significantly, with POS10-HL and POS15-HL exhibiting values of 0.57 MPa and 0.67 MPa, respectively.

Meanwhile mortars modified with nano silica (POS-HL-S series) showed even further reductions in flexural strength compared to the GOS-only specimens. POS5-HL-S recorded a flexural strength of 0.52 MPa, while POS10-HL-S and POS15-HL-S exhibited 0.49 MPa and 0.35 MPa, respectively.

6.5.2 Compressive test results

The compressive strength test was conducted to evaluate the load-bearing capacity of the repair mortars. This test is critical in the design of repair mortars in verifying their ability to provide sufficient strength to support structural loads and maintain the durability and integrity of the repaired sections. This test also assesses the compatibility of the repair mortars with the original materials in the heritage structure, as mismatched compressive strength could lead to differential stresses, cracking, and compromised structural stability.

In this case, the test was aimed at determining the influence the inclusion of GOS and nano silica on the mechanical performance of the mortars. Similar to the flexural strength test, the compressive strength test was done by subjecting the samples to an increasing uniform load of compression until the point where the samples break or crack. The maximum load under which the sample breaks was recorded and the compressive strength was determined by the expression; $f = \frac{F}{A}$ in MPa.

The final compressive strength value of each specimen was determined by the average value of the three samples tested for each mortar specimen as seen in Table 19 below.

Table 18: Determination of Compressive strength of specimen

Specimen	l (mm)	b (mm)	d (mm)	A (mm ²)	F _c - A (kN)	f _{compr,A} (MPa)	F _c - B (kN)	f _{compr,B} (MPa)	(Average) f _{compr} (MPa)
TQ-HL-1	100	40	40	1600	2.88	1.80	2.96	1.85	1.83
TQ-HL-2	100	40	40	1600	2.82	1.76	2.68	1.68	1.72
TQ-HL-3	100	40	40	1600	2.50	1.56	2.84	1.78	1.67
POS5-HL-1	100	40	40	1600	1.61	1.01	2.20	1.38	1.19
POS5-HL-2	100	40	40	1600	1.84	1.15	2.29	1.43	1.29
POS5-HL-3	100	40	40	1600	1.60	1.00	1.66	1.04	1.02
POS10-HL-1	100	40	40	1600	1.11	0.69	1.11	0.69	0.69
POS10-HL-2	100	40	40	1600	1.82	1.14	1.18	0.74	0.94
POS10-HL-3	100	40	40	1600	1.12	0.70	1.34	0.84	0.77
POS15-HL-1	100	40	40	1600	0.73	0.46	0.80	0.50	0.48
POS15-HL-2	100	40	40	1600	0.91	0.57	0.55	0.34	0.46
POS15-HL-3	100	40	40	1600	0.75	0.47	0.71	0.44	0.46
POS5-HL-S-1	100	40	40	1600	0.66	0.41	0.68	0.43	0.42
POS5-HL-S-2	100	40	40	1600	0.86	0.54	1.14	0.71	0.63
POS5-HL-S-3	100	40	40	1600	0.62	0.39	1.00	0.63	0.51
POS10-HL-S-1	100	40	40	1600	0.57	0.36	0.82	0.51	0.43
POS10-HL-S-2	100	40	40	1600	0.79	0.49	0.95	0.59	0.54
POS10-HL-S-3	100	40	40	1600	0.72	0.45	0.84	0.53	0.49
POS15-HL-S-1	100	40	40	1600	0.59	0.37	0.57	0.36	0.36
POS15-HL-S-2	100	40	40	1600	0.36	0.23	0.34	0.21	0.22
POS15-HL-S-3	100	40	40	1600	0.46	0.29	0.57	0.36	0.32

Table 19: Compressive strength of Specimens

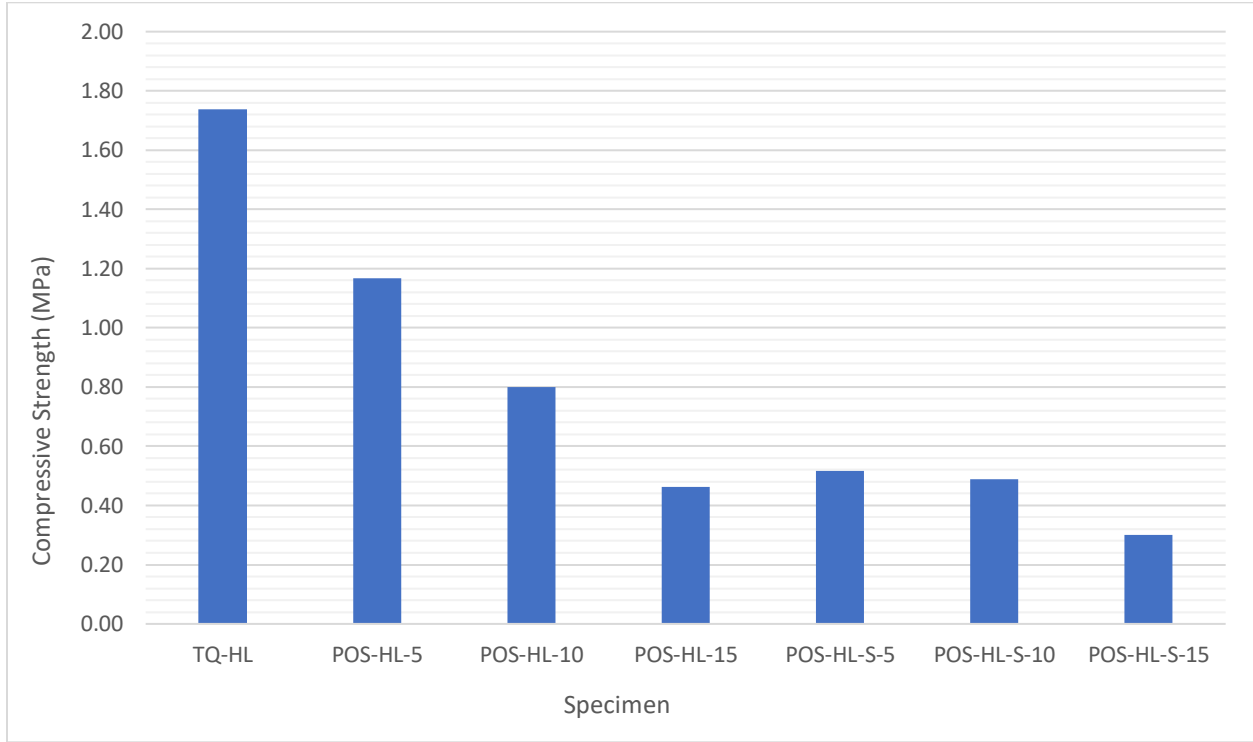


Figure 24: Graphical representation of the Specimens' compressive strength

<i>Samples</i>	<i>Compressive strength (MPa)</i>	<i>Stand. Deviation</i>
<i>TQ-HL</i>	1.74	0.08
<i>POS5-HL</i>	1.17	0.19
<i>POS10-HL</i>	0.80	0.17
<i>POS15-HL</i>	0.46	0.07
<i>POS5-HL-S</i>	0.52	0.13
<i>POS10-HL-S</i>	0.49	0.08
<i>POS15-HL-S</i>	0.30	0.07

Similar to the flexural strength test results, the results of the compressive strength reveal the reference mortar (TQ-HL) as the sample with the highest compressive strength of 1.74 MPa. The POS-HL series showed a reduction in compressive strength as GOS content increased, with POS5-HL achieving 1.17 MPa, POS10-HL recording 0.80 MPa, and POS15-HL showing a significant decline to 0.46 MPa. The nano silica-enhanced mortars (POS-HL-S series) demonstrated even lower compressive strengths compared to the GOS-only specimens, with POS5-HL-S, POS10-HL-S, and POS15-HL-S recording values of 0.52 MPa, 0.49 MPa, and 0.30 MPa, respectively.

Chapter 7: Discussion

7.1 Consistency by flow table test

The consistency test, which measured the workability of the mortar mixtures using a flow table, provides insights into the impact of GOS and nano silica on the workability of the fresh mortars. The results revealed that mortar workability decreased with the increase of GOS content. In mortar mixes with GOS, the fresh mortar became very stiff and more water was added to achieve a workable mortar.

- Effect of GOS on Workability:

The results from the test show that water demand increase with GOS. Such that the POS-HL series show an increasing water-to-binder ratio as the GOS content rises: POS5-HL: 2.21, POS10-HL: 2.27, POS15-HL: 2.30. These values are significantly higher than the reference sample which has a water-to-binder ratio of 1.75 indicating that as the proportion of GOS increases, the mortar

requires more water to achieve similar workability, a result in line with the work of Kerrai.et.al [86] whose research showed that the demand for water increased with the additive contents (Olive waste). This could attributed to the porous and organic nature of GOS as indicated by Barreca and Fichera, who mentioned that the high relative content of hemicellulose in the olive stone retards the cement hydration process [61], hence its tendency to absorb more water for ensuring proper hydration of the mortar mixture. This absorption reduces the available free water in the mortar mix, making the paste stiffer and less workable if additional water is not added. The consistency observed with the initial water content same as that of the TQ highlights the increased water demand caused by GOS's absorbent nature. The rising water-to-binder ratio for the POS-HL series demonstrates that GOS demands more water to maintain workable consistency.

- Effect of Nano Silica on Workability (POS-HL-S Series):

The results indicate a reduced water demand in the mortars containing both GOS and Nanosilica. The POS-HL-S series show a lower and consistent water-to-binder ratio of 1.88 across all GOS content levels. This ratio is notably lower than the water-to-binder ratios in the POS-HL series, where the ratios rise with increasing GOS content. This suggests that the inclusion of nano silica helps maintain workability with less water, despite the presence of GOS.

Nano silica acts as a pozzolanic material [87] and has a high surface area [88], which contributes to better particle packing and enhances the water retention capacity of the mix [89]. This leads to reduced water demand even in the presence of GOS. So the nano silica effectively might have counteracted the porous nature of GOS, allowing the mortar to achieve similar workability with less water.

Hence, while the POS-HL series without nano silica progressively needed more water to reach workable consistency as the GOS content increased, the POS-HL-S series (with nano silica)

consistently maintained a lower water-to-binder ratio, suggesting that the inclusion of nano silica in GOS-modified mortars enhances their workability without the need for excessive water, as observed in the GOS-only samples, promoting workability with less water.

7.2 Colourimetry assessment

The colourimetry assessment was conducted to examine the visual compatibility of repair mortars modified with GOS and nano silica in comparison with the reference sample. The aim was to monitor colour changes in samples containing GOS in comparison with the reference sample, ensuring that the modified repair mortars blend seamlessly with existing heritage structures, particularly when exposed to environmental factors. This analysis considers how GOS and nano silica influence the lightness (L^*), redness/greenness (a^*), and yellowness/blueness (b^*) of the mortar specimens.

- Effects of GOS on L^* (Lightness)

The reference sample (TQ) exhibits an L^* value of 88.5, representing the lightest mortar among the test samples. The following observations summarize the impact of GOS and nanosilica:

- POS5-HL: Replacing 5% of the quartz aggregate with GOS reduces the L^* value to approximately 86.4, indicating a slight darkening of the mortar.
- POS10-HL: At 10% GOS, the lightness decreases further to 84.5, confirming that additional GOS leads to darker mortars.
- POS15-HL: A 15% replacement with GOS results in an L^* value of 84.18, representing the darkest sample in the POS-HL series. In comparison to lower GOS content samples like

POS5-HL ($L^* = 86.39$), POS15-HL is noticeably darker, further supporting the trend that higher GOS content results in reduced lightness.

For the nano silica-modified counterpart (POS15-HL-S), the L value* drops further to 83.34, making it darker than the unmodified POS15-HL and the darkest sample. This shows that while nano silica helps to reduce darkening at lower GOS contents (as seen with POS5-HL-S and POS10-HL-S), it may not have the same lightening effect when the GOS content is as high as 15%.

The overall darkening effect can be attributed to the natural colour of GOS particles, which are darker than quartz aggregates. Hence as more GOS is incorporated, the lightness of the mortar decreases, regardless of whether nanosilica is added such that the higher the GOS content, the more significant the influence of its colour on the overall lightness of the mortar. These results demonstrate that increasing GOS content consistently reduces the brightness of the mortars, with nanosilica having little to no impact on the lightness.

- Effect of GOS on a^* (Green-Redness):

The a^* values provide insights into how the red or green tones of the mortars are affected by the addition of GOS, with positive a^* values representing a shift towards red and negative a^* values indicating a shift towards green. The results demonstrate that the addition of GOS has an influence on the redness of the mortar specimens. The reference sample has an a^* value of approximately 0.64, indicating a very slight shift towards the red side of the green-red axis. As the GOS content increases, the a^* values steadily rise, signifying a stronger red tint in the mortars, as seen in the following samples:

- POS5-HL: With 5% GOS, the a^* value rises to approximately 1.39, indicating a noticeable shift toward red.

- POS10-HL: With 10% GOS, the a^* value increases further to 2.05, suggesting that the mortar is becoming increasingly redder.
- POS15-HL: At 15% GOS replacement, the a^* value reaches approximately 2.3, demonstrating a significant red tint in the mortar, and the strongest red hue among the POS-HL samples.

POS5-HL-S: The inclusion of nanosilica in POS5-HL-S does not alter the red tint significantly, with an a^* value of 1.18, which is lower compared to that of POS5-HL. POS10-HL-S and POS15-HL-S maintain high a^* values that are slightly consistent with those of the POS samples without nanosilica.

- POS5-HL-S: With a^* value of 1.18 lower than that of POS5-HL
- POS10-HL-S: With a^* value of 2.24 slightly higher than that of POS10-HL
- POS15-HL-S: With a^* value of 2.66 which is higher than POS15-HL

Thus, the presence of nanosilica has little to no effect on the redness of the mortar, while increasing GOS content progressively intensifies the red tint. While nano silica can mitigate the redness at lower GOS levels, its effect is less pronounced at higher GOS concentrations, where the redness becomes more dominant.

The increase in a^* values can be explained by the reddish-brown hue of the GOS particles, which become more prominent as the GOS content increases.

- Effect of Ground Olive Stone on b^* (Blue-Yellow Axis):

The b^* values indicate the shift of the specimens on the blue-yellow axis, where positive b^* values correspond to a yellow tint, and negative b^* values indicate a shift towards blue. The results demonstrate that the addition of GOS increases the yellow tint in the mortar, while nano silica

reduces this effect to varying degrees. The reference sample in this case has a b^* value of approximately 2.48, indicating a slight yellow tint and serves as the baseline for comparison.

As the percentage of GOS increases, the b^* values also rises, indicating that the mortars are becoming more yellow as more GOS is added as seen in the progressively higher b values*.

- POS5-HL: The 5% GOS sample shows a significant increase in the b^* value of about 5.95, demonstrating that even small amounts of GOS lead to a noticeable yellowing of the mortar.
- POS10-HL: At 10% GOS, the b^* value reaches approximately 7.78, indicating a significant yellowing of the mortar.
- POS15-HL: With 15% GOS, the b^* value rises further to approximately 8.70, showing a strong yellow tint.

The POS-HL-S series, show lower b values* compared to their non-modified counterparts, indicating that nano silica helps to reduce the yellow tint to an extent.

- POS5-HL-S has a b^* value of 4.93 which is lower than the value of POS5-HL.
- POS10-HL-S with a b^* value of 6.93 also lower than POS10-HL.
- POS15-HL-S has a b^* value of 8.01 which is also lower than POS15-HL.

In all cases, the b values* for the nano silica-modified mortars are lower than those for the GOS-only specimens, indicating that nano silica mitigates the yellowing effect. However, at higher GOS content (15%), the yellow tint remains strong even with nano silica, as indicated by the b value* of 8.01 for POS15-HL-S, which is only slightly lower than the unmodified POS15-HL. Hence, the presence of nanosilica in the mortar samples does not appear to mitigate this effect very much.

However, higher GOS content results in stronger yellowing tint of the mortars likely owing to the natural colour of the olive stone particles.

- Effects of GOS and nano silica on the colour difference

The colour difference (denoted as ΔL^* , Δa^* , and Δb^*) refers to the deviation in the L^* , a^* , and b^* values between the GOS modified mortar samples and the reference sample.

As GOS content increases, the ΔL^* values become more negative, indicating that the GOS-modified mortars are darker than the reference sample. The higher the GOS content, the more pronounced the darkening effect. Nano silica helps mitigate this darkening effect at lower GOS levels (POS5-HL-S has a ΔL^* of -1.57 compared to -2.15 for POS5-HL), but this effect diminishes at higher GOS content, as seen with POS15-HL-S ($\Delta L^* = -5.20$), indicating that it is darker than even the corresponding non-modified sample POS15-HL (-4.37). This indicates that at higher GOS content (15%), the inclusion of nano silica does not lighten the sample as much as it does in the lower GOS content specimens (like POS5-HL-S or POS10-HL-S). In fact, it seems to amplify the darkening effect, possibly due to an interaction between the higher GOS content and nano silica at this concentration, which could affect the light-reflecting properties of the specimen. This suggests a potential non-linear relationship between GOS content and nano silica modification, particularly in terms of lightness (ΔL^*), where at higher GOS concentrations, the addition of nano silica may not mitigate darkening as effectively as it does at lower concentrations.

In addition, as GOS content increases, the redness increases as well (positive Δa^* values). This shift towards the red axis is a result of the natural coloration of the olive stone particles. Nano silica reduces the redness for lower GOS content (as seen in POS5-HL-S), but at higher GOS

content, the redness intensifies even in the presence of nano silica (e.g., POS15-HL-S has a Δa^* of 2.02, more than POS15-HL's 1.69).

Furthermore, GOS significantly increases yellowness, as seen from the progressively higher Δb^* values with increasing GOS content. Nano silica reduces this yellowness across all GOS content levels, though the effect diminishes a little at higher GOS contents. For instance, POS15-HL-S is still quite yellow with a Δb^* of 5.53, though less than POS15-HL's 6.22.

- Effects of GOS and Nano silica on the Total Colour difference (ΔE).

The Total Colour Difference (ΔE) is a key metric used to quantify the overall difference in colour between two samples, combining the variations in lightness (L^*), redness/greenness (a^*), and yellowness/blueness (b^*). In this case, the ΔE is calculated to compare each of the GOS and nano silica-modified samples with the reference sample. Such that a higher ΔE value indicates a greater overall colour difference.

In the POS-HL series, as GOS content increases, the total colour difference (ΔE) rises, indicating that the specimens become increasingly different from the reference sample in terms of appearance. While the POS-HL-S series with nano silica generally shows lower ΔE values compared to their GOS-only counterparts, indicating that nano silica helps reduce the total colour difference. However, at higher GOS content (POS15-HL-S), the ΔE value remains high (30.86), even slightly higher than that of POS15-HL (30.32). This suggests that at high GOS levels, nano silica is less effective in mitigating the overall colour difference.

The results highlight several significant trends when comparing the different mortar specimens containing GOS and Nano Silica to the reference sample providing insights into the visual and aesthetic implications of introducing GOS into the mortar mixtures, which is crucial for heritage

conservation. Thus, the reference sample which is the lightest among all specimens, indicate a higher light reflectance, while the samples containing GOS tend to darken progressively as the GOS content increases. This darkening trend is evident in both the unmodified and nano silica-modified mortars. As the GOS percentage rises from 5% to 15%, the mortars become progressively darker, with the POS15-HL-S specimen (with 15% GOS and nano silica) being the darkest of all.

Also, the introduction of GOS leads to noticeable changes in the redness and yellowness of the mortars. Such that as the GOS content increases, the mortars shift towards a redder and yellower hue compared to the reference sample. This is reflected in the positive Δa^* and Δb^* values across the specimens. Mortars with nano silica tend to exhibit slightly lower redness and yellowness compared to their unmodified counterparts.

The total colour difference (ΔE), which represents the overall visual difference between the specimens and the reference sample, increases as more GOS is added. This suggests that higher GOS content creates a more distinct visual deviation from the original material. However, the nano silica-modified samples generally show smaller total colour differences at lower GOS content levels. This effect diminishes at 15% GOS, where the nano silica-modified sample exhibits a slightly higher total colour difference than the unmodified sample, indicating a potential limit to nano silica's ability to mitigate colour differences at higher GOS levels.

Despite these differences, the colour variance remains subtle enough to maintain aesthetic harmony, ensuring compatibility of the GOS modified repair mortar with the appearance of the reference samples. The concept of "aesthetic harmonization" in historic masonry repair refers to the goal of making repair mortars visually compatible with the original structure [90]. This compatibility is not limited to colour; it also includes factors like texture, surface finish, and the overall visual effect of the new mortar alongside aged materials. Successful harmonization

maintains the aesthetic integrity of the original structure, so the new materials blend with the old, making repairs less noticeable and preserving the historical character of the site.

In this case, despite slight colour differences with the GOS-modified samples, they still appear visually cohesive enough to meet aesthetic harmonization requirements. It is common for some colour variance to occur, especially as the most historical mortars undergo exposure to environmental factors over time. Therefore, as long as the new mortar is not excessively different in appearance, these subtle differences should not detract from the harmony with the original structure.

7.3 Salt Crystallization tests - Results

The salt crystallization tests subjected various mortar specimens to 15 cycles of wet and dry conditions, simulating the stress that occurs in real-world environments where salts crystallize within building materials, leading to potential structural degradation. The test results provide insights into the durability of mortars modified with GOS and nano silica under these aggressive conditions.

In a 15-cycle salt crystallization test, mortars modified with GOS and nano silica were evaluated against a reference sample (TQ-HL) to assess durability under wet-dry conditions. The reference mortar (TQ-HL) showed initial mass gain but significant mass loss after the 10th cycle as indicated in Figure 26, maintaining structural integrity despite an average -4.53% mass difference by the 15th cycle (Figure 25), highlighting its relative durability.



Figure 26: TQ samples after the 10th cycle showing signs of exfoliations



Figure 25: TQ samples after the 15th cycle showing significant material loss at the end of the test

GOS-modified mortars (POS-HL series) exhibited higher initial mass gain, indicating greater salt absorption due to increased porosity from GOS. The fact that the POS-15-HL had the highest mass increase indicate its high porosity, hence its ability to adsorb more water by capillary action which in this case contains salts. However, they experienced rapid degradation in later cycles, with specimens containing higher GOS disintegrating sooner; POS15-HL completely failed by the 12th cycle (Figure 27) , with an average of -7.61% mass loss, showing GOS's detrimental impact on salt resistance.

Nano silica-modified mortars (POS-HL-S series) performed better initially by reducing water and salt absorption, showing lower initial mass gain than GOS-only mortars possibly due to the fact that some of the pores may have been filled by the nanosilica which is known to have a filler effect in mortars thereby reducing the amount of salt solution accumulated.



Figure 27: POS-15-HL after the 12th cycle showing a complete disintegration

Despite this, none survived past the 11th cycle without disintegration of some of its samples; POS10-HL-S, for instance, showed an average mass loss of 0.07% by the end of the 11th cycle with the last of its sample disintegrating after the 12th cycle (Figure 29). While POS-5-HL-S with an average mass loss of -7.58 after the 11th cycle with the last of its sample completely disintegrating at the end of the 14th cycle (Figure 28).



Figure 29: POS-10-HL-S after the 12th cycle completely disintegrated



Figure 28: POS-5-HL-S after completely disintegrated after the 14th cycle

Although nano silica improved early durability, it ultimately did not prevent long-term damage. This could be attributed to the reduced pore sizes in the nano silica modified samples, as opined by Benavente.et.al who mentioned that the salt crystallization pressure is greater materials with smaller pores, than in those with larger pores, causing minerals to precipitate deeper below the stone's surface, forming subflorescence [78].

In comparison, while the GOS-only samples absorbed more salt and deteriorated faster, the nano silica-modified specimens delayed mass loss but still failed over time. Thus, GOS reduces

durability under salt exposure, and while nano silica provides some short-term improvement, though neither modification surpasses the reference sample's resistance to salt weathering.

- Performance of the Reference Sample (TQ-HL):

With the TQ-HL serving as the baseline for comparison, the results indicate it experienced consistent mass gain during the initial cycles while showing early signs of tiny salt crystallisation on the surface (efflorescence) and minor blisters as early as after the 3rd cycle (Figure 30) , peaking at around 12.73% after the 9th cycle just before it starts to lose weight after the 10th cycle.



Figure 30: TQ samples showing signs of minor blistering and tiny salt crystals on its surface after the 3rd cycle of the salt crystallization cycle

However, it suffered significant mass loss in the later cycles, particularly after the 10th cycle, where the mass difference dropped to 11.02%, ultimately ending at -4.53% by the 15th cycle. Despite the initial signs of efflorescence on the reference samples and the subsequent blistering and detachments, all TQ-HL samples survived all 15 cycles, with the substantial reduction in mass

due to material loss. This suggests that even traditional mortar is vulnerable to prolonged salt crystallization, leading to structural weakening.



Figure 31: Visible detachment on the TQ-HL samples after the 5th cycle of the salt crystallisation test

- Effect of GOS on the Durability of Mortar (POS-HL Series):

All the just GOS-modified specimens (POS5-HL, POS10-HL, POS15-HL) experienced mass gain during the initial cycles, similar to the TQ-HL sample. This mass gain is attributed to salt accumulation within the pores of the mortar as the salts crystallized during the wet and dry cycles. As the GOS content increased, so did the mass gain. For example, POS15-HL showed the highest mass increase, with 5.46% after the 1st cycle and peaking at 16.20% by the 7th cycle, compared to 12.52% for the reference sample in the same period.

However, after the 5th cycle, all GOS-modified specimens began to lose mass, with more severe mass loss as the cycles progressed. For example: POS5-HL dropped from 13.37% in the 7th cycle to 9.23% after the 10th cycle, and by the 15th cycle, it had a final relative mass difference of -14.77% as a result of significant structural degradation. POS10-HL also followed this trend,

disintegrating before the 15th cycle, with one of its samples breaking after the 13th cycle, leaving it with a mass loss of -3.80% by the 13th cycle. POS15-HL experienced the worst degradation, with a sharp drop in mass starting from the 10th cycle, ending with -51.59% by the 12th cycle when it disintegrated.

The high water demand of GOS due to its absorbent and porous nature likely contributed to its poor performance under salt crystallization stress. The increasing mass gain in the early cycles indicates that GOS allowed for more salt solution accumulation, which, while contributing to short-term mass gain, exacerbates long-term structural damage. The fact that the specimens with higher GOS content (like POS15-HL) disintegrated earlier suggests that increased GOS makes the mortar more porous, hence its ability to absorb more water by capillarity which in this case contains salt, thereby reducing the mortar's resistance to salt crystallization.

- Effect of Nano Silica on Durability (POS-HL-S Series)

The POS-HL-S series, modified with both GOS and nano silica, showed improved initial performance compared to the GOS-only specimens, but they also ultimately disintegrated before completing all 15 cycles. The nano silica-modified specimens exhibited lower initial mass gain compared to their non-modified counterparts. For example: POS5-HL-S gained only 1.77% after the 1st cycle, compared to 3.81% for POS5-HL. Similarly, POS10-HL-S and POS15-HL-S showed less mass gain in the early cycles, suggesting that nano silica helps limit the absorption of moisture and salts in the initial stages. Unlike the reference samples, the POS-HL-S series did not show early signs of tiny salt crystals on the mortar surfaces and showed no signs of blisters in the early cycles.



Figure 32: POS-HL-S series showing no signs of suffering the salt weathering test after the 3rd cycle as compared to the TQ-HL below



Figure 33: TQ-HL showing early signs of blistering after the 3rd cycle.

Despite their improved performance in the initial cycles, the POS-HL-S specimens eventually began to lose mass.

None of the nano silica-modified samples survived beyond the 11th cycle, for, POS5-HL-S survived until cracking after the 10th cycle (Figure 34) with 1.90% average relative mass difference, and completely disintegrating by the 11th cycle. POS10-HL-S followed a similar trajectory, with mass loss accelerating after the 7th cycle, and by the 12th cycle (Figure 35), it had

dropped to -18.75%, disintegrating shortly after. POS15-HL-S also saw early failure, disintegrating after the 12th cycle (Figure 36) with a mass loss of -13.37%.



Figure 34: POS-5-HL-S after the 10th cycle



Figure 35: The last sample of POS-10-HL-S disintegrating after the 12th cycle

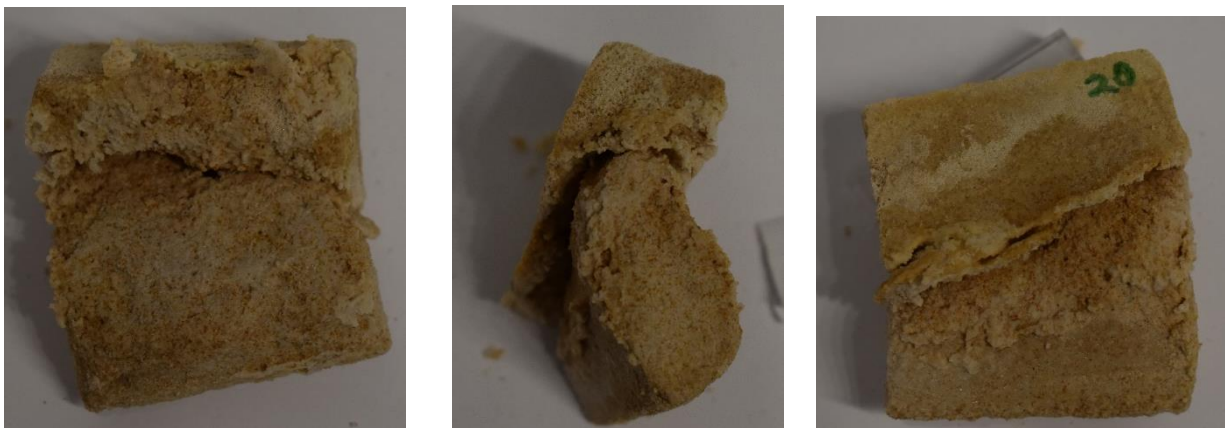


Figure 36: The last sample of POS-15-HL-S disintegrating after the 12th cycle

The inclusion of nano silica clearly improved the mortar's resistance to salt crystallization in the initial stages by reducing moisture absorption but did not offer sufficient protection under prolonged or extreme conditions. As suggested by La Russa et. al. [91], the durability of stone under salt crystallization is influenced by environmental conditions and pore size distribution, which controls fluid movement within the material, with smaller pores leading to greater pressure from growing salt crystals, increasing the potential for damage.

In this context, the nano silica may have contributed to increased mortar durability by partially filling pore spaces, thereby reducing initial salt solution uptake. However, this pore-filling effect may have also hindered the complete evaporation of the solution, leading to salt crystallization within the mortar's pore network. After extended exposure to salt crystallization cycles, this internal crystallization likely exerted pressure on the pore walls, eventually causing deterioration and disintegration of the mortar.

- Comparison Between GOS-Only and Nano Silica-Modified Specimens

The observed differences in durability between the POS-HL and nano silica-modified series under salt crystallization stress likely stem from the ways in which GOS and nano silica affect the pore structure and behaviours of the mortars. The POS-HL series, with increasing GOS content, tends to have a more open pore structure. While this initially allows for rapid absorption of the salt solution, it also leaves the material more vulnerable to salt crystallization pressures as salts accumulate and crystallize within these larger, interconnected pores. As the crystallization cycles progress, these stresses cause structural breakdown, leading to mass loss and disintegration. Hence the possible reason for the higher initial mass gain but severe mass loss and disintegration in later cycles. The higher the GOS content, the faster the specimens disintegrated under salt

crystallization stress with just two samples of lower GOS content mortar (POS-5-HL) surviving until the 15th cycle.

The nano silica-modified mortars on the other hand displayed less initial mass gain and improved durability in the early cycles, but they still failed to survive beyond the 11th or 12th cycle. Nano silica modifies the pore structure by acting as a filler, reducing the initial intake of the salt solution. This effect likely contributed to the lower initial mass gain and improved durability in early cycles, as nano silica reduces the accessible pore space for salt solution ingress. However, this partial filling of pores can also trap moisture and salts within the mortar structure, hindering the complete evaporation and migration of salts out of the material. When salts crystallize within these partially filled pores, the pressures exerted on the pore walls become concentrated, which can still lead to damage under prolonged cycles, as seen in the mortars' failure beyond the 11th or 12th cycle.

The salt crystallization test results highlight the varying degrees of resistance to salt weathering among the different mortar specimens. The reference mortar demonstrated the highest resilience throughout the test, surviving all cycles whereas the GOS-modified mortars, particularly those with higher GOS content, exhibited more pronounced degradation, with many disintegrating before the completion of the test.

This indicates that the inclusion of GOS, while potentially offering environmental benefits and reducing the density of the mortar, tends to reduce its resistance to salt crystallization due to its porous characteristics. Nano silica-modified mortars performed better than GOS-only samples, with delayed mass loss and slightly extended durability, suggesting that nano silica enhances bonding and stability against salt crystallization. However, even nano silica-modified mortars ultimately succumbed to prolonged salt exposure.

Therefore, although GOS-modified mortars may be viable for reducing environmental impact and lightening the mortar, they may exhibit weaker performance in environments subjected to salt weathering. And while the inclusion of nano silica provides some level of improvement, it does not fully prevent the damage caused by salt crystallization.

7.4 Water absorption by capillarity

The water absorption by capillarity tests were aimed at evaluating the permeability and porosity of the mortar specimens which are crucial characteristics for mortars used in the conservation and restoration of heritage structures. The test compared traditional repair mortars composed of 100% quartz aggregates with new designs incorporating GOS and nano silica.

The reference specimen demonstrated a moderate rate of water absorption in the initial stages of the test reaching a near-saturation point after approximately 24 hours, with minimal further water absorption after that time. This behaviour indicates the mortar's relatively low capillarity limited porosity. Meanwhile water absorption for POS5-HL, POS10-HL, and POS15-HL increased in direct proportion to the amount of GOS included. POS15-HL exhibited the highest level of water absorption while POS5-HL absorbed less water than POS15-HL, but still more than the reference mix, indicating that even a small percentage of GOS increases water absorption. The increased water absorption in the GOS-modified specimens suggests that GOS introduces additional porosity into the mortar matrix, allowing for greater capillary action.

Meanwhile, when nano silica was added to the GOS-modified specimens, the water absorption behaviour changed noticeably. Nano silica, known for its fine particle size and high surface area, can fill the micro-pores within the mortar, reducing overall permeability. This effect is evident in

the reduced water absorption observed in POS5-HL-S, POS10-HL-S, and POS15-HL-S compared to the non-silica mortars. For instance, POS15-HL-S absorbed less water than POS15-HL, indicating that nano silica blocked some of the capillary pathways, reducing the overall porosity of the mortar. This suggests that the combination of GOS and nano silica provides a balance between porosity and reduced capillary action, which could be beneficial for applications requiring both breathability and moisture resistance.

In comparison with the reference sample, the following observation can be made from the data:

- Effect of GOS: The inclusion of GOS increases water absorption across all specimens. The higher the percentage of GOS, the greater the water absorption, reflecting the increased porosity of the material.
- Effect of Nano Silica: Nano silica effectively reduces water absorption by filling pores in the mortar matrix. The nano silica-modified specimens show a lower water absorption rate, indicating reduced permeability. This suggests that nano silica can improve the material's resistance to water absorption while maintaining the benefits of GOS.
- Material Performance: POS15-HL, with 15% GOS, absorbed the most water, indicating high permeability and porosity. However, POS15-HL-S, with both GOS and nano silica, demonstrated a balance between increased porosity and reduced permeability.

The test showed that the reference sample reaches near-saturation more quickly and absorbs less water overall than the GOS-modified samples. This reinforces its suitability for applications where lower permeability is necessary. However, the higher long-term absorption of GOS-modified mortars suggests their use in heritage conservation could improve the breathability of structures, provided the environment is not excessively wet.

The results reveal the trade-offs between breathability and moisture resistance. The traditional repair mortars, while effective in preventing excessive moisture absorption, may not allow the structure to "breathe" as efficiently. On the other hand, the GOS-modified mortars, especially those with higher GOS content, offer enhanced breathability but require careful consideration of the environment's moisture levels to avoid potential damage from prolonged exposure to water. The incorporation of nano silica shows a promising balance of these characteristics, reducing overall water absorption while maintaining the benefits of GOS in enhancing breathability, hence offering an effective solution to mitigate some of the permeability issues and providing a more balanced approach to moisture management in restoration projects and heritage conservation applications where both permeability and durability are essential.

7.5 Mechanical tests

The flexural and compressive strength tests provided insights into the mechanical performance of the mortar specimens, which are critical for assessing their suitability for built heritage conservation. The reference sample (TQ-HL), made of 100% quartz aggregates, consistently exhibited the highest flexural and compressive strengths. In the flexural strength tests, the inclusion of GOS led to a reduction in strength as the GOS content increased, with the highest performance observed in POS5-HL, which closely matched the reference sample.

The decline in flexural strength was more pronounced in samples with higher GOS content, such as POS10-HL and POS15-HL, possibly due to the increased porosity introduced by the GOS. The addition of nano silica further reduced flexural strength across all GOS-modified samples,

suggesting that while nano silica improves durability by reducing permeability, it may negatively impact tensile properties when combined with GOS.

In the compressive strength tests, a similar trend was observed. The reference sample achieved the highest average compressive strength of 1.74 MPa, while the GOS-modified mortars showed progressively lower strengths as the GOS content increased. The POS5-HL sample demonstrated moderate compressive strength, but as GOS content increased to 15%, the strength dropped significantly, indicating that higher GOS content might have introduced voids and reduced the mortar's ability to bear axial loads.

The nano silica-modified mortars exhibited the lowest compressive strengths, which could be attributed to changes in the stress distribution within the mortar matrix due to a combination of factors related to the challenges of achieving uniform dispersion of nano silica in the presence of GOS, which introduces additional porosity and structural discontinuities in the matrix.

In a review by ALTawaiha.et.al, it was opined that even though adding nano-silica to concrete mixtures decreases porosity and enhances its pozzolanic interaction with calcium hydroxide, leading to the production of CSH and improved mechanical performance, researchers however caution the against the use of excessive amounts of nano-silica, as it may cause particle aggregation within the cement matrix, weakening the bonds in its internal structure [92]. However, the reduction in mechanical strength observed in this study cannot be attributed to an excessive use of nano-silica, as it was applied in a diluted form. The Nano Estel was diluted with distilled water at a ratio of 2:1 and subsequently incorporated into the GOS at a ratio of 0.35 relative to the quantity of GOS.

Another research by Dilbas.et.al, [93], emphasized that the strength of concrete is primarily influenced by the strength of its aggregates, the cement matrix, and the interfacial transition zone (ITZ) between them. Their research revealed that, after 28 days of curing, mortar mixes incorporating recycled aggregates and silica fume demonstrated a significant reduction in compressive strength compared to natural aggregate concrete. They attributed this short-term reduction to the presence of cracks and impurities in the recycled aggregates, which hinder the effectiveness of silica fume as these impurities weaken the bond between the cement matrix and the aggregates, thereby diminishing the pozzolanic and filler effects of silica fume. Despite the initial decrease in compressive strength, the researchers concluded that the healing and densification properties of silica fume could, over time, improve the strength and durability of the concrete.

In this research, the samples containing GOS and nano silica exhibited decreased mechanical strength, despite the known filler effect of nano silica. This outcome can be explained by considering the findings of studies such as that by Dilbas.et al. [93], which emphasize the impact of impurities and cracks within recycled aggregates on the performance of concrete. GOS, as a recycled organic material, likely introduces inherent porosity, into the mortar matrix. This characteristic disrupts the bond between the aggregates and the cementitious matrix, potentially weakening the overall structure.

Although nano silica is known for its pozzolanic and filler effects, which reduce porosity and improve the bond between the binder matrix and aggregates, its effectiveness in this case may have been limited by these structural deficiencies introduced by the GOS aggregates in this case, whose porous nature could have contributed to a weaker interfacial transition zone (ITZ) between the aggregates and the binder matrix, diminishing the ability of nano silica to effectively strengthen

the structure. Furthermore, these flaws can act as stress concentration points, reducing both flexural and compressive strength, aligning with the research findings of Dilbas.et.al. [93].

Additionally, if nano silica is not uniformly distributed within the matrix, particle aggregation may occur, further weakening the internal bonds and contributing to the reduction in mechanical strength as indicated by Li et al [94]. Li et al. noted that the uneven distribution of nano silica within the matrix can lead to particle aggregation, weakening internal bonds and reducing mechanical strength. In their study, despite containing the same quantity of nano-particles, NTC1 (a concrete mix with 1% nano-TiO₂ by weight of binder) showed superior flexural fatigue performance compared to NSC1 (a concrete mix with 1% nano-SiO₂ by weight of binder). This difference was then attributed to the specific surface area of the nano-particles. The study indicated that nano-SiO₂ has a larger specific surface area than nano-TiO₂, making it more difficult to achieve uniform dispersion within the cement paste, thus increasing the likelihood of particle aggregation for nano-SiO₂, weakening the cement matrix and adversely affecting its mechanical performance.

The explanation provided by Li et al. can be applied to understand the decrease in mechanical strength of the POS-HL-S series in this research. The reduction in mechanical strength can be attributed to a combination of factors related to the challenges of achieving uniform dispersion of nano silica in the presence of GOS, which introduces additional porosity and structural discontinuities in the matrix. Nano silica is highly effective at enhancing concrete's mechanical properties when evenly distributed, as it reacts “pozzolanically” with calcium hydroxide to form calcium silicate hydrate (C-S-H), which densifies the cement matrix. However, as noted in Li et al.'s study, nano silica has a very high specific surface area, making it challenging to disperse uniformly in the matrix, especially when combined with porous materials like GOS. As a result,

the nano silica particles are more likely to aggregate, forming clumps that can act as stress concentration points within the mortar matrix.

These aggregated nano silica particles create weak zones that disrupt the matrix's integrity, reducing the ability of the material to resist mechanical stresses. This effect is similar to the observations in Li et al.'s study, where concrete with nano-SiO₂ exhibited lower flexural fatigue performance compared to nano-TiO₂ due to the larger specific surface area of nano-SiO₂, which led to increased particle aggregation. In the case of POS-HL-S mortars, the combined effects of GOS-induced porosity and nano silica aggregation might have weakened the interfacial transition zone (ITZ) and reduced the bond strength between aggregates and the cement paste, further contributing to the decline in mechanical performance.

Therefore, the decrease in mechanical strength of the GOS- and nano silica-modified specimens can be attributed to the same principles identified by Li et al.—the challenges of dispersing nano silica uniformly and the formation of particle aggregates that weaken the matrix—compounded by the possible additional porosity and discontinuities introduced by GOS.

Chapter 8:

Conclusions

This research investigated the potential for incorporating Ground Olive Stones (GOS) as a sustainable alternative to traditional aggregates in the production of repair mortars for the conservation of built heritage. Grounded in the need for sustainable practices in the construction and restoration industry, the study focused on determining whether agricultural waste, particularly GOS, could be effectively utilized without compromising the structural integrity of historical materials. This research aimed to explore the potential of incorporating GOS as a sustainable alternative to traditional aggregates in lime-based repair mortars for built heritage conservation.

To achieve this aim the study investigated the effects of varying proportions of GOS on various properties of the mortars, including workability, colorimetric properties, water absorption by capillarity, and durability against salt crystallization. Nano-silica was also introduced in some mixtures to enhance the properties of GOS-containing mortars. The findings of this research contribute to the ongoing search for sustainable building materials that can effectively balance the preservation of heritage structures with issues of environmental concerns.

The primary objective of this research was to evaluate the viability of using GOS as a partial replacement for natural quartz aggregates in repair mortars while ensuring that the performance characteristics of the mortars remained compatible with the requirements of conservation. This was pursued through the preparation and testing of seven different mortar mixtures with varying proportions of GOS from 5% to 15% as partial replacements for quartz aggregates. Additionally, nano-silica was introduced into some formulations to enhance their properties.

The study set out to first evaluate the workability of mortars containing GOS. The consistency tests conducted via the flow table method indicated that the inclusion of GOS increases the mortar's water demand, as GOS-modified samples showed higher water-to-binder ratios, which points to reduced workability. Nano silica, however, helps to maintain workability by reducing water demand, particularly in lower GOS-content samples. This suggests nano silica can counteract the stiffening effect of GOS due to its high surface area and pozzolanic activity, aiding in particle packing and water retention

Secondly the colorimetric analysis revealed that increasing the GOS content led to darker mortars with noticeable shifts towards red and yellow hues. As GOS content rises, the mortar darkens and shifts towards red and yellow hues, primarily due to the natural colour of GOS particles. Nano silica mitigates these effects at lower GOS levels, although at 15% GOS, nano silica's impact on colour reduction diminishes, potentially due to limitations in its ability to counteract the high pigmentation of GOS. However, the colour differences between GOS-modified samples and the reference sample remain within acceptable limits for aesthetic harmonization, ensuring compatibility with historical materials while avoiding a stark visual deviation

In addition, investigating the impact of GOS on the durability of the mortars, through an accelerated weathering specifically in terms of salt crystallization resistance, revealed that GOS-modified samples, especially at higher GOS content, absorb more salt and are more susceptible to structural breakdown under cyclic salt crystallization stress. Nano silica helps improve early-cycle durability by limiting initial salt and water absorption, but it does not fully prevent disintegration under prolonged exposure. Mortars with lower GOS content performed better, but the results indicated that careful optimization of the GOS proportion is crucial to ensuring durability. The

introduction of nano-silica showed potential for enhancing the durability of these mortars, though its effect on salt crystallization resistance requires further investigation.

Also, the assessment of the water absorption by capillarity properties of the synthesised repair mortars indicated that GOS increases the porosity and water absorption capacity of the mortars, which could enhance breathability but also increases vulnerability to moisture. Nano silica reduces permeability by filling micro-pores, balancing the need for breathability and moisture resistance. The results indicate that GOS-modified mortars with nano silica could be suitable for applications where both breathability and moderate water resistance are required, though they may not be ideal for highly salt-exposed environments. The trade-off between porosity and durability must be carefully considered in conservation applications of repair mortars containing GOS.

Lastly, the mechanical tests conducted on the mortar specimens indicated that the inclusion of GOS in the repair mortars resulted in a progressive decline in mechanical strength as the GOS content increased. This decline is likely attributed to the increased porosity introduced by GOS, which weakens the bond between the aggregates and the cement matrix. Notably, the POS5-HL sample exhibited mechanical properties closest to the reference sample, indicating that lower GOS content balances sustainability with performance.

While nano silica is known for its pozzolanic and filler effects, its effectiveness was limited in the GOS-modified mortars possibly due to challenges in achieving uniform dispersion. The high specific surface area of nano silica increased the likelihood of particle aggregation, forming weak zones that may have compromised the matrix. These aggregated particles, combined with the porosity from GOS, possibly disrupted the interfacial transition zone (ITZ), reducing both flexural and compressive strengths. The findings align with previous research, which highlights that impurities and weak ITZs in recycled aggregates hinder the effectiveness of nano silica. This

underscores the need for optimizing mix designs and dispersion techniques to balance mechanical performance with sustainability in repair mortars for heritage conservation.

The use of agricultural waste such as GOS in lime-based mortars aligns with the growing emphasis on sustainable construction materials. By partially replacing traditional quartz aggregates with GOS, this research contributes to the reduction of waste and the promotion of a circular economy. However, the findings also underscore the importance of balancing sustainability with performance. In that, while GOS offers environmental benefits, its impact on the durability of repair mortars, particularly in saline environments, must be carefully considered to ensure that the long-term preservation goals of heritage conservation are not compromised.

Furthermore, the long-term performance of the mortars in real-world environments needs to be evaluated. Exposure to varying environmental conditions such as temperature fluctuations, humidity, and biological growth could affect the durability of GOS-based mortars in ways that were not captured in this study.

However, this research at least represents a significant step towards the development of sustainable repair mortars for heritage conservation. The incorporation of GOS as a partial replacement for quartz aggregates in lime mortars presents both opportunities and challenges such that while GOS contributes to sustainability by reducing the reliance on natural aggregates and repurposing agricultural waste, it also introduces complexities related to workability, aesthetic compatibility, and durability, hence the need for careful formulation and optimization of GOS-containing mortars to ensure that they meet the specific requirements of conservation projects.

Bibliography

- [1] ICOMOS International Scientific Committee for Stone (ISCS), “Illustrated glossary on stone deterioration patterns,” France, 2008.
- [2] U. J. Alengaram, B. A. A. Muhit and M. Z. b. Jumaat, “Utilization of oil palm kernel shell as lightweight aggregate in concrete – A review,” *Construction and Building Materials*, vol. 38, pp. 161-172, 2013.
- [3] V. M. Malhotra and P. Mehta, High-performance, high-volume fly ash concrete: materials, mixture proportioning, properties, construction practice, and case histories, Canada, 2002.
- [4] S. Luhar, T.-W. Cheng and I. Luhar, “Incorporation of natural waste from agricultural and aquacultural farming as supplementary materials with green concrete: A review,” *Composites Part B: Engineering*, vol. 175, 2019.
- [5] Z. Chen, W. Ge and L. Xu, “A review of mechanical properties and carbonation behavior evolution of lime mortar for architectural heritages restoration,” *Minerals and Mineral Materials*, vol. 3, 2024.
- [6] C. Groot, R. Veiga, I. Papayianni, R. Hees, M. Secco, J. Alvarez, P. Faria and M. Stefanidou, “RILEM TC 277-LHS report: lime-based mortars for restoration—a review on long-term durability aspects and experience from practice,” *Materials and Structures*, vol. 55, 2022.
- [7] P. Maravelaki-Kalaitzaki, A. Bakolas and A. Moropoulou, “Physico-chemical study of Cretan ancient mortars,” *Cement and Concrete Research*, vol. 33, no. 5, pp. 651-661, 2003.

- [8] S. Andrejkovičová, E. Ferraz, A. L. Velosa, A. S. Silva and F. Rocha, “Fine sepiolite addition to air lime-metakaolin mortars,” *Clay Minerals*, vol. 46, no. 4, pp. 621-635, 2011.
- [9] *ASTM C618: Standard specification for fly ash and raw or calcined natural pozzolan for use as a mineral admixture in Portland cement concrete*, West Conshohocken(PA, USA): ASTM International, 2003.
- [10] “Natural pozzolans,” Global cement and concrete association, [Online]. Available: <https://gccassociation.org/cement-and-concrete-innovation/clinker-substitutes/natural-pozzolans/>. [Accessed 29 April 2024].
- [11] L. Kampf, “Factors Affecting Bond of Mortar to Brick,” in *Symposium on Masonry Testing*, ASTM International, 1963, p. 127.
- [12] D. Young, “Heritage Council Victoria,” 2021. [Online]. Available: https://heritagecouncil.vic.gov.au/research-projects/technicalguide_mortars/. [Accessed 14 May 2024].
- [13] P. C. Association, “Aggregates,” 2024. [Online]. Available: <https://www.cement.org/cement-concrete/concrete-materials/aggregates>. [Accessed 08 06 2024].
- [14] P. S. Engineering, “The Effect of aggregate properties on concrete,” [Online]. Available: https://www.engr.psu.edu/ce/courses/ce584/concrete/library/materials/aggregate/aggregates_main.htm. [Accessed 08 06 2024].
- [15] L. V. Fishera and A. R. Barron, “The recycling and reuse of steelmaking slags — A review,” *Resources, Conservation & Recycling*, vol. 146, pp. 244-255, 2019.

- [16] Y. kocak, “A study on the effect of fly ash and silica fume substituted cement paste and mortars,” *Academic journals*, vol. 5, no. 9, pp. 990-998, 2010.
- [17] “Quartz,” AR Commerce , [Online]. Available: <https://arcommerce.bg/en/>. [Accessed 30 July 2024].
- [18] Q.-Y. Cao, S.-H. Wei, Q.-Y. Shao, S. U. Shar and K.-R. Zheng, “Effect of Feldspar Dissolution on Alkali–Silica Reaction at Elevated Temperatures,” *Journal of Materials in Civil Engineering*, vol. 33, no. 11, p. 04021307, 2021.
- [19] T. M.D.A. and F. K.J., “7 - Concrete aggregates and the durability of concrete,” in *Durability of Concrete and Cement Composites*, Woodhead Publishing, 2007, pp. 247-281.
- [20] C. Gillot and A. Coutelas, “Cements, Mortars, Binders,” *The SAS Encyclopedia of Archaeological Sciences (Ed.: Sandra L. López Varela)*., 2018.
- [21] J. (. Aquiline, “Types of Masonry Binders,” Limeworks.us, 2023. [Online]. Available: <https://www.limeworks.us/types-of-masonry-binders/#:~:text=There%20are%20four%20main%20binders,which%20are%20derived%20from%20limestone..> [Accessed 08 06 2024].
- [22] R. Malathy, R. Shanmugam, D. Dhamotharan, D. Kamaraj, M. Prabakaran and J. Kim, “Lime based concrete and mortar enhanced with pozzolanic materials – State of art,” *Construction and Building Materials*, vol. 390, no. 131415, 2023.
- [23] G. ESCADEILLAS, C. MAGNION, S. AMZIANE and V. NOZAHIC, “Binders,” *Bio-aggregate-based Building Materials: Applications to Hemp Concretes*, pp. 75-116, 2013.

- [24] P.-N. Maravelaki, K. Kapetanaki, I. Papayianni, I. Ioannou, P. Faria, J. Alvarez, M. Stefanidou, C. Nunes, M. Theodoridou, L. Ferrara and L. Toniolo, “RILEM TC 277-LHS report: additives and admixtures for modern lime-based mortars,” *Materials and Structures*, vol. 56, no. 5, 2023.
- [25] D. Christos, M. Zervaki, K. Sideris, M. Juenger, N. Alderete, S. Kamali-Bernard, Y. Villagrán and R. Snellings, “Natural Pozzolans,” in *Properties of Fresh and Hardened Concrete Containing*, RILEM State-of-the-Art Reports, 2017, pp. 181-231.
- [26] R. Firdous, D. Stephana and J. N. Y. Djjobob, “Natural pozzolan based geopolymers: A review on mechanical, microstructural and durability characteristics,” *Construction and Building Materials*, vol. 190, pp. 1251-1263, 2018.
- [27] C. Rispoli, A. D. Bonis, V. Guarino, S. F. Graziano, C. D. Benedetto, R. Esposito, V. Morra and P. Cappelletti, “The ancient pozzolanic mortars of the Thermal complex of Baia (Campi Flegrei, Italy),” *Journal of Cultural Heritage*, vol. 40, pp. 143-154, 2019.
- [28] E. García-Taengua, M. Sonebi, K. Hossain, M. Lachemi and J. Khatib, “Effects of the addition of nanosilica on the rheology, hydration and development of the compressive strength of cement mortars,” *Composites Part B: Engineering*, vol. 81, pp. 120-129, 2015.
- [29] D. Shanmugavel, P. KumarYadav, M. A. Khadimallah and R. Ramadoss, “Experimental analysis on the performance of egg albumen as a sustainable bio admixture in natural hydraulic lime mortars,” *Journal of Cleaner Production*, vol. 320, p. 128736, 2021.

- [30] S. Kuckova, G. Rambouskova, P. Junkova, J. Santrucek, P. Cejnar, T. A. Smirnova, O. Novotny and R. Hynek, "Analysis of protein additives degradation in aged mortars using mass spectrometry and principal component analysis," *Construction and Building Materials*, vol. 288, p. 123124, 2021.
- [31] Fotini Kesikidou and M. Stefanidou, "Natural fiber-reinforced mortars," *Journal of Building Engineering*, vol. 25, p. 100786, 2019.
- [32] M. Soria-Castro, J. Genescá-Llongueras, G. I. Hernández-Bolio and P. Castro-Borges, "Characterization of cement mortars with regional organic and inorganic additives," *RSC Advances*, vol. 14, no. 22, pp. 15468-15482, 2024.
- [33] H. Böke, S. Akkurt, B. İpekoğlu and E. Uğurlu, "Characteristics of brick used as aggregate in historic brick-lime mortars and plasters," *Cement and concrete research*, vol. 36, no. 6, pp. 1115-1122, 2006.
- [34] V. Pachta, S. Konopisi and M. Stefanidou, "The influence of brick dust and crushed brick on the properties of lime-based mortars exposed at elevated temperatures," *Construction and Building Materials*, vol. 296, p. 123743, 2021.
- [35] L. C. Botelho, G. C. Xavier, A. L. C. Paes and A. R. Azevedo, "Lime replacement by finely ground clay from the north fluminense region of RJ in mortar for coating walls and ceilings," *Journal of Materials Research and Technology*, vol. 23, pp. 5105-5114, 2023.

- [36] “Use of Water Reducers, Retarders, and Superplasticizers.,” [Online]. Available: <https://www.engr.psu.edu/ce/courses/ce584/concrete/library/materials/Admixture/AdmixturesMain.htm>. [Accessed 05 November 2024].
- [37] H. AlTawaiha, F. Alhomaidat and T. Eljufout, “A Review of the Effect of Nano-Silica on the Mechanical and Durability Properties of Cementitious Composites,” *Infrastructure*, vol. 8, no. 9, p. 132, 2023.
- [38] L. C. a. Z. Chen, Z. Xie, L. Wei, J. Hua, L. Huang and P.-S. Yap, “Recent developments on natural fiber concrete: A review of properties, sustainability, applications, barriers, and opportunities,” *Developments in the Built Environment*, vol. 16, p. 100255, 2023.
- [39] F. Khan, N. Hossain, F. Hasan, S. M. Rahman, S. Khan, A. Saifullah and M. A. Chowdhury, “Advances of natural fiber composites in diverse engineering applications—A review,” *Applications in Engineering Science*, vol. 18, p. 100184, 2024.
- [40] M. S. Hossain, V. Panov, S. Choi, J. B. kim and K. K. Yun, “Durability performance of cement mortar incorporating water-repellent admixtures,” *Construction and Building Materials*, vol. 440, p. 137262, 2024.
- [41] D. Carran, J. J. Hughes, C. Kennedy and A. Leslie, “A Short History of the Use of Lime as a Building Material Beyond Europe and North America,” *International Journal of Architectural Heritage*, vol. 6, no. 2, p. 117–146, 2012.

- [42] M. Hassibi, "An Overview Of Lime Slaking And Factors That Affect The Process," November 1999. [Online]. Available: <https://www.chemcosystems.net/literature>. [Accessed 10 06 2024].
- [43] J. Lanas and J. I. Alvarez-Galindo, "Masonry repair lime-based mortars: factors affecting the mechanical behavior," *Cement and Concrete Research*, vol. 33, no. 11, pp. 1867-1876, 2003.
- [44] C. Rodriguez-Navarro, E. Hansen and W. S. Ginell, "Calcium Hydroxide Crystal Evolution upon Aging of Lime Putty," *Journal of the American Ceramic Society*, vol. 81, no. 11, pp. 2761-3043, 1998.
- [45] B. Middendorf, J. J. Hughes, K. Callebaut and G. Baronio, "Investigative Methods for the Characterization of Historic Mortars," *Materials and Structures*, vol. 38, no. 278, pp. 695-706, 2005.
- [46] J. Ashurst and F. G. Dimes, *Conservation of Building and Decorative Stone*, Oxford: Butterworth-Heinemann, 1998.
- [47] R. Asghar, M. A. Khan, R. Alyousef, M. F. Javed and M. Ali, "Promoting the green Construction: Scientometric review on the mechanical and structural performance of geopolymer concrete," *Construction and Building Materials*, vol. 368, p. 130502, 2023.
- [48] C. I. o. A. Technologists, "Preserving the Tower of London's heritage using lime mortar," Chartered Institute of Architectural Technologists, [Online]. Available: <https://architecturaltechnology.com/resource/preserving-the-tower-of-london-s-heritage-using-lime-mortar.html>. [Accessed 29 August 2024].

- [49] L. stuff, “Tower Of London,” Lime stuff, [Online]. Available: <https://www.limestuff.co.uk/blog/tower-of-london>. [Accessed 8 August 2024].
- [50] T. Group, “TOD's for Colosseum,” [Online]. Available: <https://www.todsgroup.com/en/sustainability/colosseum-restoration-hypogea>. [Accessed 29 August 2024].
- [51] F. W. Barreiro, “ The restoration of the Oratory of the Partal Palace in the Alhambra of Granada, Grand Prix Europa Nostra,” *Built Heritage*, vol. 5, no. 1, 2021.
- [52] T. 203-RHM, “Chapter 2 - The role of mortar in masonry: An introduction to requirements for the design of repair mortars,” in *Repair Mortars for Historic Masonry - State of the Art Report of RILEM Technical Committee TC 203-RHM*, vol. 45, RILEM Publications SARL, 2016, pp. 3-14.
- [53] S. B., N. Patil, K. K. Jaiswal, T. Gowrishankar, K. K. Selvakumar, M. Jyothi, R. Jyothilakshmi and S. Kumar, “Development of sustainable alternative materials for the construction of green buildings using agricultural residues: A review,” *Construction and Building Materials*, vol. 368, 2023.
- [54] M. F. Junaid, Z. u. Rehman, M. Kuruc, I. Medved, D. Bacinskas, J. Čurpek, M. Cekon, N. Ijaz and W. S. Ansari, “Lightweight concrete from a perspective of sustainable reuse of waste byproducts,” *Construction and Building Materials*, vol. 319, 2021.

- [55] A. S. Vicente-Navarro, M. Mendivil-Giro, J. L. Santos-Ortega, E. Fraile-García and J. Ferreiro-Cabello, “Alternative Use of the Waste from Ground Olive Stones in Doping Mortar Bricks for Sustainable Façades,” *Building*, vol. 13, no. 12, 2023.
- [56] S. Blesson and A. U. Rao, “Agro-industrial-based wastes as supplementary cementitious or alkali-activated binder material: a comprehensive review,” *Innovative Infrastructure Solutions*, vol. 8, no. 125, 2023.
- [57] M. J. Marwa Khemakhem, “Composites based on (ethylene–propylene) copolymer and olive solid waste: Rheological, thermal, mechanical, and morphological behaviors,” *Polymer engineering and Science*, vol. 56, no. 1, pp. 27-35, 2016.
- [58] M. C. B. López, A. Martínez-Alonso and J. M. D. Tascón, “Mineral Matter Characterization in Olive Stones by Joint Use of LTA, XRD, FT-IR and SEM-EDX,” *Applied Spectroscopy*, vol. 54, no. 11, pp. 1712-1715, 2000.
- [59] Z. Eloueara, J. Bouzida, N. Boujelbena, M. Fekib and A. Montielc, “The use of exhausted olive cake ash (EOCA) as a low cost adsorbent for the removal of toxic metal ions from aqueous solutions,” *Fuel*, vol. 87, no. 12, pp. 2582-2589, 2008.
- [60] G. B. García, M. C. d. Hoces, C. M. García, M. T. C. Palomino, A. R. Gálvez and M. Á. Martín-Lara, “Characterization and modeling of pyrolysis of the two-phase olive mill solid waste,” *Fuel Processing Technology*, vol. 126, pp. 104-111, 2014.
- [61] F. Barreca and C. Fichera, “Use of olive stone as an additive in cement lime mortar to improve thermal insulation,” *Energy and Buildings*, vol. 62, pp. 507-513, 2013.

- [62] J. Ferreiro-Cabello, E. Fraile-Garcia, A. Pernia-Espinoza and F. J. Martinez-de-Pison, “Strength Performance of Different Mortars Doped Using Olive Stones as Lightweight Aggregate,” *Buildings*, vol. 12, no. 10, 2022.
- [63] T. Cheboub, Y. Senhadji, H. Khelafi and G. Escadeillas, “Investigation of the engineering properties of environmentally-friendly self-compacting lightweight mortar containing olive kernel shells as aggregate,” *Journal of Cleaner Production*, vol. 249, 2020.
- [64] A. Mohanad and A.-A. Nabil, “Utilization of Olive Waste Ash in Mortar Mixtures,” *Structural Concrete*, vol. 11, pp. 221-228, 2010.
- [65] John L. Clarke, *Structural lightweight aggregate concrete*, CRC Press, 1993.
- [66] Kanadasan Jegathish, Auni Filzah Ahmad Fauzi, Hashim Abdul Razak, Paramanathan Selliah, Vijaya Subramaniam and Sumiani Yusof, “Feasibility Studies of Palm Oil Mill Waste Aggregates for the Construction Industry,” *Materials*, vol. 8, no. 9, pp. 6508-6530, 2015.
- [67] İffet Gamze Mütevelli Özkan, Kıymet Aldemir, Omar Alhasan, A. Benli, O. Y. B. Mehmet Uğur Yilmazoğlu and Gökhan Kaplan, “Investigation on the sustainable use of different sizes of sawdust aggregates in eco-friendly foam concretes: Physico-mechanical, thermal insulation and durability characteristics,” *Construction and Building Materials*, vol. 438, p. 137100, 2024.
- [68] Ehsan Ghafari, Hugo Costa, Eduardo Júlio, António Portugal and Luisa Durães, “The effect of nanosilica addition on flowability, strength and transport properties of ultra high performance concrete,” *Materials and design*, vol. 59, pp. 1-9, 2014.

- [69] Ye Qing, Zhang Zenan, Kong Deyu and Chen Rongshen, "Influence of nano-SiO₂ addition on properties of hardened cement paste as compared with silica fume,," *Construction and Building Materials*, vol. 21, no. 3, pp. 539-545, 2007.
- [70] Fadi Althoey, Mohd Ahmed, Osama Zaid, R. Martínez-García., M. M. Arbili., Fahad Alsharari and Mohd Ahmed, "Impact of Nano-silica on the hydration, strength, durability, and microstructural properties of concrete: A state-of-the-art review," *Case Studies in Construction Materials* , vol. 18, 2023.
- [71] P. P. Abhilash, Dheeresh Kumar Nayak, Bhaskar Sangoju, Rajesh Kumar and Veerendra Kumar, " Effect of nano-silica in concrete: a review," *construction and building materials*, vol. 278, p. 122347, 2021.
- [72] "Nano ESTEL," CTS Conservation, [Online]. Available: <https://ctsconservation.com/it/consolidanti-protettivi-e-malte/6023-nano-estel-conf-1-kg.html>. [Accessed 10 August 2024].
- [73] F. Iucolano, A. Colella, B. Liguori and D. Calcaterra, "Suitability of silica nanoparticles for tuff consolidation," *Construction and Building Materials*, vol. 202, pp. 73-81, 2019.
- [74] "SIST EN 1015-3:2001 Methods of test for mortar for masonry - Part 3: Determination of consistence of fresh mortar (by flow table)," European Committee for Standardization (CEN), Brussels, 2001.
- [75] "UNI EN 15886 : 2010 Conservation of cultural property - Test methods - Colour measurement of surfaces," Ente Nazionale Italiano di Unificazione (UNI), 2010.

- [76] “Natural stone test methods - Determination of resistance to salt crystallisation,” SIST EN 12370, 2000.
- [77] B. Lubelli, I. Rörig-Daalgard, A. M. Aguilar, M. Aškrić, K. Beck, C. Bläuer, V. Cnudde, A. M. D’Altri, H. Derluyn, J. Desarnaud, T. Diaz Gonçalves, R. Flatt, E. Franzoni, S. Godts, D. Gulotta, R. van Hees, I. Ioannou and A. Kamat, “Recommendation of RILEM TC 271-ASC: New accelerated test procedure for the assessment of resistance of natural stone and fired-clay brick units against salt crystallization,” *MATERIALS AND STRUCTURES*, vol. 56, no. 5, p. 101, 2023.
- [78] D. Benavente, M. G. d. Cura, J. Garcia-Guinea, S. Sánchez-Moral and S. Ordóñez, “Role of pore structure in salt crystallisation in unsaturated porous stone,” *Journal of Crystal Growth*, vol. 260, no. 3-4, pp. 532-544, 2004.
- [79] Saltwiki, “Halite,” 29 August 2023. [Online]. Available: <https://www.saltwiki.net/index.php?title=Halite&oldid=7231>. [Accessed 18 September 2024].
- [80] X.-t. Yu, D. Chen, J.-r. Feng, Y. Zhang and Y.-d. Liao, “Behavior of mortar exposed to different exposure conditions of sulfate attack,” *Ocean Engineering*, vol. 157, pp. 1-12, 2018.
- [81] R. P. van Hees, “3. DAMAGE ANALYSIS AS A STEP TOWARDS COMPATIBLE REPAIR MORTARS,” in *Characterisation of Old Mortars with Respect to their Repair - Final Report of RILEM TC 167-COM*, RILEM Publications SARL, 2004, pp. 107 - 152.

- [82] I. G3SoilWorks, “Understanding Efflorescence: A Homeowner’s Guide,” 31 July 2024. [Online]. Available: <https://g3soilworks.com/2024/07/26/understanding-efflorescence-a-homeowners-guide/#:~:text=While%20efflorescence%20is%20primarily%20an,deterioration%20of%20mortar%20and%20concrete..> [Accessed 18 September 2024].
- [83] J. Desarnaud, H. Derluyn, L. Molari, S. d. Miranda, V. Cnudde and N. Shahidzadeh, “Drying of salt contaminated porous media: Effect of primary and secondary nucleation,” *Journal of applied physics*, vol. 118, no. 11, 2015.
- [84] *ISO/CIE 15801:2010; Conservation of cultural property-Test methods-Determination of water absorption by capillarity*, Milan, Italy: Ente Nazionale Italiano di Unificazione, 2010.
- [85] EUROPEAN COMMITTEE FOR STANDARDIZATION , “Methods of test for mortar for masonry - Part 11: Determination of flexural and compressive strength of hardened mortar,” 2019.
- [86] L. Kerrai, B. Salah, S. Roland and R. Z. Fetiha, “Valorisation of organic waste: Use of olive kernels and pomace for cement manufacture,” *Journal of Cleaner Production*, vol. 277, 2020.
- [87] V.V. Praveen Kumar and S. Dey, “Study on strength and durability characteristics of nano-silica based blended concrete,” *Hybrid Advances*, vol. 2, p. 100011, 2023.
- [88] S. Praveenkumar and K. Gayathiri, “Influence of Nano Silica on Fresh and Hardened Properties of Cement-based Materials – A Review,” *Silicon*, vol. 14, p. 8327–8357, 2022.

- [89] Mohammad Tabish, Mohd Moonis Zaheer and Abdul Baqi, “Effect of nano-silica on mechanical, microstructural and durability properties of cement-based materials: A review,” *Journal of Building Engineering*, vol. 65, p. 105676, 2023.
- [90] K. V. Balen, I. Papayianni, R. V. Hees, L. Binda and A. Waldum, “Introduction to requirements for and functions and properties of repair mortars,” *Materials and Structures*, vol. 38, pp. 781-785, 2005.
- [91] M. F. La Russa, S. A. Ruffolo, M. Á. de Buergo, M. Ricca, C. M. Belfiore, A. Pezzino and G. M. Crisci, “The behaviour of consolidated Neapolitan yellow Tuff against salt weathering,” *Bulletin of Engineering Geology and the Environment*, vol. 79, no. 1, p. 115–124, 2017.
- [92] H. Altawaiha, F. Alhomaidat and T. Eljufout, “A Review of the Effect of Nano-Silica on the Mechanical and Durability Properties of Cementitious Composites,” *Infrastructures*, vol. 8, no. 9, 2023.
- [93] H. Dilbas, M. Simsek and O. Cakir, “An investigation on mechanical and physical properties of recycled aggregate concrete (RAC) with and without silica fume,” *Construction and Building Materials*, vol. 61, pp. 50 - 59, 2014.
- [94] L. Hui, M.-h. Zhang and J.-p. Ou, “Flexural fatigue performance of concrete containing nanoparticles for pavement,” *International Journal of Fatigue*, vol. 29, no. 7, pp. 1292-1301, 2007.

- [95] P. S. Engineering, “The Effect of Aggregate Properties on Concrete,” [Online]. Available: <https://www.engr.psu.edu/ce/courses/ce584/concrete/library/materials/aggregate/aggregates/main.htm>. [Accessed 08 06 2024].
- [96] K. Khwaldia, N. Attour, J. Matthes, L. Beck and M. Schmid, “Olive byproducts and their bioactive compounds as available source for food packaging applications,” *Comprehensive reviews in food science and food safety*, vol. 21, no. 2, pp. 809-2073, 2022.
- [97] A. S. Vicente-Navarro, M. Mendivil-Giro, J. L. Santos-Ortega, E. Fraile-García and J. Ferreiro-Cabello, “Alternative Use of the Waste from Ground Olive Stones in Doping Mortar Bricks for Sustainable Façades,” *Buildings*, vol. 13, no. 12, 2023.

Appendix

Table 20: Description of salt damage type according to ICOMOS International Scientific Committee for Stone (ISCS), [1].

Specimen	TQ-HL		
Before accumulation			
After accumulation			

Specimen	Main categories of damage	Detailed damage and alteration type	Extent of damage or alteration	Remarks
TQ-HL	1. Surface change	a. Efflorescence b. Blistering	a. Extensive b. Extensive	The TQ samples showed early signs of surface change with tiny salt crystals on

	<p>2. Loss of cohesion</p> <p>3. Cracking</p>	<p>c. Disintegration</p> <p>d. Splitting</p>	<p>c. Limited</p> <p>d. Limited</p>	<p>the surface of the surface of the samples.</p> <p>And early sign of blistering. The sample eventually disintegrated in the final cycles.</p>
--	---	--	-------------------------------------	---

Specimen	POS-5-HL		
Before accumulation			
After accumulation			

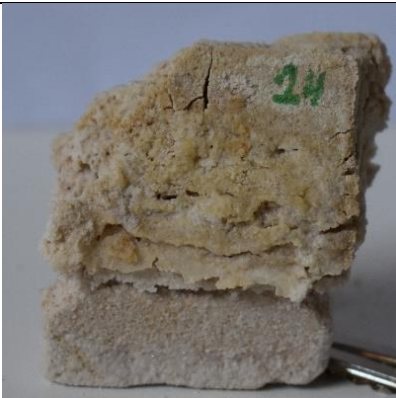
Specimen	Main categories of damage	Detailed damage and alteration type	Extent of damage or alteration	Remarks
POS-5-HL	<ol style="list-style-type: none"> 1. Surface change 2. Loss of cohesion 3. Cracking 	<ol style="list-style-type: none"> a. Efflorescence b. Blistering c. Disintegration d. Splitting 	<ol style="list-style-type: none"> a. Not so extensive b. Extensive c. Extensive d. Limited 	These samples showed less salt crystallized on the surface in the early cycles. But one of it samples completely disintegrated before the end of the 15 th cycle

Specimen	POS-10-HL		
Before accumulation			
After accumulation			

Specimen	Main categories of damage	Detailed damage and alteration type	Extent of damage or alteration	Remarks
POS-10-HL	<ol style="list-style-type: none"> 1. Surface change 2. Loss of cohesion 3. Cracking 	<ol style="list-style-type: none"> a. Efflorescence b. Blistering c. Disintegration d. Splitting e. Fragmentation 	<ol style="list-style-type: none"> a. Extensive b. Limited c. Extensive e. Extensive f. Extensive 	<p>There were some salt deposition on the surface, after the second cycle.</p> <p>There were also some blistering after the 2nd cycle and eventually, disintegration and fragmentation of all its samples before the last cycle</p>

Specimen	POS-15-HL		
Before accumulation			
After accumulation			

Specimen	Main categories of damage	Detailed damage and alteration type	Extent of damage or alteration	Remarks
POS-15-HL	<ol style="list-style-type: none"> 1. Surface change 2. Loss of cohesion 3. Cracking 	<ol style="list-style-type: none"> a. Efflorescence b. Blistering c. Disintegration d. Splitting e. Fragmentation 	<ol style="list-style-type: none"> a. Limited b. Limited c. Extensive e. Extensive f. Extensive 	<p>There was some light salt deposition on the surface, after the second cycle.</p> <p>There were also some blistering after the 2nd cycle and eventually, cracks, disintegration and fragmentation of all its samples before the last cycle</p>

Specimen	POS-5-HL-S		
Before accumulation			
After accumulation			

Specimen	Main categories of damage	Detailed damage and alteration type	Extent of damage or alteration	Remarks
POS-5-HL-S	<ol style="list-style-type: none"> 1. Surface change 2. Loss of cohesion 3. Cracking 	<ol style="list-style-type: none"> a. Efflorescence b. Blistering c. Disintegration d. Splitting e. Fragmentation 	<ol style="list-style-type: none"> a. Extensive b. Limited c. Extensive e. Extensive f. Extensive 	<p>There was some salt deposition on the surface, after the second cycle.</p> <p>There were also some blistering after the 3rd cycle and eventually, disintegration of all its samples before the last cycle</p>

Specimen	POS-10-HL-S		
Before accumulation			
After accumulation			

Specimen	Main categories of damage	Detailed damage and alteration type	Extent of damage or alteration	Remarks
POS-15-HL-S	<ol style="list-style-type: none"> 1. Surface change 2. Loss of cohesion 3. Cracking 	<ol style="list-style-type: none"> a. Efflorescence b. Blistering c. Disintegration d. Splitting e. Fragmentation 	<ol style="list-style-type: none"> a. Extensive b. Limited c. Extensive e. Extensive f. Extensive 	<p>There was some salt deposition on the surface, after the second cycle.</p> <p>There were also some blistering after the 2nd cycle and eventually, disintegration of all its samples before the last cycle</p>

Specimen	POS-15-HL-S		
Before accumulation			
After accumulation			

Specimen	Main categories of damage	Detailed damage and alteration type	Extent of damage or alteration	Remarks
POS-15-HL-S	<ol style="list-style-type: none"> 1. Surface change 2. Loss of cohesion 3. Cracking 	<ol style="list-style-type: none"> a. Efflorescence b. Blistering c. Disintegration d. Splitting e. Fragmentation 	<ol style="list-style-type: none"> a. Extensive b. Limited c. Extensive e. Extensive f. Extensive 	<p>There was some salt deposition on the surface, after the second cycle.</p> <p>There were also some blistering after the 2nd cycle and eventually, disintegration of all its samples before the last cycle</p>